

MULTIPLY CONNECTED SPACETIMES
AND CLOSED TIMELIKE CURVES
IN SEMICLASSICAL GRAVITY

Thesis by
Gunnar Klinkhammer

In Partial Fulfillment of the Requirements
for the Degree of
Doctor of Philosophy

California Institute of Technology
Pasadena, California
1992
(Defended May 15, 1992)

©1992

Gunnar Klinkhammer

All Rights Reserved

To my mother and my grandmother.

Acknowledgments

... and, mayhap, I had a tear or two myself in my eyes; but no lad of sixteen is very sad who has liberty for the first time, and twenty guineas in his pocket; and I rode away, thinking, I confess, not so much of the kind mother left alone, and of the home behind me, as of to-morrow, and all the wonders it would bring.

William Makepeace Thackeray,
The Memoirs of Barry Lyndon, Esq.

I am very happy today that five years ago, I ventured on a journey to Pasadena.

It was here that I met a most remarkable man: my thesis advisor Kip Thorne. Not only is he an outstanding scientific mentor, who leads through encouragement and respect, who is patient, yet insistent, but also he has a truly generous and liberal mind which carries him far beyond the place where he chose to be.

It has been a privilege to be involved in research at the forefront of our understanding of Nature. The California Institute of Technology and its physics department have provided an extremely stimulating environment to the apprentice in this quest.

That I feel at home in Pasadena is due especially to Betty and Doug Nickerson who made me one of their family.

My happiest hours in Southern California I spent with Sioux Bally. She filled them with love, beauty, and passion. I shall not forget her.

Back in Westphalia, the two who had raised me, my mother and my grandmother, ignored the sacrifice my distance meant to them and supported me with undiminished love. I dedicate this fruit of academic labor to them.

Abstract

In this thesis, we present three studies motivated by the recent interest in spacetimes with closed timelike curves (“CTC’s”).

First, it has been shown that certain energy conditions must be violated if spacetime is to develop CTC’s. We initiate a study of whether quantum field theory permits such violations by proving that, in Minkowski spacetime, a free scalar field will satisfy the weak and strong energy conditions averaged along any complete null or timelike geodesic. We remark that in flat, but topologically non-trivial spacetimes, the averaged weak energy condition can be violated.

Second, it has been argued that the most likely way by which Nature might prevent the creation of CTC’s is a divergent vacuum polarization at the chronology horizon where such CTC’s first arise. We derive the form of the vacuum polarization of a conformal scalar field and of a spin-1/2 field near a closed null geodesic from which the null generators of a generic compactly generated chronology horizon spring forth. We show that the tensorial structure of the polarization and its degree of divergence are the same for scalar and for spin-1/2 fields and are independent of the details of the spacetime geometry. We also show that in generic cases, there will be no cancellation of this divergence for a combination of scalar and spin-1/2 fields that has equal numbers of Fermi and Bose degrees of freedom.

Third, in anticipation of the possibility that Nature might permit CTC’s, we demonstrate that for a classical body with a hard-sphere potential and no internal degrees of freedom (a “billiard ball”) traveling nonrelativistically in a wormhole spacetime with CTC’s, the Cauchy problem is ill-posed in a peculiar way. For certain (“dangerous”) initial data, there would appear to be no self-consistent solution to the equations of motion because the ball collides with its younger self after having traversed the wormhole. However, we show that for a wide range of dangerous and non-dangerous initial data, there is an infinity of self-consistent solutions, each involving one self-collision. No initial data are found for which there is no self-consistent solution.

Contents

Acknowledgments	iv
Abstract	v
1 Introduction	1
2 Averaged energy conditions for free scalar fields in flat spacetime . . .	11
3 Vacuum polarization of scalar and spinor fields near closed null geodesics	23
4 Billiard balls in wormhole spacetimes with closed timelike curves: Classical theory	42
Epilogue	66

Chapter 1

Introduction

1 Motivation

Before the theory of general relativity, space and time were viewed as a rigid, unchanging framework in which all physical processes take place. This view reflected the everyday perception humans had, and still have, of space and time. Then, general relativity introduced the idea that space and time are themselves dynamic physical quantities whose interaction with matter is governed by nonlinear equations, the Einstein field equations. The theory thus allowed, for the first time in physics, to describe complex configurations of space and time and, hence, of causality. A striking example, provided by general relativity, of a counter-intuitive structure of space and time is a black hole, i.e., a region that is causally sealed off from the rest of the Universe.

A disturbing notion compatible with the formalism of general relativity is that of closed timelike curves. These are worldlines that, although always directed towards the future locally, return to one of their former points. Solutions of Einstein's equations exhibiting closed timelike curves have been known for a long time, but early examples were regarded as unphysical curiosities rather than viable models of something that might occur in the real Universe. Gödel's rotating spacetime, where closed timelike curves are present always and everywhere, is one such example [1].

Recently, a stronger interest in closed timelike curves has been created by the discovery of wormhole and other spacetimes that have such curves [2,3,4,5]. An effort has since been made by various researchers to answer two questions: first, whether there are viable solutions of Einstein's equations with closed timelike curves [2,5,6,7,8,9]; and second, whether a sensible initial-value problem can be formulated for matter propagating on the background of a spacetime with closed timelike curves [3,10,11,12,13,14,15,16]. The present thesis reports work on these two issues. We shall give an overview of the body of the thesis in Sec. 2 and make a few concluding remarks in Sec. 3.

2 Overview of the thesis

Chapter 2 of this thesis is devoted to the study of averaged energy conditions. When wormhole spacetimes with closed timelike curves were first discussed [2] it had already been realized that the macroscopic traversable wormholes of these spacetimes could only be sustained by matter that violates an averaged version of the weak energy condition [17]. More recently, Hawking has proved that when the boundary that separates the spacetime region with closed timelike curves from the one without (the so-called “chronology horizon”) evolves out of a compact domain, i.e., when the chronology horizon is “compactly generated”, then the weak energy condition must be violated [8].

It has been known for a long time that quantum fields can violate the *local* weak energy condition. However, by the time wormhole spacetimes with closed timelike curves were discovered, a systematic investigation of *averaged* energy conditions had not even been carried out for flat spacetime. The work described in Chapter 2 was the first such investigation. More specifically, in Chapter 2, we ask whether

$$\int d\zeta \langle T_{ab} \rangle t^a t^b$$

can ever be negative, where $\langle T_{ab} \rangle$ is the expectation value of the stress-energy tensor of a free scalar quantum field, and the integration is taken along a complete null or timelike geodesic with tangent vector t^a . We find that in ordinary Minkowski spacetime, this integral cannot be negative, and thus the averaged *weak* energy condition is satisfied. Further, we also find the averaged *strong* energy condition, which refers to the integral of $\langle T_{ab} - (1/2)g_{ab}T^c_c \rangle$, to be satisfied in Minkowski spacetime, although this places a restriction on the value of the field’s curvature coupling constant when the average is taken along a timelike geodesic. We point out, however, that in flat spacetimes with circularly closed spatial sections, the Casimir effect entails a violation of the averaged energy conditions.

In an addendum to Chapter 2, we give a simple proof that the weak energy condition averaged along a complete null geodesic in Minkowski spacetime is not

violated by the electromagnetic field, either; and we demonstrate that a violation of the *local* weak energy condition in Minkowski spacetime can arise for a spin-1/2 field in an eigenstate of particle number, whereas, for a scalar field, it can only arise in a superposition of states of different particle numbers.

The work presented in Chapter 2 initiated further investigations of averaged energy conditions [18,19,20]. It was realized that the weak energy condition averaged along a complete null geodesic (the “averaged null energy condition”) will be satisfied in curved two-dimensional spacetimes under very wide assumptions, but can be violated in curved four-dimensional spacetimes.

Chapter 3 deals with the stability of compactly generated chronology horizons. It has been shown previously that the vacuum polarization of scalar quantum fields will diverge near any chronology horizon [6], and several examples of this divergence have been discussed [6,7,9,21]. The divergence, through its back-reaction on spacetime geometry, might well alter the spacetime so strongly that closed timelike curves will not form. Hawking has recently formulated a “chronology protection conjecture” which postulates that closed timelike curves cannot arise in the real Universe [8]. He regards the divergent vacuum polarization at the chronology horizon as a likely means by which Nature will enforce this rule.

Any compactly generated chronology horizon possesses at least one smoothly closed null geodesic [8], and it is likely that all the generators of the horizon, when followed to the past, asymptote to a closed null geodesic [3]. Therefore, the divergent vacuum polarization near such a closed null geodesic might well destroy the entire chronology horizon and prevent close timelike curves from forming. In Chapter 3, we compute the vacuum polarization for a conformal scalar field near such a closed null geodesic in a *generic* spacetime with a compactly generated chronology horizon. We find that for an observer who will pass through an event on the closed null geodesic after a small interval of proper time δt , the leading-order divergence will always be proportional to $(\delta t)^{-3}$ and have the tensorial structure of the stress-energy of a null fluid that moves along the closed null geodesic. We also

compute the analogous divergence for a spin-1/2 field. The degree of divergence of the leading-order term and its tensorial structure are found to be the same as in the scalar case, but the dependence on certain parameters that describe the details of the spacetime geometry near the closed null geodesic is different. We emphasize an important consequence of this result: unlike in flat spacetime, in generic cases there will be no cancellation of the vacuum polarization for a combination of scalar and spin-1/2 fields that, in flat spacetime, would be related by supersymmetry. This finding will lend strong support to the chronology protection conjecture if Hawking's claim is correct that the divergent vacuum polarization is not rendered inconsequential by the effects of quantum gravity [6,8].

In Chapter 4, we investigate the consequences that the presence of closed time-like curves would have for the initial-value problem of a simple interacting system. For this purpose, we choose a static wormhole with an arbitrarily short throat, residing in an otherwise flat spacetime. The interacting system consists of a macroscopic body with a hard-sphere potential whose internal degrees of freedom we neglect (a "billiard ball"). The ball's motion is treated with classical, nonrelativistic mechanics. A finite set of initial conditions will have the billiard ball travel through the wormhole, backward in external time, encounter a "younger" version of itself, and scatter off itself. Such initial conditions would seem not to allow any self-consistent solution of the initial-value problem for the ball. However, as we find in Chapter 4, for a wide range of such "dangerous" initial data, there is in fact an infinite number of different self-consistent solutions for the ball's motion. Each of these solutions involves one self-collision of the ball, and the various solutions are distinguished by the number of wormhole traversals of the ball. An infinite number of such solutions exists even for a wide range of non-dangerous initial data. On the other hand, no dangerous initial data are found for which there is no such solution, although the search leaves out a certain portion of the set of dangerous initial data.

Chapter 4 represents a collaboration between F. Echeverria, K. S. Thorne, and

the author. Within this collaboration, the author's chief contribution was the derivation of the exact equations that govern the "coplanar" self-consistent solutions with one self-collision and one wormhole-traversal between the two times the ball encounters the collision event. He was also strongly involved in the presentation of all other results, with the exception of the numerical studies.

The upshot of Chapter 4 is very surprising: While the presence of closed time-like curves makes the initial-value problem for billiard ball motion ill-posed, it does so by inducing *too many* solutions rather than by allowing *none*. It seems likely that a quantum mechanical treatment of the ball's motion will make the initial-value problem well-posed again. Thorne and the author have attempted to show this [12], but, at present, some open questions remain. We shall conclude this section with a brief description of some elements of this effort.

Consider nonrelativistic motion of a billiard ball in the spacetime of Chapter 4. It is straightforward to write down an action functional that yields the correct classical equations of motion, taking self-collisions into account. A natural way to attempt a quantum mechanical formulation of the ball's dynamics is via Feynman's sum over histories. One could imagine a situation where closed timelike curves are not important for the ball's motion at early and late times. Ordinary wave functions should then describe the in state and the out state, i.e., the quantum state of the ball at some early time and the one at some late time. According to Feynman's approach, the out wave function should be related to the in wave function by a propagator that is computable as a sum over histories weighted by $\exp(iS/\hbar)$, with the sum including histories that involve self-collisions. One could take the hard-sphere potential into account by dropping from the sum all histories that ever come closer to themselves than twice the ball's radius. This procedure based on the sum over histories appears to restore a well-posed initial-value problem in the following sense: for each choice of the in state, it predicts a unique probability distribution for the outcome of any set of measurements that one might wish to make.

An interesting issue in this context is whether the evolution through the region with closed timelike curves formally obeys unitarity, i.e., whether the norm of the out wave function, computed in the standard way, equals the norm of the in wave function. One could try to answer this question in two different ways. By manipulating the propagator in its general form, one could relate it to a two-particle propagator in ordinary flat spacetime and use the unitarity properties of the latter. Or, one could choose the in state to be a quasiclassical one and then attempt a WKB approximation for the propagator. This would have the added benefit that one might then find the resultant out state to be quasiclassical also, and one would thereby see what happens to a classical billiard ball when an ill-posed initial-value problem offers it the choice of several trajectories. Unfortunately, no conclusive results about the unitarity issue have been obtained yet. It seems likely though, from a WKB calculation, that unitarity is violated: a quasiclassical in state corresponding to non-dangerous initial data will split into several outgoing wave packets, one of them corresponding to straight, collisionless propagation and having the same norm as the in state, the others corresponding to the various alternative classical solutions with collision, as described in Chapter 4; then, if the overlap between the straight piece and the scattered pieces is negligible, the overall norm of the out state will exceed the norm of the in state.

This line of investigation has stimulated research by other workers [13,16]. Very recently, e.g., it has been proposed that unitarity will be restored in the situation referred to above if one takes histories with multiple self-collisions into account [16].

3 Conclusion

In conclusion, we may say that it is quite surprising that theoretical physics as we know it does not flatly forbid closed timelike curves. If divergent vacuum polarization is indeed the universal mechanism for the prevention of closed timelike

curves, one would like to understand why it is singled out to play such a fundamental role. Perhaps, a unified theory of gravity and matter will hold definitive answers to all questions about closed timelike curves. Or perhaps, to obtain such answers, we must also understand how physics relates to the notion of free will.

Bibliography

- [1] K. Gödel, *Rev. Mod. Phys.* **21**, 447 (1949).
- [2] M. S. Morris, K. S. Thorne, and U. Yurtsever, *Phys. Rev. Lett.* **61**, 1446 (1988).
- [3] J. Friedman, M. S. Morris, I. D. Novikov, F. Echeverria, G. Klinkhammer, K. S. Thorne, and U. Yurtsever, *Phys. Rev. D* **42**, 1915 (1990).
- [4] V. P. Frolov and I. D. Novikov, *Phys. Rev. D* **42**, 1057 (1990).
- [5] J. R. Gott, *Phys. Rev. Lett.* **66**, 1126 (1991). See also C. Cutler, *Phys. Rev. D* **45**, 487 (1992).
- [6] S.-W. Kim and K. S. Thorne, *Phys. Rev. D* **43**, 3929 (1991).
- [7] V. P. Frolov, *Phys. Rev. D* **43**, 3878 (1991).
- [8] S. W. Hawking, *Phys. Rev. D* (to be published).
- [9] J. Grant, *Gravity Foundation Essay* (1992).
- [10] F. Echeverria, G. Klinkhammer, and K. S. Thorne, *Phys. Rev. D* **44**, 1077 (1991) (Chapter 4 of this thesis).
- [11] I. D. Novikov, *Phys. Rev. D* **45**, 1989 (1992).
- [12] G. Klinkhammer and K. S. Thorne (unpublished).
- [13] D. Deutsch, *Phys. Rev. D* **44**, 3197 (1991).

- [14] J. L. Friedman, N. J. Papastamatiou, and J. Z. Simon, University of Wisconsin-Milwaukee preprint WISC-MIL-91-TH-17 (1991).
- [15] D. G. Boulware, University of Washington preprint UW/PT-92-04 (1992).
- [16] H. D. Politzer and J. P. Preskill (unpublished).
- [17] M. S. Morris and K. S. Thorne, *Am. J. Phys.* **56**, 395 (1988).
- [18] U. Yurtsever, *Class. Quantum Grav. Lett.* **7**, L251 (1990).
- [19] R. M. Wald and U. Yurtsever, *Phys. Rev. D* **44**, 403 (1991).
- [20] A. Folacci, *Phys. Rev. D* (to be published).
- [21] W. A. Hiscock and D. A. Kinkowski, *Phys. Rev. D* **26**, 1225 (1982).

Chapter 2

Averaged energy conditions for free scalar fields in flat spacetime

(Originally appeared in Phys. Rev. D **43**, 2542 (1991).)

Averaged energy conditions for free scalar fields in flat spacetime

Gunnar Klinkhammer

*Theoretical Astrophysics, California Institute of Technology,
Pasadena, California 91125*

(Received 2 November 1990)

This paper initiates a research program to determine whether, and in what situations, quantum field theory enforces averaged energy conditions on the renormalized stress-energy tensors of quantum fields. This program is motivated by the important roles of averaged energy conditions in general-relativistic singularity theorems, and in preventing the existence of classical, traversable wormholes and wormhole-induced closed timelike curves. As a first step in this research program, this paper shows that a quantized, free scalar field in Minkowski spacetime has the following properties: The weak energy condition is satisfied for a wide class of states when averaged along a complete null geodesic, but it can be violated when averaged along a nongeodesic curve. If the curvature coupling constant in the scalar wave equation is restricted to a certain range, which includes conformal coupling, then the strong energy condition is satisfied for the same wide class of states when averaged along a complete timelike geodesic. It is shown, further, that this enforcement of energy conditions is not universally true in all spacetimes: by closing up Minkowski spacetime in a spatial direction (e.g., by identifying $x = 0$ with $x = L$), one can produce quantum states of a free scalar field that violate the averaged weak energy condition.

I. INTRODUCTION AND SUMMARY

Since spacetime curvature is produced by the total stress-energy tensor of all the matter that inhabits spacetime, any constraints that all stress-energy tensors must satisfy will induce corresponding constraints on spacetime curvature. At least twice in the past, physicists assumed without much proof that the stress-energy tensor was constrained in certain ways; they derived interesting resulting constraints on spacetime curvature (gravity), and then, later, they discovered counterexamples to the stress-energy constraints and thereby lost their gravitational results.

The first example of this was the belief that the stress-energy tensor must always have a non-negative trace, $T^\alpha_\alpha \geq 0$, and correspondingly that the pressure p of superdense matter can never exceed one-third its mass-energy density ρ . This belief permeated physicists' thinking about the equation of state of superdense matter during the 1930s, 1940s, and 1950s.¹ In 1961 Zel'dovich² refuted the hypothesis $T^\alpha_\alpha \geq 0$ and $p \leq \rho/3$ by exhibiting a model quantum field theory for a vector boson that produces $p = \rho$. Current theory takes seriously the possibility of nuclear-matter equations of state that imply $p > \rho/3$ at the centers of the most massive neutron stars these equations of state will sustain.³

The second example was the assumption, in the 1960s, that the stress-energy tensor always satisfies one or another energy condition: the "weak energy condition"

($T_{\mu\nu}t^\mu t^\nu \geq 0$ for all timelike or null t^μ); the "strong energy condition" [$(T_{\mu\nu} - \frac{1}{2}T^\alpha_\alpha g_{\mu\nu})t^\mu t^\nu \geq 0$ for all timelike or null t^μ]. These energy conditions, when fed into the Einstein field equations, produced theorems on the inevitability of spacetime singularities at the end point of the gravitational collapse of a star, and in the big bang.⁴⁻⁶ However, almost simultaneously with Penrose's proof of the first singularity theorem⁴ researchers in axiomatic quantum field theory (Epstein, Glaser, and Jaffe) proved that quantum fields cannot always and everywhere satisfy such energy conditions.⁷ An explicit example of a quantum violation of the dominant energy condition was constructed by Zel'dovich and Pitaevsky in 1971,⁸ and gradually in the 1970s researchers became aware that the Casimir vacuum⁹ for the electromagnetic field between two perfectly conducting plates violates the weak and strong energy conditions.¹⁰ Perhaps the simplest example of a violation of the weak energy condition is that of a free scalar field in Minkowski spacetime when its state is the vacuum plus a small admixture of a two-particle state¹¹ (see Sec. II). A wide variety of other examples have been found since the mid-1970s: quantum fields in spacetimes with moving mirrors,^{11,12} massive Dirac particles in a Kerr-Newman geometry,¹³ interacting field theories,¹⁴ and even the squeezed vacuum state of light,¹⁵ which has been constructed experimentally.¹⁶

Do these ubiquitous energy-condition violations make singularity theorems irrelevant to the real Universe in which we live? Perhaps in part (cosmological mod-

els have been constructed that use quantum fields to avoid singularities¹⁷), but perhaps not entirely: In 1978, Tipler¹⁸ exhibited a new singularity theorem which relies not on an energy condition that must be satisfied locally, everywhere, but rather on an energy condition that is satisfied only when averaged along certain curves in spacetime. Borde¹⁹ later considered weaker forms of this energy condition. Motivated by Tipler's theorem, Roman²⁰ recently has reformulated and reproven Penrose's original singularity theorem,⁴ replacing the local weak energy condition by an *averaged weak energy condition*: $\int d\zeta T_{\mu\nu}t^\mu t^\nu \geq 0$, where the integral is along null geodesics with affine parameter ζ and tangent vector $t^\mu = dx^\mu/d\zeta$. Whether quantum field theory enforces or violates this averaged energy condition is not yet known, and very little effort has been made, as yet, to find out.

This same averaged weak energy condition has recently turned out to be crucial elsewhere in physics.

If the laws of physics permit the existence of macroscopic, traversable wormholes, then generic relative motions of their mouths, and generic gravitational redshifts produced on their mouths by external bodies, inevitably will change the manner in which time links up through the wormholes and thereby will create closed timelike curves^{21,22} (CTC's). The researchers who discovered this (Morris, Yurtsever, Thorne, Frolov, and Novikov) thought, at first, that quantum field theory might protect the Universe against such CTC's by producing a divergent vacuum polarization that changes the spacetime structure just before the CTC's arise. However, Kim and Thorne²³ have recently argued that, although the vacuum polarization grows large, just before the CTC's arise, it might not grow large enough to protect against the CTC's. If this is so, then it would seem that the only way that physical law can prevent classical, traversable wormholes from creating CTC's is by preventing such wormholes from ever existing. The possibility of their existence relies crucially on the wormholes being threaded by some sort of quantum field in a state that violates the averaged weak energy condition.²¹ It therefore is important to determine whether quantum field theory enforces the averaged weak energy condition in wormhole spacetimes.

In view of the importance of averaged energy conditions to singularity theorems, to traversable wormholes, and to the existence of CTC's, it is appropriate to mount a vigorous effort to determine whether, and in what situations, quantum field theory enforces averaged energy conditions. This paper is a first step in such an effort.

Is there reason to hope that averaged energy conditions will be enforced by quantum field theory? Yes, at least under certain circumstances. Hope comes from two directions. Ford has shown, in specific examples²⁴ and very recently more generally,²⁵ that quantum field theory places certain limits on the magnitudes of fluxes of negative energies. Though these limits are not quite in the spirit of an averaged energy condition, they show clearly that quantum field theory is not entirely indifferent to

negative energies. Second it is well known that the total renormalized energy of a free quantum field, scalar or Dirac, never is negative in Minkowski spacetime.²⁶ More precisely, when one contracts the renormalized stress-energy tensor with the unit timelike normal to any spacelike hypersurface and then averages over the spacelike hypersurface, one must always get a non-negative result. This is an averaged energy condition—though, because it involves a three-dimensional average rather than a one-dimensional average, it is not of the type needed for singularity theorems and wormhole studies.

Since no systematic quantum-field-theory investigations of averaged energy conditions seem ever to have been made, this paper begins such an investigation in the simplest of situations: free, quantum, scalar fields in a flat spacetime. The fields are assumed to be test fields; i.e., the influence of their stress-energy tensor on the spacetime geometry is ignored. In this paper we shall show that, in this simple situation, the enforcement of energy conditions depends on the topology²⁷ of the flat spacetime: If the spacetime is Minkowski (Euclidean topology), then any free, quantum, scalar test field always, in every state, satisfies the averaged weak energy condition and a similar averaged strong energy condition as long as the field's curvature coupling constant is restricted to a certain range. If, instead, the flat spacetime has a cylindrical topology (e.g., $x = 0$ is identified with $x = L$, forcing the field to be spatially periodic), then there are quantum states that violate the averaged weak energy condition. These results dash previous hopes²¹ that the averaged weak energy condition might be enforced in all spacetimes, independent of topology.

We now give a summary of the structure and detailed results of this paper: In Sec. II we write down the stress-energy tensor for a free scalar field with arbitrary mass and curvature coupling constant in a Minkowski spacetime of arbitrary dimension, and we simplify it for the purpose of integration. We also discuss how the weak energy condition can fail locally. In Sec. III we prove that the averaged weak and strong energy conditions are satisfied in a Minkowski spacetime. More specifically, we choose a complete geodesic $x(\zeta)$ and compute the quantity $\int_{-\infty}^{\infty} d\zeta (T_{\mu\nu} - \frac{1}{2}T^\alpha_\alpha \eta_{\mu\nu})t^\mu t^\nu$, where ζ and $t^\mu = dx^\mu/d\zeta$ are the affine parameter and tangent vector of the geodesic, respectively. If the geodesic is null, non-negativity of this quantity corresponds to the averaged weak energy condition and also the averaged strong energy condition; if the geodesic is timelike, it corresponds to the averaged strong energy condition. We find the weak energy condition averaged along a null geodesic always to hold, but the strong energy condition averaged along a timelike geodesic to hold only for a certain range of the curvature coupling constant. This range always contains the case of conformal coupling, and for spacetime dimensions 2, 3, 4 it also contains minimal coupling. The mathematical treatment in Sec. III is somewhat heuristic, but in the Appendix we show how our results can be derived more rigorously for all state vectors

in a certain dense subspace of Fock space. This subspace is characterized by the requirements that the quantum state of the field neither involve arbitrarily large particle numbers nor arbitrarily large momenta. Finally, we argue that the results of Sec. III about the range of validity of the two averaged energy conditions apply also when the fields are classical.

In Sec. IV we show by means of a simple example that the averaged weak energy condition can fail if the curve of integration is not everywhere geodesic. We then turn to a flat, cylindrical spacetime, i.e., a Minkowski spacetime, closed in one spatial direction. In such a spacetime an effect similar to the above-mentioned Casimir effect occurs: the fact that the field modes now have a fundamental period makes the renormalized energy density and energy flux in the most natural vacuum state negative. One immediately sees from this that the averaged weak energy condition is violated in such spacetimes. This result makes it clear that the validity of the averaged weak energy condition depends on the topology of spacetime.

We conclude the paper in Sec. V, by pointing out avenues of future research as well as generalizations of the present work that are already under investigation by workers in the field.

Our notation and conventions are those of Birrell and Davies.²⁸ In particular, the metric has the signature $(+ - \dots -)$.

II. THE STRESS-ENERGY TENSOR

A free scalar field with mass m and curvature coupling constant ξ satisfies the field equation²⁸

$$[\nabla^\mu \nabla_\mu + m^2 + \xi R(x)]\phi(x) = 0, \quad (1)$$

where the Ricci scalar $R(x)$ is computed from the background metric. In n -dimensional flat spacetime, the stress-energy tensor of the field is given by²⁸

$$T_{\mu\nu} = (1 - 2\xi)\phi_{,\mu}\phi_{,\nu} - 2\xi\phi\phi_{,\mu\nu} + \left[\left(2\xi - \frac{1}{2} \right) \phi^{,\alpha}\phi_{,\alpha} + \frac{2}{n}\xi\phi\phi_{,\alpha} \right] \eta_{\mu\nu} + \left[\frac{1}{2} - 2\xi \left(1 - \frac{1}{n} \right) \right] m^2\phi^2\eta_{\mu\nu}. \quad (2)$$

Let $x^\mu(\zeta)$, with ζ an affine parameter, be a complete geodesic in n -dimensional Minkowski spacetime; $t^\mu \equiv dx^\mu/d\zeta$ is the geodesic's tangent vector. We are interested in the averaged quantity

$$T \equiv \int_{-\infty}^{\infty} d\zeta (T_{\mu\nu} - \frac{1}{2}T^\alpha_\alpha \eta_{\mu\nu})t^\mu t^\nu. \quad (3)$$

Before substituting the general expression (2) into the integral (3), we can make two simplifications. First, the two terms in Eq. (2) that are proportional to $1/n$ cancel by virtue of the flat-spacetime field equation $[\partial^\mu \partial_\mu + m^2]\phi(x) = 0$, which is satisfied by both the classical field and the quantum field operator. Second, the first two terms in Eq. (2) that are proportional to ξ become, after double contraction with t^μ ,

$$-2\xi \left[\left(\frac{d\phi}{d\zeta} \right)^2 + \phi \frac{d^2\phi}{d\zeta^2} \right]$$

and hence cancel in expression (3) by means of partial integration. This argument is evidently correct for the classical field if $\phi(d\phi/d\zeta)$ vanishes at infinity. In the quantum case, where the quadratic expressions in ϕ are replaced by the expectation values of the analogous products of field operators, the integration by parts can still be carried out, as may be seen by temporarily inserting a sum over intermediate states between the operators. The latter procedure is not in conflict with stress-energy tensor renormalization, which in Minkowski spacetime amounts only to normal ordering of the creation and an-

ihilation parts of the field operators. With these simplifications, expression (3) reduces to

$$T = \int_{-\infty}^{\infty} d\zeta \{ \phi_{,\mu}\phi_{,\nu} + [a\phi^{,\alpha}\phi_{,\alpha} - (a + \frac{1}{2})m^2\phi^2] \eta_{\mu\nu} \} t^\mu t^\nu, \quad (4)$$

where

$$a \equiv (n - 4)/4 + (3 - n)\xi.$$

(The factors of n stem from the trace of the metric.)

If t^μ is null and the field is treated classically, then the integrand in expression (4) becomes a squared quantity and hence non-negative. To see that this is not necessarily true in the quantum case, we need to insert the field operator

$$\phi(x) = \int d^{n-1}\mathbf{k} [u_{\mathbf{k}}(x)a_{\mathbf{k}} + u_{\mathbf{k}}^*(x)a_{\mathbf{k}}^\dagger], \quad (5)$$

where

$$\begin{aligned} u_{\mathbf{k}}(x) &= (2\pi)^{-(n-1)/2} (2\omega_{\mathbf{k}})^{-1/2} e^{-ik_\mu x^\mu}, \\ \omega_{\mathbf{k}} &= (\mathbf{k}^2 + m^2)^{1/2}, \\ k^\mu &= (\omega_{\mathbf{k}}, \mathbf{k}), \\ [a_{\mathbf{k}}, a_{\mathbf{k}'}^\dagger] &= \delta^{(n-1)}(\mathbf{k} - \mathbf{k}'). \end{aligned}$$

With this field operator and employing normal ordering, we obtain

$$T_{\mu\nu}t^\mu t^\nu = \iint d^{n-1}\mathbf{k} d^{n-1}\mathbf{k}' (2u_{\mathbf{k}}^* u_{\mathbf{k}'} a_{\mathbf{k}}^\dagger a_{\mathbf{k}'} - u_{\mathbf{k}} u_{\mathbf{k}'} a_{\mathbf{k}} a_{\mathbf{k}'} - u_{\mathbf{k}}^* u_{\mathbf{k}'}^* a_{\mathbf{k}}^\dagger a_{\mathbf{k}'}^\dagger) k_\mu t^\mu k'_\nu t^\nu \quad (6)$$

if t^μ is null. (We have dropped the spacetime dependence of the modes $u_{\mathbf{k}}$ for ease of notation. We have also omitted those terms that cancel when integrated along the geodesic.) Since this expression is quadratic in the creation and annihilation operators, $\langle 0|T_{\mu\nu}t^\mu t^\nu|2\rangle$ will be nonzero at an arbitrary spacetime point x for a suitably chosen two-particle state $|2\rangle$ and the vacuum state $|0\rangle$. If $|\psi\rangle = |0\rangle + \epsilon|2\rangle$, then for small ϵ the dominant contribution to the expectation value $\langle\psi|T_{\mu\nu}t^\mu t^\nu|\psi\rangle/\langle\psi|\psi\rangle$ at x will be $2\text{Re}(\epsilon\langle 0|T_{\mu\nu}t^\mu t^\nu|2\rangle)$, and ϵ can be so adjusted as to make this quantity negative. The state $|\psi\rangle$ then violates the weak energy condition at x —an ancient, well-known result.¹¹ $|\psi\rangle$ can be regarded as an approximation to a weakly squeezed state. Braunstein¹⁵ pointed out some time ago that squeezed states violate the (local) weak energy condition and that a natural interpretation of the extent of this violation in terms of the zero-point energy can be given. In the next section we shall ask whether a violation of the *averaged* weak energy condition is equally possible.

III. THE AVERAGED ENERGY CONDITIONS

We wish to carry out the integration over ζ in Eq. (3) for various choices of the geodesic $x^\mu(\zeta)$. The integrand itself is defined by an integration over a multiple of the one-particle momentum space such as that in Eq. (6). In calculating T , we will interchange these two types of integration, thereby obtaining delta functions. We assume that the states with respect to which expectation values of T are formed guarantee the validity of this procedure. Indeed, in the Appendix we will identify a dense subspace of Fock space on which the manipulations of this section can be carried out in a rigorous fashion: For every vector in this subspace there exist two arbitrarily large, but finite numbers N and K such that in the corresponding physical state the field cannot be found to contain more

than N particles or a particle whose momentum exceeds K in magnitude. For a state of this kind, as is also shown in the Appendix, the expectation value of the integrand in Eq. (3) is nowhere singular.

We now specialize, temporarily, to expression (6); i.e., the case of a null geodesic. Because of Poincaré invariance of the field theory, we do not lose generality by assuming that $x^\mu(\zeta) = \zeta t^\mu$, where $\vec{t} = \vec{e}_0 + \vec{e}_1$ is in the x^0, x^1 hyperplane. Here and throughout, spacetime indices run from 0 to $n-1$, with x^0 the time coordinate.

The first term in expression (6) is obviously a non-negative operator, since it can be written as the product of $\int d^{n-1}\mathbf{k} u_{\mathbf{k}} a_{\mathbf{k}} k_\mu t^\mu$ and its Hermitian conjugate. To investigate the contribution of the remaining terms to T , we note that

$$\begin{aligned} & \int_{-\infty}^{\infty} d\zeta u_{\mathbf{k}}(x(\zeta)) u_{\mathbf{k}'}(x(\zeta)) \\ &= \frac{1}{2(2\pi)^{n-2}(\omega_{\mathbf{k}}\omega_{\mathbf{k}'})^{1/2}} \delta(\omega_{\mathbf{k}} + \omega_{\mathbf{k}'} - k^1 - k'^1). \end{aligned} \quad (7)$$

For a massive field, $\omega_{\mathbf{k}}$ is strictly greater than the 1 component of \mathbf{k} , and thus the delta function in Eq. (7) is without support. In the case of a massless field, it has support only where both \mathbf{k} and \mathbf{k}' lie completely in the positive x^1 direction. For such momenta, however, the factors $k_\mu t^\mu = \omega_{\mathbf{k}} - k^1$ and $k'_\nu t^\nu = \omega_{\mathbf{k}'} - k'^1$ in expression (6) vanish. Therefore, both for the massive and the massless field, the only contribution to T stems from the first term in expression (6) and is manifestly non-negative. This implies that the *averaged weak energy condition and the averaged strong energy condition are satisfied when one averages along any complete, null geodesic*.

Consider, next, a timelike geodesic. We may assume, again by Poincaré invariance of the field theory, that $x^\mu(\zeta) = \zeta t^\mu$, but now with $\vec{t} = \vec{e}_0$, i.e., $x^0 = \zeta$ and $x^i = 0$ for $i = 1, \dots, n-1$. For this geodesic,

$$\int_{-\infty}^{\infty} d\zeta u_{\mathbf{k}}^*(x(\zeta)) u_{\mathbf{k}'}(x(\zeta)) = \frac{1}{2(2\pi)^{n-2}\omega_{\mathbf{k}}} \delta(\omega_{\mathbf{k}} - \omega_{\mathbf{k}'}) = \frac{1}{2(2\pi)^{n-2}|\mathbf{k}|} \delta(|\mathbf{k}| - |\mathbf{k}'|), \quad (8)$$

whereas

$$\int_{-\infty}^{\infty} d\zeta u_{\mathbf{k}}(x(\zeta)) u_{\mathbf{k}'}(x(\zeta)) = \int_{-\infty}^{\infty} d\zeta u_{\mathbf{k}}^*(x(\zeta)) u_{\mathbf{k}'}^*(x(\zeta)) = \frac{1}{2(2\pi)^{n-2}\omega_{\mathbf{k}}} \delta(\omega_{\mathbf{k}} + \omega_{\mathbf{k}'}), \quad (9)$$

which we can consider zero. Hence, when substituting the field (5) into expression (4), we only need to retain terms proportional to $a_{\mathbf{k}}^\dagger a_{\mathbf{k}'}$, and we thereby obtain

$$T = \iint d^{n-1}\mathbf{k} d^{n-1}\mathbf{k}' \frac{\delta(|\mathbf{k}| - |\mathbf{k}'|)}{(2\pi)^{n-2}|\mathbf{k}|} [\omega_{\mathbf{k}}\omega_{\mathbf{k}'} + a k^\alpha k'_\alpha - (a + \frac{1}{2})m^2] a_{\mathbf{k}}^\dagger a_{\mathbf{k}'}$$

Using polar coordinates for the momenta, $\int d^{n-1}\mathbf{k} = \int_0^\infty k^{n-2} dk \int d\Omega$, where $k \equiv |\mathbf{k}|$, we can reexpress this as

$$\begin{aligned}
\mathcal{T} &= \int_0^\infty dk \frac{k^{2n-5}}{(2\pi)^{n-2}} \int d\Omega \int d\Omega' [\omega_{\mathbf{k}}^2 + a(\omega_{\mathbf{k}}^2 - \mathbf{k} \cdot \mathbf{k}') - (a + \frac{1}{2})m^2] a_{\mathbf{k}}^\dagger a_{\mathbf{k}'}, \\
&= \int_0^\infty dk \frac{k^{2n-5}}{(2\pi)^{n-2}} \left([\frac{1}{2}m^2 + (a+1)k^2] A_{\mathbf{k}}^\dagger A_{\mathbf{k}} - ak^2 \sum_{i=1}^{n-1} A_{\mathbf{k}}^{i\dagger} A_{\mathbf{k}}^i \right), \tag{10}
\end{aligned}$$

where

$$A_{\mathbf{k}} \equiv \int d\Omega a_{\mathbf{k}}, \quad A_{\mathbf{k}}^i \equiv k^{-1} \int d\Omega k^i a_{\mathbf{k}}$$

contain momenta of magnitude k only.

The operator (10) is manifestly non-negative as long as $a + 1 \geq 0$ and $-a \geq 0$, i.e. for

$$-1 \leq a \leq 0. \tag{11}$$

This is equivalent to

$$\begin{aligned}
\frac{n-4}{4(n-3)} \leq \xi \leq \frac{n}{n-3}, \quad n \geq 4, \\
-\infty < \xi < \infty, \quad n = 3, \\
-2 \leq \xi \leq \frac{1}{2}, \quad n = 2,
\end{aligned} \tag{12}$$

which includes conformal coupling $\xi = (n-2)/4(n-1)$ for all n and minimal coupling $\xi = 0$ for $n = 2, 3$, and 4. Thus, we conclude that *the averaged strong energy condition is satisfied when the average is taken along any complete, timelike geodesic and ξ lies in the range (13)*. For values of ξ outside the range (13), however, it is not difficult to construct states of the field such that the expectation value of \mathcal{T} is negative.

We would like to add that the value of the curvature coupling constant is also crucial for the weak energy condition averaged along any complete, timelike geodesic. By the same methods we have used above, one finds that for it to be satisfied the absolute value of ξ must not exceed $\frac{1}{4}$, regardless of the spacetime dimension. Minimal and conformal coupling are included in this range.

It is interesting to notice that the manipulations in this section remain valid if the field (5) is understood to be classical with the $a_{\mathbf{k}}$'s being complex expansion coefficients. Our observations about the sign of \mathcal{T} in expression (10) are not affected by this change of viewpoint, because the averaging of the operator $T_{\mu\nu}$ has removed from \mathcal{T} all terms that do not conserve particle number.

IV. NONGEODESIC CURVES AND CYLINDRICAL SPACETIMES

Does the validity of the averaged energy conditions depend on the geodesic nature of the curve of integration? As an example of nongeodesic curves, consider a piecewise straight null curve in two-dimensional Minkowski spacetime (coordinates x and t) that issues from past null infinity, runs in the positive x direction most of the time, has only one short segment running in the negative x direction, and extends to future null infinity. Let the field be massless and in a state where only right-moving modes have nonzero amplitudes to contain par-

ticles. Then the expectation value of the operator (6) will vanish everywhere along the right-going segments of the line, because there the tangent vector t^μ is in the same direction as the (null) momenta k^μ of the occupied modes. Hence, the only contribution to the expectation value of \mathcal{T} arises from the left-going segment of the curve and is determined by the local expectation value of the operator (6) if this segment is very short. However, that local value of the energy density is negative for an appropriately chosen state of the field, as was shown at the end of Sec. II. Thus, we see that *the averaged weak energy condition can be violated for nongeodesic, complete, null curves*, by contrast with null geodesics.

The averaged weak energy condition can also break down in spacetimes that are flat, but topologically nontrivial. Consider, as an example, a two-dimensional flat spacetime that is spatially closed along the x axis with circumference L . In this spacetime the field modes are periodic in x . It is a well-known result that when the field is in the vacuum state with respect to these modes, the renormalized energy density and pressure of the field are negative. More precisely,²⁸

$$\langle T_{tt} \rangle = \langle T_{xx} \rangle = -\pi/6L^2, \quad \langle T_{tx} \rangle = 0, \tag{13}$$

where the brackets denote expectation values with respect to that vacuum state and the field is taken to be massless and minimally coupled. From the expectation values (13) it follows that *the averaged weak energy condition is violated along every null geodesic in this cylindrical spacetime*.

V. CONCLUSION

We have seen that rather simple methods suffice to answer the question whether free scalar fields in flat spacetimes can violate averaged energy conditions. The answer found, when the spacetime topology is trivial, is mainly negative: If the averaging curves are complete, causal geodesics, violations cannot occur; though, in the case of timelike geodesics this answer requires certain restrictions, which do not seem worrisome, on the curvature coupling. For nontrivial topologies, however, violations can occur.

The easy success of this paper's initial study is strong motivation to push onward into more interesting situations: higher-spin fields in flat spacetime, and most especially, spacetimes with curvature. Analyses with sufficient generality to give insight into the validity of energy conditions in singularity theorems are likely to be very difficult. Less difficult, perhaps, will be studies that tackle the traversable wormhole problem. For example,

in static, spherical wormhole spacetimes, is the averaged weak energy condition enforced for radial null geodesics that thread the wormhole? If it is enforced, then such wormholes cannot exist. However, to be compelling, such a conclusion will require studies not only of free fields, but also of interacting fields—a formidable task.

The first steps in extending this paper's results to curved spacetimes have already been taken: Yurtsever²⁹ has proven the validity of the averaged weak energy condition for a massless, conformally coupled, free scalar field in any curved two-dimensional spacetime that meets certain asymptotic regularity requirements; and Wald and Yurtsever,³⁰ using algebraic quantum-field-theory techniques, can now even dispense with those regularity assumptions. Thus, we may hope to witness significant progress in the near future.

ACKNOWLEDGMENTS

Michael Morris and Ulvi Yurtsever have pursued many aspects of this work in parallel with the author, and he wishes to thank them for stimulating exchanges of ideas. He is also indebted to W. A. J. Luxemburg, David Politzer, and John Preskill for technical discussions. Finally, the author's special thanks go to Kip Thorne for advice about the presentation, an introduction into the history of energy conditions, and for general encouragement. This research was supported in part by the National Science Foundation, Grant No. AST 88-17792.

APPENDIX

Let \mathcal{V} be the set of all Fock-space state vectors that can be written as

$$|\psi\rangle = \sum_{j=0}^N |\psi_j\rangle, \quad (\text{A1})$$

$$\begin{aligned} \langle \psi_{j-2} | T_{\mu\nu} t^\mu t^\nu | \psi_j \rangle &= - \int d^{n-1} \mathbf{k} d^{n-1} \mathbf{k}' u_{\mathbf{k}} u_{\mathbf{k}'} \langle \psi_{j-2} | a_{\mathbf{k}} a_{\mathbf{k}'} | \psi_j \rangle \\ &= - \frac{j!}{2(2\pi)^{n-1}} \int_{\mathcal{K}^j} d\mu^{(j)} [(\omega_{\mathbf{k}_1} - k_1^1)(\omega_{\mathbf{k}_2} - k_2^1)(\omega_{\mathbf{k}_1} \omega_{\mathbf{k}_2})^{-1/2}] \exp[-i\zeta(\omega_{\mathbf{k}_1} - k_1^1 + \omega_{\mathbf{k}_2} - k_2^1)] \\ &\quad \times f^{(j-2)*}(\mathbf{k}_3, \dots, \mathbf{k}_j) f^{(j)}(\mathbf{k}_1, \dots, \mathbf{k}_j). \end{aligned} \quad (\text{A4})$$

In this integral, the factor in front of the exponential never becomes singular. Together with the integrability properties of the $f^{(n)}$'s this implies that the whole integrand is in $L^1[\mathcal{K}^j]$. Thus, the matrix element (A4) exists. The diagonal matrix elements can likewise be shown to exist. The finiteness of the sum (A3) then guarantees that the integrand in expression (A2) is nowhere singular (as was asserted in the first paragraph of Sec. III).

If we integrate the off-diagonal matrix element (A4) along a finite stretch of the geodesic, say, from $\zeta = -Z$ to $\zeta = Z$, we may interchange the order of integration, obtaining

$$- \frac{j!}{(2\pi)^{n-1}} \int_{\mathcal{K}^j} d\mu^{(j)} [(\omega_{\mathbf{k}_1} - k_1^1)(\omega_{\mathbf{k}_2} - k_2^1)(\omega_{\mathbf{k}_1} \omega_{\mathbf{k}_2})^{-1/2} (\omega_{\mathbf{k}_1} - k_1^1 + \omega_{\mathbf{k}_2} - k_2^1)^{-1}] \sin[Z(\omega_{\mathbf{k}_1} - k_1^1 + \omega_{\mathbf{k}_2} - k_2^1)] \times f^{(j-2)*}(\mathbf{k}_3, \dots, \mathbf{k}_j) f^{(j)}(\mathbf{k}_1, \dots, \mathbf{k}_j). \quad (\text{A5})$$

where

$$|\psi_j\rangle = \int_{\mathcal{K}^j} d\mu^{(j)} f^{(j)} a_{\mathbf{k}_1}^\dagger \dots a_{\mathbf{k}_j}^\dagger |0\rangle,$$

$$\mathcal{K}^j = \{(\mathbf{k}_1, \dots, \mathbf{k}_j) \mid \mathbf{k}_i \in R^{n-1}, |\mathbf{k}_i| \leq K\},$$

$$d\mu^{(j)} = d^{n-1} \mathbf{k}_1 \dots d^{n-1} \mathbf{k}_j,$$

$$f^{(j)} \in L^2[\mathcal{K}^j],$$

K and N are finite and depend on $|\psi\rangle$, $f^{(j)}$ is invariant under interchange of any two of its j vector arguments, and $|\psi_0\rangle$ is a multiple of the vacuum $|0\rangle$. \mathcal{V} is a dense subspace of Fock space, whose physical significance is discussed in the first paragraph of Sec. III. The results of that section can be proven rigorously when the expectation value of $T_{\mu\nu}$ is formed with respect to a state vector in \mathcal{V} . We will demonstrate this here for the case of the weak energy condition averaged along a null geodesic. The case of the strong energy condition averaged along a timelike geodesic can be treated in an analogous way.

In this appendix, then, we prove the non-negativity of

$$\int_{-\infty}^{\infty} d\zeta \langle \psi | T_{\mu\nu}(x(\zeta)) t^\mu t^\nu | \psi \rangle, \quad (\text{A2})$$

where the geodesic $x(\zeta)$ is as in Sec. III and $|\psi\rangle$ has the form (A1) with unit norm. Since $T_{\mu\nu}$ is quadratic in the creation and annihilation operators, the integrand in expression (A2) can be expanded as

$$\sum_j \langle \psi_j | T_{\mu\nu} t^\mu t^\nu | \psi_j \rangle + \sum_{|j-k|=2} \langle \psi_j | T_{\mu\nu} t^\mu t^\nu | \psi_k \rangle. \quad (\text{A3})$$

Here a typical off-diagonal element has the form [see Eq. (6)]

The first factor in the integrand is again nonsingular, and so the whole integrand without the sine is in $L^1[\mathcal{K}^j]$. To infer the vanishing of the expression (A5) in the limit $Z \rightarrow \infty$, we could immediately apply to the Riemann-Lebesgue lemma of Fourier analysis if the argument of the sine were linear in the momenta k_i . A simple coordinate transformation, $k_1^1 \mapsto \omega_{k_1} - k_1^1$ and $k_2^1 \mapsto \omega_{k_2} - k_2^1$, however, produces such linearity, and we thus conclude that the off-diagonal elements do not contribute to the integral (A2). The validity of the averaged weak energy condition now follows from the fact that the diagonal elements in the sum (A3) cannot be negative (see Sec. III).

-
- ¹See, e.g., the discussion in Secs. 6.11 and 6.12 of Ya. B. Zel'dovich and I. D. Novikov, *Relativistic Astrophysics, Vol. 1: Stars and Relativity* (University of Chicago Press, Chicago, 1971).
- ²Ya. B. Zel'dovich, *Zh. Eksp. Teor. Fiz.* **41**, 1609 (1961) [*Sov. Phys. JETP* **14**, 1143 (1962)].
- ³See Figs. 4 and 7 in W. D. Arnett and R. L. Bowers, *Astrophys. J. Suppl. Ser.* **33**, 415 (1977).
- ⁴R. Penrose, *Phys. Rev. Lett.* **14**, 57 (1965).
- ⁵S. W. Hawking, *Proc. R. Soc. London A* **300**, 182 (1967).
- ⁶S. W. Hawking and G. F. R. Ellis, *The Large Scale Structure of Space-Time* (Cambridge University Press, Cambridge, England, 1973).
- ⁷H. Epstein, V. Glaser, and A. Jaffe, *Nuovo Cimento* **36**, 1016 (1965).
- ⁸Ya. B. Zel'dovich and L. P. Pitaevsky, *Commun. Math. Phys.* **23**, 185 (1971).
- ⁹H. B. G. Casimir, *Proc. K. Ned. Akad. Wet.* **51**, 793 (1948).
- ¹⁰L. S. Brown and G. J. Maclay, *Phys. Rev.* **184**, 1272 (1969).
- ¹¹P. C. W. Davies and S. A. Fulling, *Proc. R. Soc. London A* **356**, 237 (1977). It seems to us that the Appendix to this paper contains the first reference in the literature to that very simple example of a violation of the weak energy condition.
- ¹²S. A. Fulling and P. C. W. Davies, *Proc. R. Soc. London A* **348**, 393 (1976).
- ¹³S. M. Wagh and N. Dadhich, *Phys. Rev. D* **32**, 1863 (1985).
- ¹⁴B. Rose, *Class. Quantum Grav.* **3**, 975 (1986); **4**, 1019 (1987).
- ¹⁵Unpublished work by S. Braunstein, described by M. Morris and K. S. Thorne, *Am. J. Phys.* **56**, 395 (1988).
- ¹⁶See, e.g., L.-A. Wu, H. J. Kimble, J. L. Hall, and H. Wu, *Phys. Rev. Lett.* **57**, 2520 (1986).
- ¹⁷See, e.g., L. Parker and S. A. Fulling, *Phys. Rev. D* **7**, 2357 (1973); or, more recently, S. Gottlober, *Ann. Phys. (Leipzig)* **45**, 452 (1988).
- ¹⁸F. J. Tipler, *Phys. Rev. D* **17**, 2521 (1978).
- ¹⁹A. Borde, *Class. Quantum Grav.* **4**, 343 (1987).
- ²⁰T. A. Roman, *Phys. Rev. D* **33**, 3526 (1986); **37**, 546 (1988).
- ²¹M. S. Morris, K. S. Thorne, and U. Yurtsever, *Phys. Rev. Lett.* **61**, 1446 (1988).
- ²²V. P. Frolov and I. D. Novikov, *Phys. Rev. D* **42**, 1057 (1990); see also I. D. Novikov, *Zh. Eksp. Teor. Fiz.* **95**, 769 (1989) [*Sov. Phys. JETP* **68**, 439 (1989)].
- ²³S.-W. Kim and K. S. Thorne, *Phys. Rev. D* (to be published).
- ²⁴L. H. Ford, *Proc. R. Soc. London A* **364**, 227 (1978).
- ²⁵L. H. Ford (in preparation).
- ²⁶See, e.g., F. Mandl and G. Shaw, *Quantum Field Theory* (Wiley, Chichester, 1984).
- ²⁷Fulling [S. A. Fulling, *Aspects of Quantum Field Theory in Curved Space-Time* (Cambridge University Press, Cambridge, England, 1989)] has criticized attributing Casimir-type stress-energy tensors to spacetime topology. Rather, he argues, they are related to boundary conditions. We shall not belabor the point here. Throughout this paper we follow widespread usage, referring to Casimir-type effects as topological.
- ²⁸N. D. Birrell and P. C. W. Davies, *Quantum Fields in Curved Space* (Cambridge University Press, Cambridge, England, 1982).
- ²⁹U. Yurtsever, *Class. Quantum Grav.* **7**, L251 (1990).
- ³⁰R. M. Wald and U. Yurtsever (unpublished).

Addendum to Chapter 2

In this addendum we shall make two further observations about the stress-energy tensor of quantum fields in four-dimensional Minkowski spacetime. First, we show that the stress-energy tensor of the electromagnetic field, like the one of a scalar field, satisfies the weak energy condition averaged along a complete null geodesic. This result was recently proven by Folacci [1], using point-splitting renormalization. We shall rederive it here with much simpler means: renormalization by normal ordering, and the Gupta–Bleuler formalism for gauge fields [2]. Second, we demonstrate that the stress-energy tensor of a spin-1/2 field can violate the local weak energy condition. Whereas, in the case of a scalar field, such a violation requires the field to be in a superposition of states of different particle number, we show that a massive Dirac spinor can violate the local weak energy condition in an eigenstate of particle number. We retain the conventions of the main part of Chapter II here.

The stress-energy tensor of the electromagnetic field is given by

$$T_{\mu\nu} = \frac{1}{4}\eta_{\mu\nu}F^{\alpha\beta}F_{\alpha\beta} - F_{\mu}{}^{\alpha}F_{\nu\alpha}, \quad (2.1)$$

where $F_{\mu\nu} = A_{\mu,\nu} - A_{\nu,\mu}$. In computing the integral $\int_{-\infty}^{\infty} d\zeta \langle T_{\mu\nu} \rangle t^{\mu}t^{\nu}$, we take the null geodesic to be given by $x^{\mu}(\zeta) = \zeta t^{\mu}$, where $\vec{t} = \vec{e}_0 + \vec{e}_1$. We then have

$$T_{\mu\nu}t^{\mu}t^{\nu} = (F_{20} + F_{21})^2 + (F_{30} + F_{31})^2. \quad (2.2)$$

We insert the vector potential

$$A^{\mu} = \int d^3\mathbf{k} \sum_{\alpha=0}^3 (u_{\mathbf{k}}\epsilon_{\mathbf{k}\alpha}^{\mu} a_{\mathbf{k}\alpha} + \text{h.c.}), \quad (2.3)$$

where $u_{\mathbf{k}} = [2(2\pi)^3|\mathbf{k}|]^{-1/2} \exp(-ik_{\mu}x^{\mu})$, the $\vec{\epsilon}_{\mathbf{k}\alpha}$ are polarization vectors with $\eta_{\mu\nu}\epsilon_{\mathbf{k}\alpha}^{\mu}\epsilon_{\mathbf{k}\beta}^{\nu} = \eta_{\alpha\beta}$, and the $a_{\mathbf{k}\alpha}$ are annihilation operators. The first squared term in (2.2) then equals, after normal ordering,

$$2T^{\dagger}T - T^2 - T^{\dagger 2}, \quad (2.4)$$

where

$$T = \int d^3\mathbf{k} \sum_{\alpha=0}^3 u_{\mathbf{k}} a_{\mathbf{k}\alpha} (f_{20}(\mathbf{k}, \alpha) + f_{21}(\mathbf{k}, \alpha)) \quad (2.5)$$

with

$$f^{\mu\nu}(\mathbf{k}, \alpha) = \epsilon_{\mathbf{k}\alpha}^{\mu} k^{\nu} - \epsilon_{\mathbf{k}\alpha}^{\nu} k^{\mu}. \quad (2.6)$$

When the integration along the geodesic is carried out, delta functions appear in T^2 and $T^{\dagger 2}$ which select photon momenta of the form $k^{\mu} = |\mathbf{k}|t^{\mu}$. For such momenta, the last factor in (2.5), $\epsilon_2 k_0 - \epsilon_0 k_2 + \epsilon_2 k_1 - \epsilon_1 k_2$, vanishes identically (we have dropped the label $\mathbf{k}\alpha$ from the polarization vectors), and therefore the integral of $-T^2 - T^{\dagger 2}$ along the geodesic vanishes also. To make this delta-function argument rigorous we could proceed in the same way as in the main part of Chapter II, where we treat the scalar field. The product $T^{\dagger}T$ will produce nonnegative expectation values even before integration along the geodesic if we remove all negative-norm states by applying the Gupta-Bleuler procedure. The second term in (2.5) can, of course, be treated in the same way as the first, and so we find the averaged null energy condition to be satisfied for the electromagnetic field in Minkowski spacetime.

The plane-wave decomposition for a massive Dirac spinor reads [2]

$$\psi = \sum_{r=1}^2 \int d^3\mathbf{k} \left(\frac{m}{(2\pi)^3 \omega_{\mathbf{k}}} \right)^{1/2} (u_{r\mathbf{k}} e^{-ik_{\mu}x^{\mu}} c_{r\mathbf{k}} + v_{r\mathbf{k}} e^{ik_{\mu}x^{\mu}} d_{r\mathbf{k}}^{\dagger}). \quad (2.7)$$

Here, the $u_{r\mathbf{k}}$ and $v_{r\mathbf{k}}$ are positive-energy and negative-energy four-spinors, respectively. The operator $c_{r\mathbf{k}}$ destroys a particle, whereas the operator $d_{r\mathbf{k}}^{\dagger}$ creates an antiparticle. The stress-energy tensor is given by

$$T_{\mu\nu} = \frac{i}{2} (\bar{\psi} \gamma_{(\mu} \psi_{,\nu)} - \bar{\psi}_{,(\mu} \gamma_{\nu)} \psi), \quad (2.8)$$

where $\bar{\psi} = \psi^{\dagger} \gamma^0$, and the gamma matrices satisfy $\{\gamma^{\mu}, \gamma^{\nu}\} = 2\eta^{\mu\nu}$. We renormalize the stress-energy tensor by normal ordering, i.e., by taking all anticommutators to vanish. It is clear from (2.7) and (2.8) that if we form the expectation value of T_{00} with respect to a state that contains no antiparticles only one term will contribute:

$$\frac{m}{2(2\pi)^3} \sum_{r,r'} \int \int d^3\mathbf{k} d^3\mathbf{k}' \frac{(\omega_{\mathbf{k}} + \omega_{\mathbf{k}'})}{(\omega_{\mathbf{k}} \omega_{\mathbf{k}'})^{1/2}} u_{r\mathbf{k}}^{\dagger} u_{r'\mathbf{k}'} e^{i(k_{\mu} - k'_{\mu})x^{\mu}} c_{r\mathbf{k}}^{\dagger} c_{r'\mathbf{k}'}. \quad (2.9)$$

This expression does not factorize into an operator and its hermitian conjugate. Indeed, we can construct states in which the expectation value of T_{00} is negative at a given spacetime point. Let the spinors be normalized so that $u_{\mathbf{r}\mathbf{k}}^\dagger u_{\mathbf{r}\mathbf{k}} = \omega_{\mathbf{k}}/m$. If $\mathbf{k} = k\mathbf{e}_3$, then, in the Dirac–Pauli representation,

$$u_{1\mathbf{k}} = [2m(\omega_{\mathbf{k}} + m)]^{-1/2} \begin{pmatrix} \omega_{\mathbf{k}} + m \\ 0 \\ k \\ 0 \end{pmatrix}. \quad (2.10)$$

Choose a state of the form

$$|\psi\rangle = 5^{-1/2}(2c_{1\mathbf{k}_1}^\dagger - c_{1\mathbf{k}_2}^\dagger)|0\rangle, \quad (2.11)$$

with $\mathbf{k}_1 = k_1\mathbf{e}_3$ and $\mathbf{k}_2 = \lambda\mathbf{k}_1$, where $\lambda > 1$. If $k_1 \gg m$ we find, after a bit of algebra,

$$\langle T_{00}(x=0) \rangle_\psi \approx \frac{|k_1|}{5(2\pi)^3}(2 - \lambda), \quad (2.12)$$

which can obviously be made negative. Since we have used a one-particle state in this calculation, the result will hold equally well if the Dirac field is regarded as a classical field, with the $c_{\mathbf{r}\mathbf{k}}$ playing the role of expansion coefficients. As has been noted elsewhere [3], the failure of the Dirac field, if treated classically, to satisfy energy conditions is related to the fact that the exclusion principle forces one to regard half-odd-integer-spin fields as quantum fields in any case.

Acknowledgments

We thank Eanna Flanagan for a stimulating discussion of the second item in this addendum.

Bibliography

- [1] A. Folacci, Phys. Rev. D (to be published).
- [2] See, e.g., F. Mandl and G. Shaw, *Quantum Field Theory* (John Wiley & Sons, Chichester, 1984).
- [3] See, e.g., the corresponding remark on page 368 of of R. Penrose and W. Rindler, *Spinors and space-time, Volume I: Two-spinor calculus and relativistic fields* (Cambridge University Press, Cambridge, England, 1984).

Chapter 3

Vacuum polarization of scalar and
spinor fields near closed null geodesics

Abstract

Hawking has recently proposed a “chronology protection conjecture”, which states that closed timelike curves cannot form in the real Universe. The most likely mechanism for enforcing this conjecture, if it is correct, is a divergent vacuum polarization at the Cauchy horizon (“chronology horizon”) where closed timelike curves first try to form. Hawking has proved that, if the chronology horizon is compactly generated, then it contains one or more smoothly closed null geodesics. Because it seems likely that all the horizon’s generators emerge from these closed null geodesics, a sufficiently strongly divergent vacuum polarization at the closed null geodesics is likely to destroy the chronology horizon completely and thereby prevent closed timelike curves from forming. In this paper we compute the details of the divergence near the closed null geodesics, in a *generic* spacetime with a compactly generated chronology horizon — thereby generalizing earlier computations, in special spacetimes, by Hiscock and Konkowski, Kim and Thorne, and Frolov. We carry out the computation for both a conformal scalar field and a two-component spinor field. We show that for an observer who will pass through a point on the closed null geodesic after a small interval of proper time δt , the leading-order divergence is always proportional to $(\delta t)^{-3}$ and has the same tensorial structure as the stress-energy of a null fluid moving along the closed null geodesic. We also show that, by contrast with flat spacetime, there is in general no cancellation between the divergent vacuum energies of a combination of fields that, in flat spacetime, would be related by supersymmetry: two conformal scalar fields and one two-component spinor field. We discuss the implications of these results for Hawking’s chronology protection conjecture.

1 Introduction and summary

An effort has been made, over the last few years, to investigate the attitude of twentieth-century physics towards the notion of “backward time travel.” This investigation rests on two pillars: general relativity and quantum field theory. General relativity’s geometric approach towards space and time allows a “time machine” to be conceptualized in terms of closed timelike curves on a Lorentzian manifold. Quantum field theory is needed to determine whether there is a stable semiclassical solution of Einstein’s equations in which quantum matter sustains a classical spacetime with closed timelike curves. Quantum field theory should also tell us whether a sensible initial-value problem can be formulated for matter propagating on the background of such a spacetime [1].

The effort described above was sparked when Morris, Thorne, and Yurtsever realized that accelerated relative motion of the mouths of a traversable macroscopic wormhole creates closed timelike curves [2]. Morris and Thorne had found earlier that the matter sustaining a traversable wormhole has to violate an averaged version of the weak energy condition [3]. Since then, some research has been devoted to averaged energy conditions [4], but it is not yet clear whether a spacetime with a macroscopic wormhole can be a solution of the semiclassical theory. However, Gott [5] has recently found a spacetime in which the relative motion of two infinite cosmic strings results in closed timelike curves. These strings do not violate classical energy conditions.

In the spacetime of Morris et al., and also in that of Gott, closed timelike curves are not present everywhere. A Cauchy horizon separates the spacetime region with closed timelike curves from the one without. Following a suggestion of Hawking’s, we shall call such a Cauchy horizon a “chronology horizon.” Geometric considerations suggest quite generally that the stress-energy tensor of any field propagating through the region without closed timelike curves might diverge as the field approaches the chronology horizon. Morris et al. found that the defocusing

effect of the wormhole can prevent *classical* fields from developing such a divergence [2]. Later, however, several researchers independently realized that the stress-energy tensor of a scalar *quantum* field will always diverge as one approaches any event that is connected to itself by a null geodesic [6]; and Kim and Thorne then showed that all events on any chronology horizon are limit points of a sequence of such self-connected events, and therefore the vacuum polarization must diverge everywhere on any chronology horizon [7]. Kim and Thorne went on to compute the details of that divergence for a chronology horizon produced by the relative motion of two wormhole mouths, and Frolov computed the details for a chronology horizon produced by a difference in gravitational redshift between two wormhole mouths [8], and very recently, Grant has computed the details of the divergence for scalar field in Gott's spacetime [9].

Whether a divergent vacuum polarization at the chronology horizon, via its back-reaction on the spacetime geometry, would actually alter the causal structure drastically and prevent closed timelike curves altogether, is still controversial. Because the divergence only becomes appreciable in a tiny neighborhood of the chronology horizon, its influence on the spacetime metric has to be compared to the fluctuations that quantum gravity is likely to predict for spacetime geometry on very small scales [7]. Hawking has formulated a "chronology protection conjecture" according to which the laws of physics do not allow the appearance of closed timelike curves [10]. He views divergent vacuum polarization as a likely means by which Nature will enforce this rule. Indeed, the divergent vacuum polarization of quantum fields is the only mechanism known so far that has the potential to prevent the creation of closed timelike curves in every spacetime which would otherwise produce them [7].

In his discussion of the chronology protection conjecture, Hawking concentrates on spacetimes that possess what he calls "compactly generated" chronology horizons. All past directed null geodesic generators of such a chronology horizon enter and remain within a compact set. As he points out, the formulation of a Cauchy

problem for fields propagating on a spacetime that develops closed timelike curves will be more promising if the chronology horizon is compactly generated than if it is not. He goes on to show that if the region with closed timelike curves develops from a non-compact spacelike hypersurface and the chronology horizon is compactly generated then the weak energy condition must be violated. He adds that if the initial hypersurface is compact then a compactly generated chronology horizon can form without a violation of the weak energy condition, but such a horizon will be unstable if any matter passes through it. Therefore, in generic cases, a compactly generated chronology horizon requires a violation of the weak energy condition, whether or not the initial hypersurface is non-compact. As a corollary he concludes that one cannot create closed timelike curves by moving finite loops of cosmic string within a finite region of spacetime. Gott's spacetime, with its infinite cosmic strings, by contrast, has a non-compactly generated chronology horizon and therefore manages to create closed timelike curves without violating the weak energy condition. The various wormhole spacetimes mentioned above do have compactly generated chronology horizons.

A compactly generated chronology horizon contains, Hawking proves, at least one closed null geodesic. After going around such a geodesic once, the direction of its tangent vector has been reproduced, whereas the length of the tangent vector has been boosted by some factor e^h . It seems likely that in generic cases, all the generators of the chronology horizon, when followed to the past, will asymptote to such closed null geodesics [11]. If this is true, then the divergent vacuum polarization near these closed null geodesics will be of particular importance for the chronology protection conjecture: the divergence, if sufficiently strong, will be likely to destroy the entire chronology horizon and thus prevent closed timelike curves from forming.

In this paper we elaborate two remarks that Hawking makes about divergent vacuum polarization at compactly generated chronology horizons. The first remark is that the result one finds for the divergent stress-energy tensor of a quantum

field near a closed null geodesic must always have the same form, regardless of the spacetime and the quantum state of the field. In Sec. 2, we compute the expectation value of the stress-energy tensor of a conformal scalar field near a point X that lies on a closed null geodesic γ in an arbitrary spacetime with a compactly generated chronology horizon. We show that in the reference frame of an observer who will pass through X after a small interval of proper time δt the leading-order divergence of the stress-energy tensor will always be proportional to $(\delta t)^{-3}$, and the tensorial structure of this leading-order term will be the same as for a null fluid that moves along γ . We also find that the dependence of this term on the boost parameter h always has the same form. Our results in Sec. 2 include as special cases the results of Kim and Thorne and of Frolov.

Hawking's second remark is that one would not expect a cancellation of the divergent stress-energy tensor between fields of different spins, or at least not when the boost parameter h is nonzero. A cancellation of the vacuum energies does occur between fields related by supersymmetry in Minkowski spacetime [12]. However, collections of fields of various spins on a curved classical background cannot be constructed as supersymmetric theories unless the background admits a covariantly constant spinor field [13], and in a spacetime with a compactly generated chronology horizon, a spinor field cannot be covariantly constant along the closed null geodesic if $h \neq 0$. This was the basis for Hawking's remark. To show explicitly that a cancellation of the vacuum polarization does not occur, we compute, in Sec. 3, the expectation value of the stress-energy tensor of a two-component (Weyl) spinor field near the closed null geodesic γ . The degree of divergence, $(\delta t)^{-3}$, and the tensorial structure, that of a null fluid, are found to be the same as in the case of a scalar field. The dependence on the boost parameter h , however, is different. Moreover, the spinor stress-energy tensor, unlike its scalar counterpart, also depends on the angle θ through which a spatial plane orthogonal to the tangent vector of γ is rotated by parallel transport from X to X along γ . A cancellation of the vacuum energies between two conformal scalar fields and one spinor field, as

is known to happen in the supersymmetric case in Minkowski spacetime, is shown to be impossible unless $h = \theta = 0$.

In Sec. 4 we compare our results to those of others and discuss their relevance for the chronology protection conjecture.

We shall use the metric signature $(-+++)$ and natural units ($G = c = 1$) throughout.

2 Scalar fields

We consider an arbitrary spacetime M with a compactly generated chronology horizon and a closed null geodesic γ on this horizon. All steps of our analysis depend only on the fact that γ causally links a spacetime point X to itself in a non-trivial way, i.e., γ encompasses other spacetime points than X . Nevertheless, for ease of presentation, we shall pretend that γ cannot be continuously deformed to a trivial curve. Thus, M becomes multiply connected, with a universal covering space \tilde{M} . (We can always make M multiply connected by excising from it an appropriately chosen curve that γ loops around.) Since we are only concerned with γ and nearby curves, we may assume that the fundamental group of M has only one generator, and we may take γ to represent this generator. The copies of M in \tilde{M} , called the “fundamental domains”, can be labeled by the integers. Accordingly, the copies in \tilde{M} of a point X' in M shall be denoted by X'_n , where n ranges through the integers.

Our calculation of the vacuum polarization of a conformally coupled massless scalar field ϕ in M shall be based on the Hadamard function $G^1(X, X') = \langle \phi(X)\phi(X') + \phi(X')\phi(X) \rangle$, where the expectation value is defined with respect to a suitably defined vacuum state. The region before the chronology horizon does not contain closed timelike curves, and so the definition of a vacuum state and the computation of vacuum stress-energy in this region can proceed in the familiar way. The Hadamard function G^1 , defined in M , can be represented in terms of

the analogous Hadamard function \tilde{G}^1 in \tilde{M} . For an untwisted field the relation is simple:

$$G^1(X, X') = \sum_{n=-\infty}^{\infty} \tilde{G}^1(X_0, X'_n). \quad (3.1)$$

We shall assume that \tilde{G}^1 has the familiar singularity structure:

$$\tilde{G}^1(X, X') = \frac{\Delta^{1/2}}{4\pi^2} \left[\frac{1}{\sigma} + O(\ln |\sigma|) \right], \quad (3.2)$$

where $\sigma(X, X')$ is the geodetic interval between X and X' , and $\Delta(X, X')$ is the Van Vleck–Morette determinant, which remains regular as σ goes to zero.

The expectation value of the stress-energy tensor $\langle T_{ab} \rangle$ is obtained by applying to G^1 a differential operator D_{ab} which is derived from the classical formula for T_{ab} and by then taking the coincidence limit $X' \rightarrow X$. For a conformally coupled massless scalar field we can take D_{ab} to be

$$\begin{aligned} D_{ab} = & \frac{1}{6}(\nabla_{a'}\nabla_b + \nabla_a\nabla_{b'}) - \frac{1}{12}g_{ab}\nabla_c\nabla^{c'} - \frac{1}{12}(\nabla_a\nabla_b + \nabla_{a'}\nabla_{b'}) \\ & + \frac{1}{48}g_{ab}(\nabla_c\nabla^c + \nabla_{c'}\nabla^{c'}) - R_{ab} + \frac{1}{4}g_{ab}R, \end{aligned} \quad (3.3)$$

where R_{ab} is the Ricci tensor. To renormalize the otherwise singular expression for $\langle T_{ab} \rangle$, a subtraction is made from G^1 before D_{ab} is applied. Because the standard renormalization prescription is concerned with the short-distance behavior of G^1 , the subtracted term equals, up to a piece that will not diverge for null separation of X and X' , the $n = 0$ term in (3.1), i.e., the term in which the copies of X and X' in \tilde{M} lie in the same fundamental domain. Thus, we have, up to a non-divergent term,

$$\langle T_{ab}(X) \rangle = \lim_{X' \rightarrow X} \sum_{n \neq 0} D_{ab} \tilde{G}^1(X_0, X'_n). \quad (3.4)$$

It is immediately clear from (3.2) and (3.4) that $\langle T_{ab}(X) \rangle$ will diverge when X lies on γ because the geodetic interval vanishes when taken along a null geodesic [6]. This divergence is not taken care of by standard renormalization, because it is linked to a global feature of M , namely the fact that there is a closed null geodesic.

Obviously, the divergent vacuum polarization at a point X on γ will have contributions for all non-zero winding numbers n . In what follows, we shall drop

the primes from the X'_n in (3.4) because it is the coincidence limit $X' \rightarrow X$ that we are interested in. Dropping these primes will create no confusion about how the operator D_{ab} is to be applied because the term with $n = 0$ is not included in (3.4). We shall label the points X_n so that, for positive n , going along the null geodesic from X_0 to X_n in \tilde{M} corresponds, in M , to going n times around γ in the future direction. This will boost the tangent vector of γ by a factor of e^{nh} , and Hawking shows that h cannot be negative. In \tilde{M} , the gradients of $\sigma(X_0, X_n)$ at X_0 and X_n are directly related to the tangent vectors of the null geodesic at these points. These gradients can therefore be expressed in terms of the initial tangent vector k^a of γ at X . Let k^a be normalized so that $k^a u_a = -1$, where u^a is the four-velocity of an observer who passes through X . Further, let ζ be an affine parameter for γ such that $k^a = dX^a/d\zeta$, and let ζ_n be the total affine parameter distance for going n times around γ . Then we have

$$\nabla_a \sigma = -\zeta_n k_a, \quad \nabla_{a'} \sigma = e^{nh} \zeta_n k_a, \quad (3.5)$$

where unprimed indices refer to X_0 and primed ones refer to X_n . If the observer will pass through X only after a small interval of proper time δt , then his current spacetime position is connected to itself by a closed spacelike geodesic that is nearly null. The geodetic interval for going n times around this geodesic will be, to linear order in δt ,

$$\sigma = -u^a (\nabla_a \sigma + \nabla_{a'} \sigma) \delta t = \zeta_n (e^{nh} - 1) \delta t. \quad (3.6)$$

By combining (3.2), (3.3), (3.5), and (3.6), we find the contribution to (3.4) with a given winding number n :

$$-\frac{\Delta_n^{1/2}}{24\pi^2 \zeta_n (\delta t)^3} \frac{1 + 4e^{nh} + e^{2nh}}{(e^{nh} - 1)^3} k_a k_b + O((\delta t)^{-2}), \quad (3.7)$$

where Δ_n is the Van Vleck–Morette determinant associated with the null geodesic from X_0 to X_n .

It is not hard to see what happens to the leading term in (3.7) when one switches the sign of n , i.e., when one switches from n circuits around γ in the

future direction to n circuits in the past direction. We can write this term as

$$-\frac{\Delta_n^{1/2}}{24\pi^2\sigma(\delta t)^2} \frac{1 + 4e^{nh} + e^{2nh}}{(e^{nh} - 1)^2} k_a k_b.$$

The geodetic interval σ is, of course, not affected by a switch of direction. Neither is, in fact, the Van Vleck–Morette determinant. The rational function of e^h appearing in the last expression is also invariant when one changes the sign of n . Taking all this into account, we find, not surprisingly, that the contribution to (3.4) with winding number $-n$ is the same as the one with winding number n . Therefore, we can write

$$\langle T_{ab} \rangle = -\frac{1}{12\pi^2(\delta t)^3} \left[\sum_{n=1}^{\infty} \frac{\Delta_n^{1/2}}{\zeta_n} \frac{1 + 4e^{nh} + e^{2nh}}{(e^{nh} - 1)^3} \right] k_a k_b + O((\delta t)^{-2}). \quad (3.8)$$

Thus, the leading-order divergence of the scalar vacuum polarization near γ is proportional to $(\delta t)^{-3}$ and has the tensorial structure of the stress-energy of a null fluid moving along γ . In general, there will be additional divergent terms that diverge as lower powers of $(\delta t)^{-1}$ and have a more complicated tensorial structure.

The details of the spacetime geometry around γ leave their imprint on the form of the leading-order term in (3.8) only in a very restricted way: through the boost parameter h and through the winding-number-dependent factors $\Delta_n^{1/2}/\zeta_n$. To understand how the latter scale with n , we turn to the analysis of Kim and Thorne [7]. They show that $\Delta_n^{1/2}/\zeta_n \equiv \Delta^{1/2}(X_0, X_n)/\zeta_n$ can be constructed in the following way: Consider a high-frequency classical scalar wave emitted at X_0 . Normalize the wave so that in the vicinity of X_0 its amplitude equals $1/\zeta$. Propagate the wave along the null geodesic from X_0 to X_n , using geometrical optics. Then $\Delta^{1/2}(X_0, X_n)/\zeta_n$ will equal the amplitude of the wave at X_n . Without spacetime curvature $\Delta_n^{1/2}/\zeta_n$ would simply equal $1/\zeta_n$. However, this would imply that classical fields diverge at the chronology horizon [2]. Hence, we should assume that spacetime curvature will exert a defocusing effect that drives the wave amplitude down more strongly. This defocusing effect (which results from a violation of the weak energy condition), after one circuit around γ , will be characterized by an

effective focal length. Once the wave has traveled around γ enough times that the radius of curvature of the wave fronts is much larger than this focal length, the wave will interact with the spacetime curvature in essentially the same way every additional time it goes around γ . The amplitude reduction due to curvature with each trip around γ will then be expressed by some factor $\alpha < 1$, which is independent of n and of the location of X on γ , i.e., we will have

$$\frac{\Delta_{n+1}^{1/2}/\zeta_{n+1}}{\Delta_n^{1/2}/\zeta_n} = \alpha.$$

We see now from (3.8) that the contributions to the $(\delta t)^{-3}$ divergence of the vacuum polarization will be proportional to

$$\alpha^n e^{-nh}$$

for sufficiently large n . Clearly, the contributions from high winding numbers are suppressed and the series appearing in (3.8) is convergent.

3 Spin-1/2 fields

To find the vacuum polarization of a spinor field, we shall develop a computational technique that is very similar to the one used in the preceding section. Our treatment largely follows Christensen's well-known work [14]. Some modifications are needed, though, because his presentation refers to a neutral Dirac spinor, i.e., a real four-component spinor, whereas we consider a complex two-component (Weyl) spinor. In dealing with Weyl spinors, we shall use the definitions found in the appendix of Ref. [15], which are suited to our choice of the metric signature. The complex conjugate of the spinor ψ^α will be denoted by $\bar{\psi}^{\dot{\alpha}}$. Spinor indices can be lowered with the antisymmetric tensor: $\psi_\alpha = \varepsilon_{\alpha\beta}\psi^\beta$. In a given local Lorentz frame, sigma matrices can be used to relate spacetime indices to spinor indices. We employ the matrices $\sigma^0 = \bar{\sigma}^0$, being equal to minus the identity, and $\sigma^i = -\bar{\sigma}^i$, $i = 1, 2, 3$, being equal to the familiar Pauli matrices. Their spin-index structure is given by $\sigma_{\alpha\dot{\alpha}}$ and $\bar{\sigma}^{\dot{\alpha}\alpha}$.

The stress-energy tensor of a Weyl spinor field is

$$T^{ab} = \frac{i}{2} \sigma_{\alpha\dot{\alpha}}^{(a} [\bar{\psi}^{\dot{\alpha}} \nabla^{b)} \psi^{\alpha} - (\nabla^{b)} \bar{\psi}^{\dot{\alpha}}] \psi^{\alpha}. \quad (3.9)$$

Noting that ψ is an anticommuting field, we can write the expectation value of (3.9) as the following coincidence limit:

$$\langle T^{ab}(X) \rangle = \lim_{X' \rightarrow X} \frac{i}{4} \sigma_{\alpha\dot{\alpha}}^{(a} (\nabla^{b')} - \nabla^{b'}) S^{\dot{\alpha}\alpha'}(X, X'), \quad (3.10)$$

where the bispinor

$$S^{\dot{\alpha}\alpha'}(X, X') = \langle [\bar{\psi}^{\dot{\alpha}}(X), \psi^{\alpha'}(X')] \rangle$$

is the expectation value of the field commutator. S is related to a Hadamard-type Green's function, \mathcal{G}^1 [16]:

$$S^{\dot{\alpha}\alpha'}(X, X') = -i \bar{\sigma}_c^{\dot{\alpha}\beta} \nabla^c \mathcal{G}_{\beta}^{1\alpha'}(X, X'). \quad (3.11)$$

Substituting this in (3.10), we find

$$\langle T^{ab}(X) \rangle = \lim_{X' \rightarrow X} \frac{1}{4} \sigma_{\alpha\dot{\alpha}}^{(a} \bar{\sigma}_c^{\dot{\alpha}\beta} (\nabla^{b')} - \nabla^{b'}) \nabla^c \mathcal{G}_{\beta}^{1\alpha'}(X, X'). \quad (3.12)$$

In both (3.10) and (3.12) a summation over the index pair α, α' is understood. Strictly speaking, a bispinor of parallel transport should be inserted so that this index pair refers to the same spacetime point. However, this bispinor becomes the unit matrix in the coincidence limit $X' \rightarrow X$.

The Green's function \mathcal{G}^1 can be related to the corresponding Green's function $\tilde{\mathcal{G}}^1$ in \tilde{M} . Again we assume an untwisted field, and a formula just like (3.1) will hold:

$$\mathcal{G}^1(X, X') = \sum_{n=-\infty}^{\infty} \tilde{\mathcal{G}}^1(X_0, X'_n). \quad (3.13)$$

$\tilde{\mathcal{G}}^1$ has a singularity structure analogous to (3.2):

$$\tilde{\mathcal{G}}^1(X, X') = \frac{\Delta^{1/2}}{4\pi^2} \left[\frac{1}{\sigma} \mathcal{I} + O(\ln |\sigma|) \right], \quad (3.14)$$

where $\mathcal{I}_{\beta}^{\alpha'}$ describes the parallel transport of a spinor of the type ψ^{β} from X to X' (or, equivalently, of a spinor of the type $\psi_{\alpha'}$ from X' to X). Standard

renormalization in M will again consist in the subtraction of $\tilde{\mathcal{G}}^1(X_0, X'_0)$ from $\mathcal{G}(X, X')$ (up to a non-divergent term). As in the case of scalar fields, it is evident that the remaining terms $\tilde{\mathcal{G}}^1(X_0, X'_n)$ with $n \neq 1$ will lead to a divergent stress-energy tensor near γ . In the coincidence limit, these terms contain non-trivial spinor propagators $\mathcal{I}(X_0, X_n)$ describing parallel transport of spinors as one goes n times around γ , from X to X .

We turn next to the computation of the spinor propagator for a given winding number n . Let us choose a local Lorentz basis e_0^a, \dots, e_3^a at X so that $u^a = e_0^a$ and $k^a = e_0^a + e_3^a$. Further, let us use the matrices $\bar{\sigma}^0, \dots, \bar{\sigma}^3$ introduced at the beginning of this section to represent this Lorentz basis in terms of bispinors. If the sigma matrices are understood to refer to a basis o^α, ι^α of the spinor space at X , then k^a will be represented by

$$k^a \bar{\sigma}_a^{\dot{\alpha}\alpha} = 2\bar{\iota}^{\dot{\alpha}} \iota^\alpha. \quad (3.15)$$

Parallel transport of a vector tetrad n times around γ is equivalent to a Lorentz transformation L . We have seen in Sec. 2 that

$$L^a_b k^b = e^{nh} k^a.$$

Obviously, then, L will take ι^α into $\lambda \iota^\alpha$, where $\lambda = e^{n(h+i\theta)/2}$ and θ is a real number depending on the spacetime M . Since L is represented in the spinor basis by a matrix of unit determinant, the general form of $\mathcal{I}(X_0, X_n)$ in this basis is

$$\mathcal{I}_\beta^{\alpha'}(X_0, X_n) = \begin{pmatrix} \lambda^{-1} & \mu \\ 0 & \lambda \end{pmatrix}, \quad (3.16)$$

where μ is a complex number depending on the spacetime M . (Remember that we have defined $\mathcal{I}(X, X')$ so that it multiplies a spinor at X from the right.)

Below, we shall see that μ drops out of our calculation. The meaning of θ is elucidated by the following [17]. As long as $\lambda \neq 1$, it is clear that the matrix (3.16) can be diagonalized by a suitable redefinition of o^α . When this has been done, $\bar{o}^{\dot{\alpha}} o^\alpha$ represents a null vector l^a such that $L^a_b l^b = e^{-nh} l^a$. Also, $\bar{o}^{\dot{\alpha}} \iota^\alpha$ represents a

complex vector m^a that is multiplied by $e^{in\theta}$ under the action of L . The spacelike plane spanned by real linear combinations of m^a and its complex conjugate \bar{m}^a is orthogonal to k^a and l^a . In this plane, L acts as a rotation, and the rotation angle is $n\theta$. That L involves an inverse boost in a null direction different from k^a and generally also effects a rotation in a spacelike plane has been noted by Hawking [10].

Returning to our original spinor basis, we now insert the term $\tilde{\mathcal{G}}^1(X_0, X'_n)$ into the expression (3.12). From (3.5) we see that in the leading-order divergence of (3.12) the matrices $\bar{\sigma}^a$ will only appear in the combination (3.15). It is straightforward to check that

$$k^a \bar{\sigma}_a \mathcal{I}(X_0, X_n) = \lambda k^a \bar{\sigma}_a,$$

where we have suppressed spinor indices. Using

$$\text{Tr } \sigma^a \bar{\sigma}^b = -2g^{ab}$$

we easily find the contribution to (3.12) with winding number n :

$$\frac{\Delta_n^{1/2}}{4\pi^2 \zeta_n (\delta t)^3} e^{in\theta/2} \frac{e^{nh/2} + e^{3nh/2}}{(e^{nh} - 1)^3} k_a k_b + O((\delta t)^{-2}), \quad (3.17)$$

where we have used the geometric quantities defined in the previous section.

Again, we would like to see how (3.17) transforms when the sign of n is changed. It follows from the definition of the spinor propagators that $\mathcal{I}(X_0, X_{-n})$ is the matrix inverse of $\mathcal{I}(X_0, X_n)$:

$$\mathcal{I}_\beta^{\alpha'}(X_0, X_{-n}) = \begin{pmatrix} \lambda & -\mu \\ 0 & \lambda^{-1} \end{pmatrix}. \quad (3.18)$$

This allows us to modify the argument we used in Sec. 2 when changing the sign of n in (3.7), and we find that the contribution to (3.12) with winding number $-n$ is the complex conjugate of the one with winding number n . Hence, we can write, analogously to the scalar case,

$$\langle T_{ab} \rangle = \frac{1}{2\pi^2 (\delta t)^3} \left[\sum_{n=1}^{\infty} \frac{\Delta_n^{1/2}}{\zeta_n} \cos(n\theta/2) \frac{e^{nh/2} + e^{3nh/2}}{(e^{nh} - 1)^3} \right] k_a k_b + O((\delta t)^{-2}). \quad (3.19)$$

The leading-order divergence of the spinor vacuum polarization thus shares its tensorial structure and degree of divergence with its scalar counterpart (3.8). For sufficiently large n , the terms in (3.19) will be proportional to

$$\alpha^n e^{-3nh/2},$$

where α describes the defocusing effect of the spacetime curvature around γ , as explained in Sec. 2.

Now, suppose that Nature provides us with a combination of conformal scalar fields and spin-1/2 fields in accord with supersymmetry: two scalar fields for each spin-1/2 field. Then, by comparing (3.19) with (3.8) we see that for $h = \theta = 0$ there will be an exact cancellation of the leading $(\delta t)^{-3}$ divergence. For general h and θ , the total stress-energy tensor for each spin-1/2 field together with its associated pair of scalar fields will be

$$\langle T_{ab} \rangle^{\text{tot}} = -\frac{1}{6\pi^2(\delta t)^3} \left[\sum_{n=1}^{\infty} \frac{\Delta_n^{1/2}}{\zeta_n(e^{nh} - 1)^3} P_n(e^{nh/2}, \theta) \right] k_a k_b + O((\delta t)^{-2}), \quad (3.20)$$

where

$$P_n(x, \theta) = x^4 + 4x^2 + 1 - 3 \cos(n\theta/2)(x^3 + x).$$

It is easy to see that $P_n(x, \theta) > 0$ whenever $x \neq 1$, regardless of the value of θ . Thus, the case $h = \theta = 0$ is the only one that results in a cancellation of the leading-order divergence.

4 Conclusion

We have seen that the vacuum polarization near closed null geodesics on compactly generated chronology horizons exhibits a remarkable universality. Apart from the factors Δ_n/ζ_n , the form of the leading-order divergence is completely determined by one or two parameters that describe parallel transport around the closed null geodesic: h in the case of a scalar field, and h and θ in the case of a spin-1/2 field.

The form of the vacuum polarization we have found should be compared with other results. The general divergence in Misner space, derived by Hiscock and Kinkowski [18] and quoted by Hawking [10], appears different from ours because it diverges as the inverse of the fourth power of a time coordinate and because it does not have a double null tensorial structure. However, these differences can be removed by a Lorentz transformation that becomes singular at the chronology horizon of Misner space [18,19] — and that makes Misner space exhibit the same near-horizon spacetime structure as generic spacetimes with compactly generated chronology horizons. Grant finds a weaker, $(\delta t)^{-2}$ divergence at the chronology horizon of Gott's spacetime [9]. This has to do with the fact that the chronology horizon of Gott's spacetime is not compactly generated and does not possess a smoothly closed null geodesic. Indeed, Grant speculates that this feature might exempt Gott's spacetime from the chronology protection conjecture. The wormhole spacetimes considered by Kim and Thorne [7] and by Frolov [8] do have compactly generated horizons. As a consequence, their results for the scalar vacuum polarization, when specialized to the vicinity of the closed null geodesics of their spacetimes, are in perfect agreement with ours. On the other hand, at points of their chronology horizons that are away from the closed null geodesics, the wormhole spacetimes exhibit the same type of weakened divergence as Grant finds everywhere on the horizon of Gott's spacetime [7].

Our result that a cancellation of vacuum energies between scalar and spinor fields will not carry over from flat spacetime to a compactly generated chronology horizon also enjoys universality. If it is agreed on that the divergences discussed here will not be rendered inconsequential by the effects of quantum gravity then our result will lend strong support to the chronology protection conjecture. It should be remarked that a cancellation can occur for special, but non-trivial values of \hbar and θ if a different combination of scalar and spinor fields is considered (more specifically, if the number of spinor fields is greater than half the number of scalar fields). However, if one believes that the fields in the actual Universe are governed

by supersymmetry then one is forced to dismiss as unphysical such combinations, because they do not have equal numbers of Fermi and Bose degrees of freedom.

Finally, we would like to mention a speculation of Hawking's [10] according to which the back-reaction of the matter fields might drive an arbitrary spacetime that is about to form closed timelike curves into the special configuration $h = \theta = 0$ for which there is a cancellation of the vacuum polarization. Might Nature in this way try to circumvent the chronology protection conjecture rather than enforce it?

Acknowledgements

This paper was originally written to report some results about spinor vacuum polarization in locally static spacetimes with closed timelike curves. The author is indebted to Kip Thorne for pointing out that these results actually apply to any spacetime with a compactly generated chronology horizon. The author is also grateful to Thorne for encouraging the present work and for general support. He thanks Stephen Hawking, John Preskill, Curt Cutler, and Steven Christensen for helpful discussions. This research was supported in part by the National Science Foundation, Grant AST 88-17792.

Bibliography

- [1] J. L. Friedman, N. J. Papastamatiou, and J. Z. Simon, University of Wisconsin-Milwaukee preprint WISC-MIL-91-TH-17 (1991); D. G. Boulware, University of Washington preprint UW/PT-92-04 (1992). See also D. Deutsch, *Phys. Rev. D* **44**, 3197 (1991).
- [2] M. S. Morris, K. S. Thorne, and U. Yurtsever, *Phys. Rev. Lett.* **61**, 1446 (1988).
- [3] M. S. Morris and K. S. Thorne, *Am. J. Phys.* **56**, 395 (1988).
- [4] G. Klinkhammer, *Phys. Rev. D* **43**, 2542 (1991); U. Yurtsever, *Class. Quantum Grav. Lett.* **7**, L251 (1990); R. M. Wald and U. Yurtsever, *Phys. Rev. D* **44**, 403 (1991).
- [5] J. R. Gott, *Phys. Rev. Lett.* **66**, 1126 (1991). See also C. Cutler, *Phys. Rev. D* **45**, 487 (1992).
- [6] Independent unpublished work by V. P. Frolov, N. N. Gnedin, D. A. Kompaneets, and K. S. Thorne.
- [7] S.-W. Kim and K. S. Thorne, *Phys. Rev. D* **43**, 3929 (1991).
- [8] V. P. Frolov, *Phys. Rev. D* **43**, 3878 (1991).
- [9] J. Grant, *Gravity Foundation Essay* (1992).
- [10] S. W. Hawking, *Phys. Rev. D* (to be published).

- [11] See the appendix to J. Friedman, M. S. Morris, I. D. Novikov, F. Echeverria, G. Klinkhammer, K. S. Thorne, and U. Yurtsever, *Phys. Rev. D* **42**, 1915 (1990).
- [12] B. Zumino, *Nucl. Phys.* **B89**, 535 (1975).
- [13] R. Kallosh, Stanford University preprint SU-ITP-92-1 (1992).
- [14] S. M. Christensen, *Phys. Rev. D* **17**, 946 (1978).
- [15] J. Wess and J. Bagger, *Supersymmetry and Supergravity* (Princeton University Press, Princeton, 1983).
- [16] Such a relation is well-known for Dirac spinors. For Weyl spinors as well as for Dirac spinors, \mathcal{S} will satisfy the appropriate spinor wave equation with zero boundary conditions if \mathcal{G}^1 satisfies a scalar-field-type wave equation with zero boundary conditions. The normalization can be checked by considering \mathcal{S} and \mathcal{G}^1 in flat spacetime, where they are known explicitly.
- [17] The author owes this derivation of the general behavior of L to a discussion with C. Cutler.
- [18] W. A. Hiscock and D. A. Kinkowski, *Phys. Rev. D* **26**, 1225 (1982).
- [19] K. S. Thorne (unpublished).

Chapter 4

Billiard balls in wormhole spacetimes with closed timelike curves: Classical theory

(By F. Echeverria, G. Klinkhammer, and K. S. Thorne. Originally appeared in Phys. Rev. D **44**, 1077 (1991).)

Billiard balls in wormhole spacetimes with closed timelike curves: Classical theory

Fernando Echeverria, Gunnar Klinkhammer, and Kip S. Thorne

Theoretical Astrophysics, California Institute of Technology, Pasadena, California 91125

(Received 27 February 1991)

The effects of self-interaction in classical physics, in the presence of closed timelike curves, are probed by means of a simple model problem: The motion and self-collisions of a nonrelativistic, classical billiard ball in a space endowed with a wormhole that takes the ball backward in time. The central question asked is whether the Cauchy problem is well posed for this model problem, in the following sense: We define the *multiplicity* of an initial trajectory for the ball to be the number of self-consistent solutions of the ball's equations of motion, which begin with that trajectory. For the Cauchy problem to be well posed, all initial trajectories must have multiplicity one. A simple analog of the science-fiction scenario of going back in time and killing oneself is an initial trajectory which is *dangerous* in this sense: When followed assuming no collisions, the trajectory takes the ball through the wormhole and thereby back in time, and then sends the ball into collision with itself. In contrast with one's naive expectation that dangerous trajectories might have multiplicity zero and thereby make the Cauchy problem ill posed ("no solutions"), it is shown that *all* dangerous initial trajectories in a wide class have *infinite* multiplicity and thereby make the Cauchy problem ill posed in an unexpected way: "far too many solutions." The wide class of infinite-multiplicity, dangerous trajectories includes all those that are nearly coplanar with the line of centers between the wormhole mouths, and a ball and wormhole restricted by (ball radius) \ll (wormhole radius) \ll (separation between wormhole mouths). Two of the infinity of solutions are slight perturbations of the self-inconsistent, collision-free motion, and all the others are strongly different from it. Not all initial trajectories have infinite multiplicity: trajectories where the ball is initially at rest far from the wormhole have multiplicity one, as also, probably, do those where it is almost at rest. A search is made for initial trajectories with zero multiplicity, and none are found. The search entails constructing a set of highly nonlinear, coupled, algebraic equations that embody all the ball's laws of motion, collision, and wormhole traversal, and then constructing perturbation theory and numerical solutions of the equations. A future paper (paper II) will show that, when one takes account of the effects of quantum mechanics, the classically ill-posed Cauchy problem ("too many classical solutions") becomes quantum-mechanically well posed in the sense of producing unique probability distributions for the outcomes of all measurements.

I. INTRODUCTION AND SUMMARY

A. Motivation

This is one of a series of papers that try to sharpen our understanding of causality by exploring whether the standard laws of physics can accommodate themselves, in a reasonable manner, to closed timelike curves (CTC's).

Previous papers have provided a natural spacetime arena for such an exploration: The arena of spacetimes that contain classical, traversible wormholes (i.e., multiply connected spatial slices). Morris, Thorne, and Yurtsever [1] showed that generic relative motions of the mouths of a traversible wormhole produce CTC's that loop through the wormhole's throat, and Frolov and Novikov [2] showed that generic gravitational redshifts at a wormhole's two mouths, due to generic external gravitational fields, also produce CTC's. (It is not clear whether the laws of physics permit the existence of such traversible wormholes; the attempt to find out is a separate line of research [1, 3-5], which we shall not discuss here.)

A consortium [6] of researchers from Moscow, Milwaukee, Chicago, and Pasadena (henceforth referred to as

"the consortium") has raised the issue of whether the Cauchy problem is well posed in spacetimes with CTC's, and has explored many facets of the issue. This paper is one of several that elaborate on the ideas raised by the consortium [6].

Two examples of wormhole spacetimes with CTC's are depicted in Fig. 1. Both of these spacetimes are flat and Minkowski, except for the vicinity of the wormhole throat. The wormhole is arbitrarily short, and its two mouths move along two world tubes that are depicted as thick lines in the figure. The mouths are so small compared to their separation that one cannot see in the figure their finite size. Proper time τ at the wormhole throat is marked off along the mouths' world tubes; points with the same values of τ are the same event, on the throat, as seen through the two different mouths.

In Fig. 1(a) mouth 1 remains forever at rest, while mouth 2 accelerates away from 1 at high speed, then returns and decelerates to rest. Because the motions of the two mouths are like those of the twins in the standard special-relativistic twin paradox, we shall refer to this as the "twin-paradox spacetime." The same relative aging as occurs in the twin paradox produces, here, closed timelike curves that loop through the wormhole [1]. The

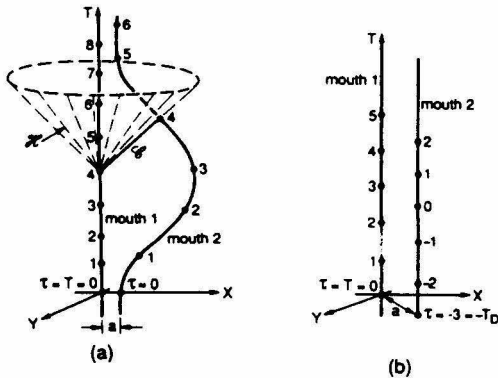


FIG. 1. Two examples of wormhole spacetimes with closed timelike curves. (a) The "twin-paradox spacetime," (b) the "eternal-time-machine spacetime."

light-cone-like hypersurface \mathcal{H} shown in the figure is a Cauchy horizon. Through every event to the future of this Cauchy horizon \mathcal{H} there are CTC's; nowhere in the past of \mathcal{H} are there any CTC's.

In Fig. 1(b) the two mouths are both forever at rest, but with a time delay T_d between them that is greater than the distance a separating them. Because there are CTC's looping through the wormhole throughout this spacetime, the wormhole can be used in principle as a "time machine" for traveling arbitrarily far into the past or the future. For this reason, it has become conventional to call this the "eternal-time-machine spacetime."

Many aspects of the twin-paradox spacetime and the eternal-time-machine spacetime have been studied elsewhere in the literature [1, 6, 3, 7]. Most importantly for us, the consortium [6], and Friedman and Morris [7] have used these spacetimes as "testbed arenas" for studying whether the Cauchy problem is well posed in the presence of CTC's.

As the consortium has shown [6], it is an exceedingly delicate enterprise to pose initial data in a region of spacetime that is threaded by CTC's (the region to the future of the Cauchy horizon in the twin-paradox spacetime; anywhere, except past null infinity, in the eternal-time-machine spacetime). The delicacy is caused by the absence of well-behaved spacelike or null hypersurfaces in such a region, on which to pose the data. Various aspects of this delicacy are discussed by the consortium [6] and by Yurtsever [8], and we shall not in this paper attempt to elucidate them further. Rather, we shall confine attention to the more straightforward situation of initial data that are posed in regions to the past of all CTC's; i.e., data posed on a spacelike or null Cauchy surface to the past of the Cauchy horizon \mathcal{H} in the twin-paradox spacetime, and data posed on past null infinity in the eternal-time-machine spacetime. We shall ask (as did the consortium [6]) whether the Cauchy problem is well posed for such initial data, in the following sense:

If one gives the same standard initial data as one would do in a spacetime without CTC's, then for each choice of those data does there exist a self-consistent, global solution of the standard, local evolution equations, and if so is the self-consistent solution unique? (The demand for self-consistency has been discussed in depth by the consortium [6].)

One can ask about the well posedness of the Cauchy problem for a variety of types of evolving systems in spacetimes with CTC's. The first step, carried out by Friedman and Morris [7], was to study the evolution of a classical, massless scalar field ϕ . Friedman and Morris showed rigorously that the Cauchy problem is well posed for such a field in the eternal-time-machine spacetime: Every arbitrary initial value of the field $r\phi$ (where r is radial distance), posed at past null infinity (limit as $T - r \rightarrow -\infty$), gives rise, via the standard local evolution equation $\square\phi = 0$, to a unique, globally self-consistent field ϕ throughout the eternal-time-machine spacetime. It seems highly likely that this behavior is prototypical in the sense that, for any zero-rest-mass, noninteracting, classical field (e.g., the vacuum electromagnetic field) in any stable wormhole spacetime with CTC's, the Cauchy problem will be well posed [1, 6, 7].

It seems probable that the well posedness of the Cauchy problem for the field ϕ results from the fact that ϕ has no self-interactions. More likely to produce peculiar results is a system that, after traveling around a nearly closed timelike world line, can interact with its younger self (e.g., a person who tries to kill his younger self). The simplest such classical system is a single, classical particle that carries a hard-sphere, repulsive potential and has no internal degrees of freedom (a "billiard ball"), and that travels with a speed small compared to light so special-relativistic effects can be ignored. The purpose of this paper is to study the Cauchy problem for such a billiard ball in the twin-paradox and the eternal-time-machine spacetimes.

Other papers in this series study the well posedness of the Cauchy problem for systems that embody other pieces of physics: A companion paper to this one (paper II [9]) studies the effects of nonrelativistic quantum mechanics on the Cauchy problem for this paper's billiard ball; Novikov and Petrova [10] are currently studying a classical billiard ball that has huge numbers of internal degrees of freedom and thus can behave inelastically when it collides with itself; and Novikov [11] has examined, semiquantitatively, a number of complicated classical systems (e.g., a bomb that explodes in response to a trigger signal, sending explosive debris through a wormhole and backward in time where it tries to trigger the explosion before the explosion actually occurs). For his complicated classical systems, Novikov shows that it is *plausible* that there always exists at least one self-consistent solution, no matter how paradoxical the initial data may appear. Unfortunately, for such complicated systems it seems hopeless to obtain firm results. Accordingly, in this paper, in a quest for firmness, we examine the simplest system we can think of that has self-interactions: the perfectly elastic, nonrelativistic billiard ball.

B. The Cauchy problem for classical billiard balls

In this paper we pose our initial data (initial billiard ball trajectory, by which we mean *initial path and speed*), in the region of spacetime that is devoid of CTC's: before the Cauchy horizon for the twin-paradox spacetime [Fig. 1(a)], or at past null infinity for the eternal-time-machine spacetime [Fig. 1(b)]. For the twin-paradox spacetime, we confine attention for simplicity to initial trajectories that take the ball into the vicinity of the wormhole long after mouth 2 has returned to rest. This permits us, throughout the calculation, to ignore the early-time, relative motion of the wormhole mouths and to treat the twin-paradox spacetime as though it were the same as the eternal-time-machine spacetime, i.e., the same as Fig. 1(b).

The structure of this (common) spacetime can be understood easily as follows [6]: Take ordinary, flat, Minkowski spacetime, cut out of it the world tubes of two balls that are at rest in a chosen Lorentz coordinate system (T, X, Y, Z) , and identify the surfaces of the balls, with a time delay T_d between them. The surfaces of the two balls are the mouths of the wormhole, and because they have been identified with each other, the wormhole is vanishingly short.

We shall denote by D the separation between the centers of the two mouths as measured in the Lorentz frame where they are at rest, by b the radii of the two mouths (radius of curvature of their surfaces), by T_d the time delay between the two mouths, and by r the radius of the billiard ball. Throughout this paper we shall measure spatial distances in units of D (so the wormhole mouth separation is unity) and times in units of T_d (so the time delay between the two mouths is unity); and we shall denote by $B \equiv b/D$ and $R \equiv r/D$ the wormhole radius and the billiard ball radius, measured in these units, and by v the billiard ball speed, measured in these units (units of D/T_d).

The identification we shall use for the two wormhole mouths is one in which diametrically opposed points (points obtained by reflection in the plane half way between the two mouths) are identical. Stated more pedestrianly (see Fig. 2): Adjust the Lorentz frame's spatial, Cartesian coordinates so the line of centers between the two mouths lies on the X axis. Then set up a right-handed spherical polar coordinate system (Θ, Φ) on the right mouth with the polar axis pointed in the $-X$ di-

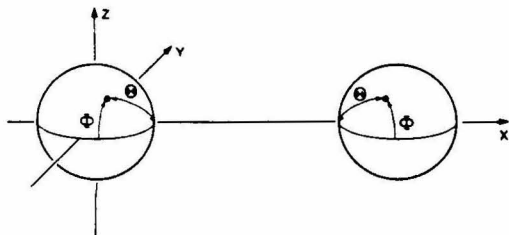


FIG. 2. The identification of points on the two mouths of the wormhole.

rection (along the line of centers, toward the left mouth) and with $\Phi = 0$ along the $-Y$ direction; and set up a left-handed spherical polar coordinate system (Θ, Φ) on the left mouth with polar axis pointed in the $+X$ direction (along the line of centers, toward the right mouth) and with $\Phi = 0$ along the $-Y$ direction. Then points on the two mouths with the same values of Θ and Φ are identified.

In our study of the Cauchy problem for a billiard ball in the above spacetime, we shall focus on the issue of the *multiplicity* of solutions to the ball's equations of motion. For each initial trajectory (initial path and speed) we define the multiplicity to be the number of self-consistent solutions of the equations of motion that begin with that trajectory. Not surprisingly, it will turn out that each initial trajectory has a discrete set of solutions, and thus has multiplicity zero or one or two or In the absence of CTC's, all trajectories have multiplicity one, which is just a fancy way of saying that the Cauchy problem is well posed. From exposure to science-fiction scenarios (e.g., those in which one goes back in time and kills oneself), one might expect CTC's to give rise to initial trajectories with zero multiplicity—a severe form of ill posedness for the Cauchy problem. However, we have searched hard for initial trajectories with zero multiplicity and have found none. On the other hand, our search has not covered all initial trajectories (see especially Sec. V), so we cannot guarantee the nonexistence of zero-multiplicity trajectories.

The only trajectories that have any possibility for zero multiplicity are those which, when followed assuming no collision, produce a collision. We call such trajectories *dangerous*. A trajectory can be dangerous only if it leads the ball into the wormhole, and this can happen only if the trajectory is nearly coplanar with the line that connects the centers of the wormhole mouths—more specifically, only if it is within a distance $B = (\text{mouth radius})$ of being coplanar with the line of centers. For this reason, in this paper we restrict attention to nearly coplanar trajectories. The analysis of the billiard ball motion is fairly manageable when the initial trajectory is precisely coplanar (Secs. II, III, and IV); and the *slightly* noncoplanar case (within a distance $\ll B$ of coplanar) can be treated using perturbation theory (Sec. V). However, we have not found a manageable way to analyze the case of coplanarity to within a distance $\sim B$.

For the slightly noncoplanar case, and for $R \ll B \ll D \equiv 1$ (ball small compared to mouths and mouths small compared to separation of mouths), we shall derive a rather remarkable result (Sec. IV A): *All dangerous initial trajectories have infinite multiplicity*. What a contrast with one's naive, science-fiction-based expectation of zero multiplicity.

Figure 3 gives insight into two of the infinite set of solutions in the precisely coplanar case. Figure 3(a) is the self-inconsistent solution which tells us that the initial trajectory, labeled α , is dangerous. When, as in Fig. 3(a), we assume that the ball travels freely along α without suffering a collision, it passes through the wormhole, emerges along β before it went in, and hits itself so hard that it knocks itself along α' , preventing itself from go-

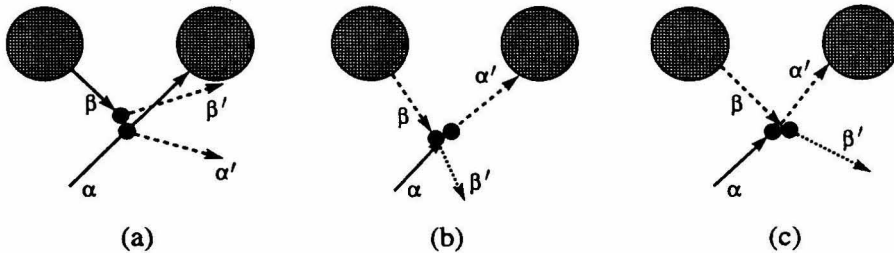


FIG. 3. Spatial diagrams showing a prototypical example of initial data that produce two self-consistent solutions to the billiard-ball equations of motion. Each diagram shows the ball's spatial trajectory, and also shows the ball itself (young version in black and old version in grey) at the moment of self-collision. (a) The self-inconsistent solution which arises if one assumes the ball does not get hit before traversing the wormhole. (b) A "class-I" self-consistent solution in which the ball is speeded up and deflected rightward slightly by a collision before entering the wormhole. (c) A "class-II" self-consistent solution in which the ball is slowed and deflected leftward slightly by a collision before entering the wormhole.

ing through the wormhole. Figure 3(b) is what we call a "self-consistent solution of class I" for this same initial trajectory α . The ball, while traveling toward the wormhole on α , gets hit gently on its left rear side and is speeded up a bit and deflected rightward a bit (along trajectory α'); it then enters the wormhole and reemerges before it went down (trajectory β), it tries to pass behind its younger self, but gets hit a gentle, glancing blow by its younger self and deflected slightly (along trajectory β'). Figure 3(c) is what we call a "self-consistent solution of class II." While traveling toward the wormhole, the ball (trajectory α) gets hit gently on its front right side and is slowed a bit and deflected leftward a bit (along trajectory α'), it enters the wormhole and reemerges before it went down (trajectory β), it passes in front of its younger self and, just before getting all the way past, it gets hit a gentle, glancing blow by its younger self and deflected slightly (along trajectory β'). We shall study the details of such coplanar class-I and class-II solutions in Sec. IV and in Appendixes A and B—and shall do so not only for $R \ll B \ll D \equiv 1$, but also for wormholes with large mouths and balls with large radii.

The class-I and class-II solutions are small perturbations of the self-inconsistent solution, in the sense that the ball's path is displaced by only enough (typically of order the ball's radius R) to permit the ball to undergo a glancing collision rather than a head-on collision. By contrast, the other self-consistent solutions are quite different from the self-inconsistent one. They (or at least the ones studied in this paper) involve a collision that occurs somewhat farther from the wormhole than for class I and class II, and correspondingly the distance the ball travels, from its first encounter with the collision to its second, is rather larger than in the class-I and class-II solutions. This means the ball must travel farther back in time to achieve such a solution. It does so by undergoing several wormhole traversals. In Sec. III we shall exhibit a self-consistent solution corresponding to each value of the integer $n \equiv$ (number of wormhole traversals); and we shall do so not only when the initial trajectory is dangerous, but in fact for almost all coplanar initial trajectories with speeds $v_1 > D/T_d \equiv 1$. Figure 9 (in Sec. III) is an example with eight traversals.

Our analysis of these multiple-traversal solutions, by contrast with our analysis of the class-I and class-II solutions, is restricted to $R \ll B \ll D \equiv 1$. This restriction permits us to ignore the details of the balls' relative geometry during the collision event (aside from proving, in Sec. II, that the necessary geometry exists). By decoupling the details of the collision geometry from the rest of the solution, we bring the multiple-traversal analysis into an elegant geometric form that contrasts with the complicated algebraic calculations used to analyze the class-I and class-II solutions. This difference motivates our presenting the multiple-traversal analysis (Sec. III) before the class-I-class-II analysis (Sec. IV).

This paper restricts attention, for simplicity, to solutions that entail a single self-collision. There presumably are also multiple-collision solutions, and we speculate about some possible, rather strange ones in the paragraph containing Eq. (3.11). Such solutions can only increase the tendency of initial trajectories to have high, even infinite, multiplicity.

Having identified this tendency toward high multiplicity, we ask ourselves in Sec. III C whether there exist any solutions with multiplicity 1; and in Secs. IV and V, whether there exist any with multiplicity zero. Our search for multiplicity zero comes up empty handed; all initial trajectories that we have examined have self-consistent solutions. By contrast, there is at least a small (measure-zero) class of initial trajectories with unit multiplicity: those in which the ball is initially at rest far from the wormhole. We suspect, but have not proved, that the (finite-measure) initial trajectories with speeds $v_1 \ll D/T_d \equiv 1$ and with impact parameters $h \gg D \equiv 1$ also have unit multiplicity; see Sec. III.

The above conclusions are derived for the precisely coplanar case in Secs. II, III, and IV; and they then are all extended to the slightly noncoplanar case in Sec. V. This extension is accomplished by demonstrating (via perturbation theory) that for each slightly noncoplanar initial trajectory there is a one-to-one correspondence between its self-consistent solutions and those of a nearby, precisely coplanar initial trajectory.

This paper's principal conclusion, that the Cauchy problem is ill posed for classical billiard balls in the

eternal-time-machine spacetime, suggests at first sight that the laws of physics might not be able to accommodate themselves in any reasonable way to CTC's. However, the laws of classical mechanics are only an approximation to the more fundamental laws of quantum mechanics, and in paper II [9] it will be shown that quantum mechanics can cure the multiple-solution ill posedness (and can also cure a zero-multiplicity ill posedness, if it occurs): For each initial quantum state of a nonrelativistic billiard ball, posed before the region of CTC's, the sum-over-histories formulation of quantum mechanics predicts unique probabilities for the outcomes of all sets of measurements that one might make in the region of CTC's.

C. Outline of this paper

We begin our quantitative analysis of coplanar solutions in Sec. II, by laying some foundations. In Sec. IIA we derive simple "wormhole traversal" rules for the change of a billiard ball's velocity when it goes through the wormhole. Then in Sec. IIB we analyze the kinematics of a billiard ball's self-collision when there is only one collision event along the ball's world line. Our analysis simplifies subsequent calculations by embodying all the kinematics (energy conservation, momentum conservation, and friction-free billiard-ball contact at the collision event) in one simple rule: the collision must produce either a direct "velocity exchange," or a "mirror exchange" of velocities.

In Sec. III, by combining the wormhole traversal rules with velocity-exchange and mirror-exchange collisions, and restricting attention to $R \ll B \ll D \equiv 1$, we show that multiple solutions to the billiard ball's equations of motion are ubiquitous. More specifically, we show that a finite measure of such (coplanar) initial trajectories produce not only multiple solutions (Sec. III A), but in fact an infinity of solutions (infinite multiplicity; Sec. III B). We then show that *not all* initial trajectories have infinite multiplicity; there do exist some with only one solution (unit multiplicity; Sec. III C).

In Sec. IV we turn our attention to *dangerous*, coplanar initial trajectories. We begin in Sec. IV A by proving, as a corollary of the Sec. III B analysis, that for $R \ll B \ll D \equiv 1$ almost all such trajectories have infinite multiplicity. Then we extend our search for multiplicity zero to balls that are large enough for the geometry of the collision to couple significantly into the rest of the solution, $R \not\ll B$. In Appendix A and Sec. IV B we derive a set of highly nonlinear, coupled equations governing self-consistent solutions with such collisions. Those equations are valid not only for $R \not\ll B$, but also for $B \not\ll D \equiv 1$. However, in Appendix B and Sec. IV C we return to the restriction $B \ll D$ and there search for solutions of the equations. We find analytic, perturbation-theory solutions of classes I and II for almost all initial trajectories; and we construct numerical solutions for some typical initial trajectories in the extreme regions where the perturbation-theory solutions fail. Our spot checks in these extreme regions have not turned up any initial trajectories for which numerical solutions do not exist.

In Sec. V, using perturbation theory, we extend to slightly noncoplanar initial trajectories all the coplanar results of the previous sections.

II. FOUNDATIONS: WORMHOLE TRAVERSALS AND SELF-COLLISIONS

In this section we give brief analyses of coplanar wormhole traversals and billiard-ball self-collisions—analyses that produce simple rules for use in subsequent sections.

A. Coplanar wormhole traversals

For nearly all the wormhole traversals encountered in this paper, the ball's trajectory is coplanar with the line of centers of the wormhole mouths, and the ball enters mouth 2 and exits from mouth 1, thereby traveling backward in time. In this section we shall confine attention to such traversals.

For all traversals, we shall presume that the ball is small enough (ball radius R sufficiently small compared to mouth radius B) that we can ignore the impulsive tidal force exerted on the ball's hard-sphere potential by the concentrated spacetime curvature at the wormhole throat. Just how small R must be for this depends on one's model for the internal structure of the ball.

In this paper our model for the ball will have the following features. (i) We shall refuse to consider collisions that occur while the center of the ball is on one side of the wormhole throat and its colliding surface is on the other; thereby we shall avoid worrying about instantaneous tidal deformations of the ball's hard-sphere potential during the traversal. (ii) We shall assume (for simplicity and definiteness) that, even if R is as large as, say, $B/2$, the ball's center moves through the wormhole in the same manner as would an arbitrarily small ball. (iii) We shall assume that, even for R as large as $B/2$, the ball recovers from its tidal distortions and resumes its radius- R , spherical shape arbitrarily quickly after a traversal. These features of our model are sufficient to permit R to be as large as $B/2$. (Our choice of $B/2$ rather than $B/4$ or $9B/10$ is quite arbitrary.)

Since the ball's center moves through the wormhole in the same manner as would an arbitrarily small ball, its motion must be on a straight line and with constant speed, as seen by an observer at rest on the throat. Such motion guarantees energy and momentum conservation during the traversal, as seen by the observer. (We presume that the wormhole recoils negligibly; i.e., we treat the ball as a "test object" that moves through the fixed wormhole geometry.)

Since the wormhole mouths are both at rest in the external space, constant speed as seen on the throat implies that the speed of the ball, as measured in the exterior, is unchanged by the traversal: $v_{\text{out}} = v_{\text{in}}$.

Straight-line motion, as measured on the throat, implies that the ball's outgoing velocity \mathbf{v}_{out} makes the same angle θ , with the outgoing mouth's outward normal, as the ball's ingoing velocity \mathbf{v}_{in} makes with the ingoing mouth's inward normal. This in turn implies (cf. Fig. 4) that the angle ψ from the mouths' line of centers

(the X axis) to the ball's velocity vector changes during the wormhole traversal from $\psi = \theta + \phi$ to $\psi = \theta - \phi$. Here ϕ is the angular location of the traversal on the wormhole throat as depicted in Fig. 4 (not to be confused with the Φ of Fig. 2).

These conclusions are summarized by the following "wormhole traversal rules":

$$v_{\text{out}} = v_{\text{in}} , \quad (2.1a)$$

$$\psi_{\text{out}} = \psi_{\text{in}} - 2\phi . \quad (2.1b)$$

Here and throughout, an italic v denotes the magnitude (speed) of the velocity \mathbf{v} .

B. Coplanar self-collisions

In this section and throughout this paper we restrict attention to self-consistent solutions that involve a single self-collision. We shall denote by \mathbf{v}_1 the ball's velocity as it enters the collision the first time, by \mathbf{v}'_1 its velocity as it leaves the collision the first time, by \mathbf{v}_2 its velocity as it enters the second time, and by \mathbf{v}'_2 its velocity as it leaves the second time. In other words, the sequence of velocities as measured by the ball itself is $\mathbf{v}_1, \mathbf{v}'_1, \mathbf{v}_2, \mathbf{v}'_2$.

No matter how many wormhole traversals the ball may make between its two visits to the collision event, the "speed in equals speed out" wormhole traversal rule implies that

$$v'_1 = v_2 ; \quad (2.2a)$$

and this, combined with energy conservation, implies that

$$v'_2 = v_1 . \quad (2.2b)$$

These two speed relations, together with the collision's law of momentum conservation,

$$\mathbf{v}'_1 + \mathbf{v}'_2 = \mathbf{v}_1 + \mathbf{v}_2 , \quad (2.2c)$$

are a complete set of conservation laws for the ball's velocity.

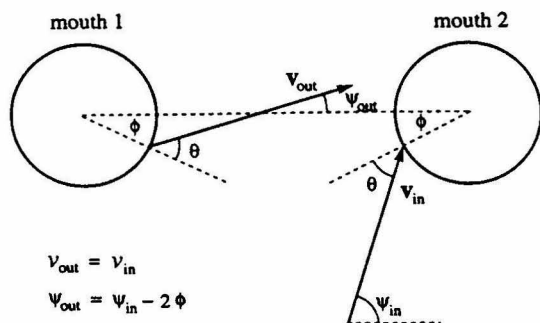


FIG. 4. The "wormhole traversal rules" [Eqs. (2.1)], which govern coplanar wormhole traversals from mouth 2 to mouth 1.

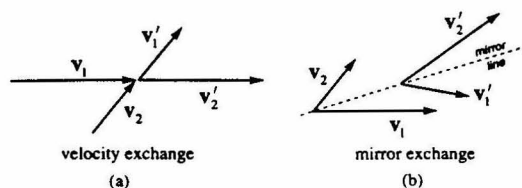


FIG. 5. The two solutions to the self-collision equations: "velocity exchange" [Eq. (2.3a)], and "mirror exchange" [Eq. (2.4a)].

These conservation laws can be satisfied in precisely two ways (Fig. 5): (i) *velocity exchange*,

$$\mathbf{v}'_1 = \mathbf{v}_2 , \quad \mathbf{v}'_2 = \mathbf{v}_1 , \quad (2.3a)$$

for which the relative position of the balls at the moment of collision (the vector separation of their centers) is

$$\mathbf{r}_1 - \mathbf{r}_2 = 2R \frac{\mathbf{v}_2 - \mathbf{v}_1}{|\mathbf{v}_2 - \mathbf{v}_1|} ; \quad (2.3b)$$

and (ii) *mirror exchange*,

$$\begin{aligned} \mathbf{v}'_1 &= (\mathbf{v}_2)_{\text{reflected in line parallel to } \mathbf{v}_1 + \mathbf{v}_2} , \\ \mathbf{v}'_2 &= (\mathbf{v}_1)_{\text{reflected in line parallel to } \mathbf{v}_1 + \mathbf{v}_2} , \end{aligned} \quad (2.4a)$$

for which the relative position of the balls at the moment of collision is

$$\mathbf{r}_1 - \mathbf{r}_2 = 2Rs \frac{\mathbf{v}_2 + \mathbf{v}_1}{|\mathbf{v}_2 + \mathbf{v}_1|} , \quad (2.4b)$$

where $s = \text{sign}(v_2 - v_1)$. [The relative position of the balls when they collide, Eq. (2.3b) or (2.4b), is determined by the fact that the momentum transfer $\mathbf{v}'_1 - \mathbf{v}_1$ must be along the balls' line-of-centers direction $\mathbf{r}_1 - \mathbf{r}_2$, and the centers must be separated by a distance $2R$.]

In summary, all the constraints on velocity that a self-collision must satisfy are embodied in the simple statement that *either the balls undergo velocity exchange (2.3a), or they undergo mirror exchange (2.4a).*

III. UBIQUITY OF MULTIPLE SOLUTIONS FOR COPLANAR INITIAL TRAJECTORIES

In this section we shall use the geometry of the velocity exchange, mirror exchange, and wormhole traversal rules to show that multiple solutions to the billiard ball's equations of motion are ubiquitous. Our discussion will be confined to coplanar initial data. However later, in Sec. V, we shall see that all coplanar solutions are stable (continue to exist) when one perturbs the initial data in an arbitrary but infinitesimal, noncoplanar way. In our discussion, as in Sec. I, we shall refer to the number of solutions that an initial trajectory produces as its "multiplicity."

We begin in Sec. IIIA by showing that all coplanar initial trajectories that are aimed between the wormhole mouths have multiplicity at least two. One solution is unperturbed straight-line motion, and a second is com-

posed of a wormhole traversal and a velocity-exchange collision. Then in Sec. III B we show that there is a wide variety of coplanar initial trajectories (a set of finite measure) with infinite multiplicities. Each of the solutions we exhibit, for these initial trajectories, has a single mirror-exchange collision, together with some number n of wormhole traversals; n ranges over positive integers up to infinity. Finally, in Sec. III C, we show that a ball initially at rest far from the wormhole has only one solution to its equations of motion: the trivial solution where it remains forever at rest. We also argue, but do not prove firmly, that there is only a single solution for any ball with (i) an initial speed that is sufficiently slow but not zero, and (ii) an initial path of motion that, if extended forever, remains far from the wormhole.

A. Multiplicity larger than 1 is generic

Consider a ball whose initial path is coplanar with the mouths' line of centers and is directed between the mouths, and whose initial speed is arbitrary but nonzero. An obvious solution to the ball's equation of motion is collision-free, wormhole-traversal-free, straight-line motion [Fig. 6(a)]. A second solution is shown, for the case of an arbitrarily small ball, in Fig. 6(b). The ball is hit as it crosses the mouths' line of centers and gets knocked radially into mouth 2. Regardless of the ball's initial speed v_1 , it is hit with just the right impulse to give it a speed $v'_1 = (D - 2B)/T_d \equiv 1 - 2B$. It travels through the wormhole and returns to its impact point at just the right moment to hit itself and be deflected back onto its

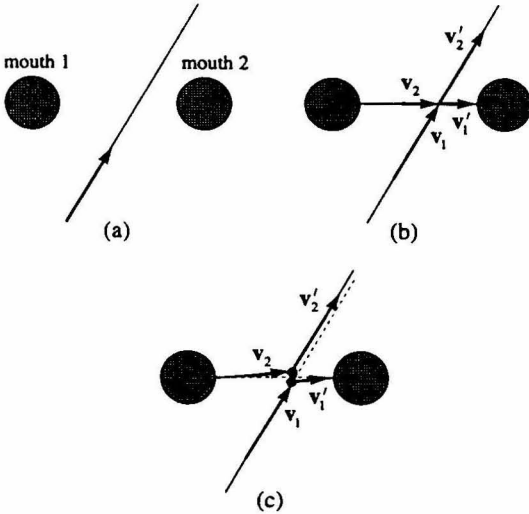


FIG. 6. Solutions to the equations of motion for a coplanar initial trajectory that is directed between the wormhole mouths. The ball's speed is arbitrary. (a) The trivial solution. (b) A solution with one wormhole traversal and a velocity-exchange collision. (c) Modification of solution (b) when the radius of the ball is not negligible.

original trajectory. Since the wormhole traversal rules (2.1) are trivially obeyed, and the ball has obviously undergone a velocity-exchange collision, all the equations of motion are satisfied.

If the ball's radius is not arbitrarily small, both solutions, (a) and (b), still exist. However, the details of solution (b) are modified slightly, as shown in (c). The collision still entails a precise velocity exchange, and the wormhole traversal rule is still satisfied (but not quite so trivially as before). However, there is now an offset of the various pieces of the ball's path (solid lines) relative to the previous path (dotted lines).

It is not hard to convince oneself that, when the ball is given a finite but small size $R \ll B$, all the solutions described in the remainder of Sec. III remain valid with tiny modifications similar to those in Fig. 6(c). However, for ease of presentation we henceforth in Sec. III shall keep the ball's size infinitesimal.

B. Infinite multiplicity is generic

As a first step in demonstrating that infinite multiplicity is generic (i.e., that all the initial trajectories in a set of finite measure have infinite multiplicity), consider the highly symmetric initial trajectory shown in Fig. 7. The ball's initial speed is arbitrary, and its initial path is coplanar with and perpendicular to the line of centers and is directed half way between the two mouths. Figures 7(a)–7(d) are four self-consistent solutions for this initial trajectory, and they obviously are generalizable to produce an infinite set of solutions. Yet another solution is that of Fig. 6(b), which involves velocity exchange by contrast with the mirror exchange of Fig. 7.

The solution shown in Fig. 7(b) was pointed out to us by Forward [12] (and it motivated our discovery of the infinite multiplicity of solutions). In this solution the ball experiences a mirror-exchange collision, which knocks it radially into mouth 2. It then emerges radially from mouth 1, earlier in external time by precisely the right amount $T_d = 1$ to enable it to return to the collision event. The wormhole-traversal rules (2.1) are trivially satisfied ($\psi_{in} = \phi$, $\psi_{out} = -\phi$; $v'_1 = v_2$), and the mirror-exchange rule is satisfied with the mirror line parallel to the line of centers (horizontal dashed line). Since the mirror line must be along $\mathbf{v}_1 + \mathbf{v}_2$, the speed v_2 must be $v_2 = v_1 / \sin \psi$ (where ψ , as shown in the figure, is the ψ_{in} of the wormhole-traversal rule). The total distance traveled by the ball between collisions (in the limit, for simplicity, that $B \ll 1$) is $1/\cos \psi$, so the total time lapse as measured by the ball between collisions is $(1/\cos \psi)(1/v_2) = \tan \psi / v_1$. This ball-measured time lapse must be equal to the amount of backward time travel, $T_d = 1$, during the ball's wormhole traversal, in order that the ball return to the collision event. Correspondingly, the value of ψ must be given by

$$\tan \psi = v_1. \quad (3.1)$$

Notice that there is no constraint whatsoever on the initial speed v_1 . All the equations of motion are satisfied in Fig. 7(b), when ψ has the value (3.1), regardless of

how large or how small v_1 might be.

In the limit as v_1 goes to zero, the ball is initially at rest on the mouths' line of centers; it gets hit and knocked radially into mouth 2 at speed $v_2 = 1$; it travels backward in external time by $T_d = 1$ while traversing the wormhole; and it then emerges radially from mouth 1, travels to the collision event, hits itself, and comes to rest. Note that this solution is really a continuous infinity of solutions: the time T of the collision is completely arbitrary.

The solution in Fig. 7(c) involves two wormhole traversals. As measured by the ball, using its own local time, the sequence of events is the following: (i) initial path α , (ii) mirror-exchange collision, (iii) path β from collision to mouth 2, (iv) first wormhole traversal, (v) path γ from mouth 1 to mouth 2, (vi) second wormhole traversal, (vii) path δ from mouth 1 to collision event, (viii) path ε (opposite to initial path).

As seen by external observers, the sequence is quite different. It is straightforward to verify, by the same method as was used in solution (b), that in the limit $B \ll 1$ the angle ψ is given by

$$\sin \psi + \tan \psi = 2v_1, \tag{3.2}$$

and that the sequence of events is as follows. (i) At time $T = -1/(1 + \cos \psi)$ before the collision, the ball emerges from mouth 1 and starts traveling along δ toward the collision event, while (in its younger incarnation) it is also traveling up α . (ii) At time $T = -\cos \psi/(1 + \cos \psi)$, the ball emerges from mouth 1 and starts traveling along γ toward mouth 2; there are now three incarnations of the ball present. (iii) At time $T = 0$, the collision between incarnations α and δ occurs, knocking incarnation α along β and incarnation δ along ε ; the third incarnation is still traveling along γ . (iv) At $T = \cos \psi/(1 + \cos \psi)$, the ball on γ enters mouth 2 and disappears, leaving just two balls: one on ε , the other on β . At $T = 1/(1 + \cos \psi)$, the ball on β enters mouth 2 and disappears, leaving just one ball, traveling along the final trajectory ε .

Figure 7(d) involves three wormhole traversals. The sequence of paths as measured by the ball is in Greek alphabetical order. It is left as an exercise for the reader to compute the angle ψ in the limit $B \ll 1$ and compute the detailed timings of events as seen by external observers. The reader should also be able to verify (perhaps with the aid of Fig. 9 below and the associated discussion) that the wormhole-traversal rules and mirror-exchange rules are satisfied.

The generalization of the solutions of Fig. 7 to an arbitrarily high number of wormhole traversals should be obvious. We shall examine, in Fig. 9 below, the details of the sequence of wormhole traversals involved in that generalization.

The generalization of these mirror-exchange solutions to arbitrary coplanar initial trajectories is not quite so easy as in the velocity-exchange case of Fig. 6. The method of generalization, for a one-traversal solution, is shown in Fig. 8. The steps in the method are as follows: (i) Specify the initial path α , but not the initial speed v_1 ; the initial speed will be calculated as the last step in the method. Specify, instead of the initial speed, the location P along the initial trajectory α at which the collision occurs. (ii) By trial and error find a path that takes the

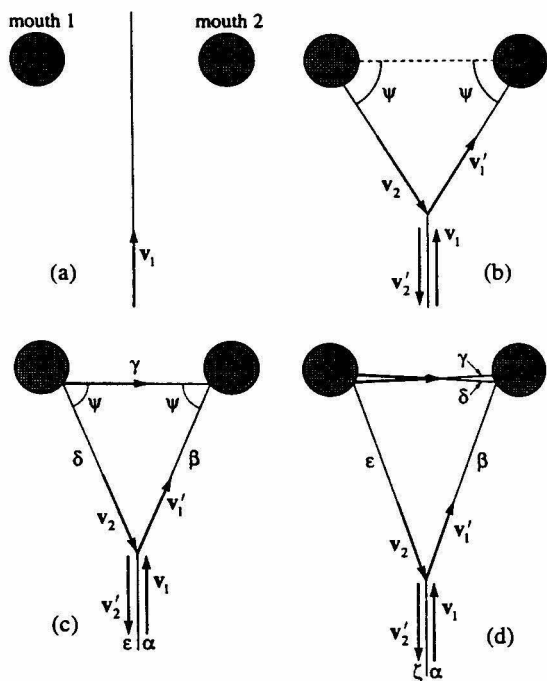


FIG. 7. A specific example of an initial trajectory with an infinite number of solutions (infinite multiplicity). (a) The trivial solution. (b) Solution with one mirror-exchange collision and one wormhole traversal. (c) Solution with one mirror-exchange collision and two wormhole traversals. (d) Solution with one mirror-exchange collision and three wormhole traversals. Solution (b) was pointed out to us by Forward [12] and motivated our discovery of solutions (c) and (d) and their generalizations.

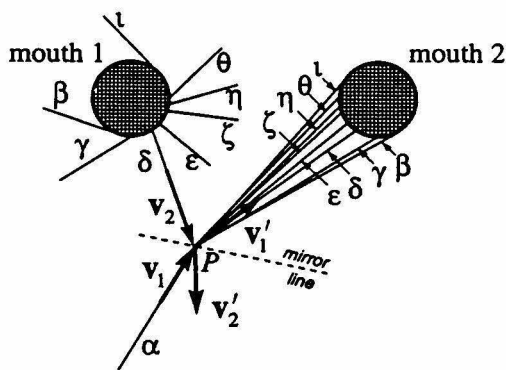


FIG. 8. Trial-and-error method of generating a one-traversal, mirror-exchange solution for an arbitrary, coplanar initial trajectory.

ball from point P to mouth 2, then through the wormhole in accord with the wormhole-traversal rule, then back to point P . That the trial and error will produce precisely one path of the desired type is demonstrated by the sequence of trials $\beta, \gamma, \delta, \dots, \iota$. The wormhole traversal rule (2.1b) guarantees that the modest displacements of the path into mouth 2, in going from β to γ to \dots to ι , will produce the large swing of the path around mouth 1 that is shown in Fig. 8. This large swing, in fact, is an obvious consequence of the "diverging-lens" property of any wormhole mouth [13, 1]. And this monotonic, "diverging-lens swing" will obviously produce precisely one path of the desired form: path δ in Fig. 8. (iii) From the collision-to-collision travel distance along path δ and the backward time travel $T_d = 1$ of the wormhole traversal, compute the speed $v_2 = v'_1$ with which δ must be traversed. This, together with the path δ , gives the velocities v_2 and v'_1 . (iv) From the fact that these v_2 and v'_1 must be the reflection of each other in the mirror line, infer the mirror line's orientation. (v) From the fact that the mirror line must be parallel to $v_1 + v_2$, and from the known value of v_2 and direction of v_1 (along α), compute the ball's initial speed v_1 . (vi) From the initial speed and direction infer the initial velocity v_1 . (vii) Reflect this v_1 in the mirror line to get v'_2 . All details of the solution are now known, and all the ball's equations of motion have been satisfied.

This same method can be used to produce solutions with one mirror-exchange collision and an arbitrary number of wormhole traversals:

For simplicity, restrict attention to a ball with radius R and a wormhole with mouth separation $D \equiv 1$ and mouth radius B satisfying

$$R \ll B \ll 1. \tag{3.3}$$

Consider an arbitrary coplanar initial trajectory, as shown in Fig. 9(a). It is characterized by the ball's initial speed v_1 , the angle ψ_A that its initial velocity makes with the mouths' line of centers, and its initial impact parameter h with respect to the center of mouth 2. (The subscript A is used on ψ_A because, in the limit that the collision point is infinitely far from the wormhole, the angle ψ_0 , at which the ball first hits mouth 2, asymptotically approaches ψ_A ; cf. Eq. (3.10) below: ψ_A is the asymptotic value of ψ_0 .) By suitable choices of these parameters in the range $0 \leq v_1 < \infty$, $0 \leq \psi_A \leq \pi$, and $-\infty < h < \infty$, we can describe all possible coplanar initial trajectories. (Trajectories with $-\pi < \psi_A < 0$ are obtained from those with $0 < \psi_A < \pi$ by reflection in the line of centers.) As we shall see, to obtain an infinite number of solutions, each with a single mirror-exchange collision and all with the same initial trajectory, we need only place two constraints on the initial trajectory:

$$v_1 > 1, \quad \psi_A > B. \tag{3.4}$$

There typically will be solutions (e.g., the class-I and class-II solutions of Fig. 3) in which the collision occurs in the vicinity of the wormhole. However, in this section, in order to demonstrate the existence of infinite numbers of solutions, we can and shall restrict attention to collisions

that occur far from the wormhole, i.e., at

$$L \gg 1 \text{ and } L \gg h, \tag{3.5}$$

where L is the distance, along the initial trajectory, from the collision to the point of closest approach to mouth 2; cf. Fig. 9(a). As was the case in Fig. 7, for a fixed incoming trajectory, the location L of the collision will turn out to depend on the number n of wormhole traversals, and in the limit $n \rightarrow \infty$, L will become arbitrarily large. In the discussion associated with Fig. 8, we regarded the initial path and L as fixed, and solved for the initial speed v_1 . Here we shall regard the initial path and speed (i.e., ψ_A, h , and v_1) as fixed and shall solve for L in terms of ψ_A, h, v_1 , and n .

Because $L \gg 1$, the velocity v'_1 with which the ball

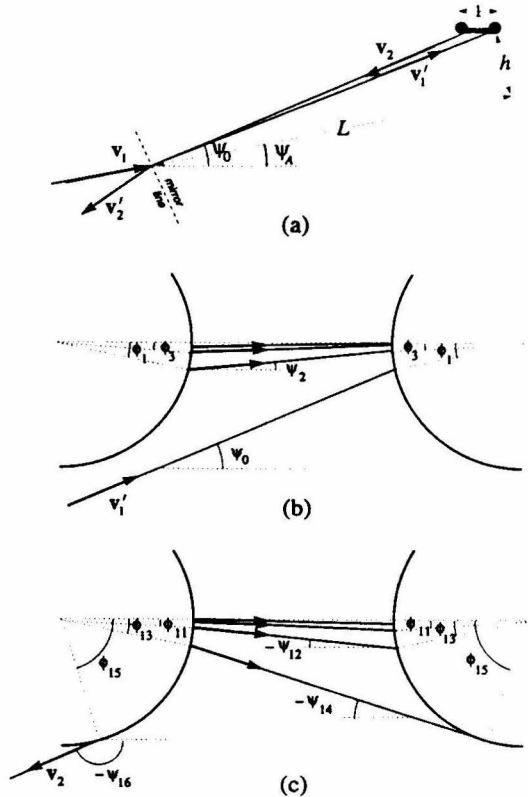


FIG. 9. A solution to the equations of motion for $R \ll B \ll 1$, with an arbitrary number n of wormhole traversals. The figure is drawn for $n = 8$. The initial trajectory, characterized by v_1, ψ_A , and h , is arbitrary except that $v_1 > 1$ and $\psi_A > B$. (a) The large-scale geometry of the solution. (b) The sequence of wormhole traversals as the ball works its way up toward the line of centers. (c) The sequence of traversals as the ball works its way back down from the line of centers. The angles ψ_{2k} and ψ_{2k+1} are given by the diverging-lens map (3.6).

heads toward the wormhole and the velocity v_2 with which it returns are very nearly antiparallel. Since these velocities must be the reflections of each other, the mirror line (which is along $v_1 + v_2$) must be very nearly orthogonal to v_2 , and correspondingly, the speeds must be related by

$$v_2 = v'_1 = v_1 \cos(h/L) = v_1 [1 - \frac{1}{2}(h/L)^2], \quad (3.6)$$

where we ignore corrections of higher order in h/L . In its sequence of n wormhole traversals, the ball goes backward in time by $\Delta T = -nT_d = -n$. Correspondingly, in order to return to the collision point at the moment of collision, it must travel a total distance nv_2 . The total distance traveled, for large L and n , is easily seen from the diagram to be $2L + n$ (aside from unimportant fractional corrections of order h^2/L^2). By equating these distances to each other and using the value (3.6) for the speed v_2 , we obtain the relation

$$n = \frac{2L}{v_1 - 1 - \frac{1}{2}(h/L)^2 v_1}. \quad (3.7)$$

This is the promised relation which determines the location L of the collision in terms of the initial trajectory (characterized here by h and v_1) and the number n of wormhole traversals.

Notice that this relation cannot be satisfied, for arbitrarily large n and positive L , unless $v_1 > 1$. This is the origin of the first of constraints (3.4) on our initial trajectory. The second of those constraints, $\psi_A > B$, is required to ensure that, for arbitrarily large L and n [which means for $\psi_A \simeq \psi_0 \simeq 2\phi_1$ in Fig. 9(b), see discussion below], the ball can reach mouth 2 on its after-collision inward trajectory, without first running into mouth 1.

For a wide class of initial trajectories, there is a lower bound on the number n of wormhole traversals that can produce a self-consistent solution. In the regime of our analysis ($n \gg 1$, $L \gg 1$, $L \gg h$) this lower bound shows up as the fact that n viewed as a function of L with fixed v_1 and h [Eq. (3.7)] has a minimum:

$$n_{\min} = \frac{3\sqrt{3v_1/2}}{(v_1 - 1)^{3/2}} |h|. \quad (3.8)$$

As the initial speed v_1 decreases toward unity (with h fixed), the minimum number of traversals n_{\min} increases toward infinity.

To recapitulate, for every choice of initial conditions in the range $v_1 > 1$ and $\psi_A > B$, there is an infinite number of solutions (labeled by n) to (i) the laws of energy and momentum conservation in the billiard-ball collision [embodied in Eq. (3.6) which produces mirror-exchange], and (ii) the condition that the ball return to its collision point at the same time T as it left it [Eq. (3.7)]. We can be sure that each $n > n_{\min}$ gives a full solution to the equations of motion as soon as we have verified one more thing: that there is a path leading from the collision point of Fig. 9(a), to mouth 2, then through the wormhole n times [and obeying the rules (2.1) at each traversal], then out of mouth 1 and back to the collision point. We shall now demonstrate that this is so.

We shall label the wormhole traversals by odd integers

1, 3, 5, ..., $2n - 1$, and shall label the path up to mouth 2, the paths between traversals, and the path back to the collision point by even integers 0, 2, 4, ..., $2n$. Figure 9 is drawn for $n = 8$, $2n = 16$. The location of traversal $2k - 1$ is described by its angle ϕ_{2k-1} on the wormhole mouths relative to the line of centers, and the direction of path $2k$ is described by the angle ψ_{2k} from the line of centers to the path's velocity direction. The wormhole traversal rule (2.1b), in this notation, reads

$$\psi_{2k+2} - \psi_{2k} = -2\phi_{2k+1} \quad \text{for } 0 \leq k \leq n-1; \quad (3.9a)$$

and the expression for the slope of path $2k$ in terms of the locations of its end points reads (for $B \ll 1$ so $|\psi_{2k}| \ll 1$)

$$\sin \phi_{2k+1} - \sin \phi_{2k-1} = -\frac{\psi_{2k}}{B} \quad \text{for } 1 \leq k \leq n-1. \quad (3.9b)$$

For all except the first and last traversals, the angle ϕ is small compared to unity. Therefore, in (3.9b) the $\sin \phi_{2k \pm 1}$ can be approximated by $\phi_{2k \pm 1}$, except for $\sin \phi_1$ and $\sin \phi_{2n-1}$.

Equations (3.9a) and (3.9b) constitute a map from the direction ψ_0 of the ingoing path to the direction ψ_{2n} of the outgoing path. This map embodies all the equations-of-motion constraints on the trial-and-error search for the desired ingoing path. In this map we are to take ψ_0 as fixed by our chosen location for the collision

$$\psi_0 = \psi_A + h/L \quad (3.10)$$

[cf. Fig. 9(a)], and we are to adjust the location ϕ_1 of the ingoing path so as to produce n wormhole traversals followed by an outgoing path with direction $\psi_{2n} = \psi_0 - \pi$. The diverging-lens behavior of the wormhole guarantees that ϕ_1 can be so adjusted: By elementary geometric optics it should be clear that the correct route must work its way up toward the mouths' line of centers in the manner of Fig. 9(b) during the first half of its trip, and must then work its way back down in the manner of Fig. 9(c) during the second half. In order to do this successfully, the paths on the upward route must have $\psi_{2k+2} \ll \psi_{2k}$ and, correspondingly [cf. Eq. (3.9a)], $\phi_{2k+1} \simeq 2\psi_{2k}$ —or, as one sees from a more precise study of the map (3.9a) and (3.9b), $\phi_{2k+1} = 2\psi_{2k}[1 + O(B)]$, where $O(B)$ denotes a k -dependent quantity of order B . In particular (choosing $k = 0$), ϕ_1 must be equal to $\frac{1}{2}\psi_0[1 + O(B)]$.

We can understand qualitatively (but not quantitatively), with the aid of Fig. 8, how the pattern of paths in the vicinity of the hole changes as the trial-and-error value of ϕ_1 is gradually decreased toward and then past the fixed $\frac{1}{2}\psi_0$. Initially, for $\phi_1 \simeq \pi/2$, there is just one wormhole traversal and the outgoing path at mouth 1 has the form β of Fig. 8. As ϕ_1 is decreased, the outgoing path at mouth 1 swings from β to γ , which is the desired path in our present trial-and-error search [point P very far down path γ as in Fig. 9(a)]. We thereby obtain a solution with one wormhole traversal. As ϕ_1 is further decreased, the output path at mouth 1 swings through δ and ϵ and up to ζ . Suddenly at ζ the output path plunges down mouth 2 and emerges from mouth 1

along β . A further decrease of ϕ_1 swings the output path around to γ , the desired position. We now have a solution with two wormhole traversals. By continuing to decrease the trial-and-error ϕ_1 toward $2\psi_0$, we cause the output path to swing again from γ to ζ , there enter the wormhole a second time and emerge on β , then swing down to γ , producing a solution with three traversals, then continue its swing to produce solutions with four traversals, five traversals, six traversals, Ultimately, as ϕ_1 decreases through the singular limit point of an infinite number of traversals [$\phi_1 =$ a certain value $\phi_{1\text{crit}} = \frac{1}{2}\psi_0 + O(\psi_0 B)$], the output path flips over to path η , which passes just above mouth 2; and further decreases of ϕ_1 cause it to swing through a pattern η, θ, ι , reduction of traversals by 1; then η, θ, ι , reduction by 1; . . . until the number of traversals is reduced to zero. During this reduction sequence we get no acceptable solutions because the output path is not swinging through the required position γ .

This completes our demonstration that for each coplanar initial trajectory with $v_1 > 1$ and $\psi_A > B$ (and for a ball and wormhole satisfying $R \ll B \ll 1$), there exists an infinite number of solutions of the billiard-ball equations of motion, one corresponding to each value $n > n_{\text{min}}$ of the number of wormhole traversals. To construct the solution with n traversals one can (i) specify the initial trajectory (the parameters ψ_A, h, v_1), (ii) then compute the location L of the collision from Eq. (3.7), and (iii) then find the location ϕ_1 at which the ball first enters mouth 2 by the above geometrical trial-and-error method. (Readers who seek higher rigor than we do might worry that our analysis has examined only the leading-order effects in the small parameters $B, R/B, 1/L$, and h/L and has not proved rigorously that higher-order corrections are negligible. We are not worried.)

C. Initial trajectories with only one solution

In this section we turn attention from initial trajectories with infinite multiplicity (an infinite number of solutions), to the issue of whether there exist trajectories with only one solution: collision-free motion. As in the last section, we shall restrict attention to initial trajectories that are coplanar with the wormhole's line of centers and shall describe them by the parameters v_1, h , and ψ_A of Fig. 9(a).

We learned in the last section that for speeds $v_1 > 1$ the multiplicity is almost always infinite. This suggests that we should seek unit multiplicity in the regime $v_1 \ll 1$. Moreover, it seems intuitively clear that a good strategy for avoiding collisions is to keep the initial trajectory far from the wormhole, i.e., to choose $h \gg 1$.

That $h \gg 1$ and $v_1 \ll 1$ are indeed likely to produce unit multiplicity we can see from the following: If there were a solution with one or more collisions, the first collision encountered by the ball presumably would have to be of the type depicted in Fig. 9(a): the old incarnation of the ball flies out from near the wormhole and knocks the young incarnation inward, toward it, and then the old incarnation flies away never to collide again. Such a colli-

sion can only be of the mirror-exchange type and not the velocity-exchange type. Moreover, even if the ball encounters many additional collisions near the wormhole, energy conservation in the entire sequence of collisions implies that $v_2 = v'_1$ in the ball's first, distant collision; and this, together with the argument preceding Eq. (3.6), implies that

$$v_2 = v'_1 = v_1 \cos(\psi_0 - \psi_A) < v_1 \ll 1. \quad (3.11)$$

In other words, after its first collision, the ball heads toward the wormhole with a speed $v'_1 = v_2$ very small compared to $D/T_d = 1$, and after it has finished all its near-wormhole activity, it heads back out toward its first collision with the same tiny speed. This implies, in turn, that the ball must travel backward in time, via wormhole traversals, by a huge amount, $\Delta T > 2h/v_2 > 2h/v_1 \gg 2h \gg 1$. Since each traversal produces a backward time travel of only $T_d = 1$, and there is a forward time travel of at least $D/v = 1/v$ between traversals, the only way the ball can achieve such an evolution is by a peculiar sequence of multiple collisions near the wormhole that build up speeds $v > 1$, temporarily, followed (from the ball's viewpoint) by multiple wormhole traversals into the past at these high speeds, and then followed (from the ball's viewpoint) by collisions that reduce the ball back to $v_2 \ll 1$ and send it back out toward its first collision event. We have searched cursorily for such peculiar solutions, without success, and we suspect they do not exist. However, we have no proof.

On the other hand, in the limit that the ball's initial velocity is precisely zero, and the ball's initial location is far from the wormhole mouths, it is easy to prove (with one caveat; see below) that there is only one solution, the trivial one where the ball remains always at rest. The proof makes use of a sequence of nested convex surfaces that enclose the wormhole mouths, which for concreteness we take to be ellipsoids of revolution (Fig. 10). The ellipsoids are labeled by a generalized radius r which increases outward. We require that the ball initially reside at a radius r_0 larger than that, r_{min} , of the ellipsoid which barely encloses both wormhole mouths.

Now, suppose that there were a solution to the equations of motion other than the one in which the ball re-

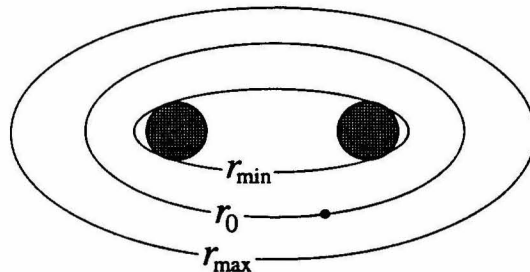


FIG. 10. Nested ellipsoids of revolution surrounding the wormhole, which are used to prove that a ball initially at rest sufficiently far from the wormhole must always remain at rest.

mains at rest. In this solution, the ball would have to undergo one or more self-collisions. There are two possibilities: (i) As seen by the ball there is an infinite sequence of self-collisions that goes on and on forever. We have not been able to rule out such a solution rigorously, but it seems exceedingly unlikely that one could exist. (ii) As seen by the ball there is a last collision. We restrict ourselves to this case.

After completing all its collisions, in order to conserve energy (cf. Fig. 5 of Ref. [6]), the ball would have to return to rest. Let r_{\max} be the largest radius the ball reaches while it is in motion. Since $r_{\max} \geq r_0 > r_{\min}$, this largest radius must lie outside the wormhole, and there thus must be a collision at this r_{\max} , for otherwise the moving ball would be at larger radii momentarily before or after it is at r_{\max} . However, the object that the ball collides with, as it rises to r_{\max} and then gets deflected back downward, can only be the ball itself (since there exist no objects in this problem except the ball and the wormhole), on a path that is coming downward from radii $r > r_{\max}$. We thus reach a contradiction; r_{\max} is not the ball's maximum radius. Therefore, there exist no solutions except the trivial one.

Note that this proof fails if the ball is initially at rest inside radius r_{\min} , since the maximum radius then can lie at the wormhole mouth, and the wormhole rather than a collision can be responsible for deflecting the ball back inward toward smaller radii. A specific example of a non-trivial solution of this type is the one where the ball is initially at rest on the mouths' line of centers, gets hit and knocked into mouth 2, emerges earlier from mouth 1, hits itself and returns to rest; cf. the second paragraph after Eq. (3.1).

IV. SEARCH FOR COPLANAR INITIAL TRAJECTORIES WITH NO SELF-CONSISTENT SOLUTIONS

We now turn attention to the issue of whether there exist coplanar initial trajectories with vanishing multiplicity—i.e., initial trajectories that have no self-consistent solutions whatsoever. If there are such initial trajectories, they must be of the "dangerous" type, i.e. they must be trajectories that, when followed assuming no self-collision, produce a self-collision; cf. the discussion in Sec. I B.

Our search for zero multiplicity among the dangerous trajectories will be carried out in three pieces. In subsection A we shall consider the restrictive case of a ball and wormhole satisfying $R \ll B \ll 1$, and shall show that in this case all (coplanar) dangerous initial trajectories have infinite multiplicity. In Sec. IV B and Appendix A, we shall completely relax these restrictions, and require only that $B < \frac{1}{2}$ so the wormhole mouths do not overlap each other, and $R/B < \frac{1}{2}$ so the ball can pass through the wormhole and we can ignore the effects of tidal forces on the ball during and after its traversal (cf. Sec. II A). For this case we shall derive a pair of coupled, highly nonlinear algebraic equations that govern self-consistent solutions. These equations have solutions in all regimes we have examined (the multiplicity

is nonzero), but their high nonlinearity has prevented us from proving definitively that there always is a solution. In Sec. IV C and Appendix B we shall examine the intermediate case $R/B < \frac{1}{2}$ but $B \ll 1$. In this case we shall show that for a wide range of dangerous initial trajectories there is always at least one self-consistent solution, and we shall argue that this is probably so for all initial trajectories, i.e., the multiplicity is probably always nonzero.

To summarize, our search will turn up no evidence at all for initial trajectories with zero multiplicity.

As a by-product of our search, we shall obtain a detailed understanding of the class-I and class-II solutions depicted in Fig. 3, above.

A. Ball and wormhole with $R \ll B \ll 1$

When $R \ll B \ll 1$, we can infer from the analysis given in Sec. III B above that all dangerous initial trajectories have infinite multiplicity. The argument goes as follows.

Each dangerous initial trajectory, if followed assuming no self-collision, must travel backward in time by a mouth-2 to mouth-1 wormhole traversal so as to produce a self-collision. This means that it must hit mouth 2 upon nearing the wormhole, and not be blocked from doing so by mouth 1, which in turn means that the angle ψ_A in Fig. 9(a) must be larger than B :

$$\psi_A > B \quad (4.1a)$$

[cf. Eq. (4.7) below with $\psi_A = \theta + \phi$]. Moreover, it is easy to see that, if n is the total number of mouth-2 to mouth-1 wormhole traversals that the (self-inconsistent) trajectory undergoes before hitting itself, then the total distance it travels from its first encounter with the event of self-inconsistent collision to its second encounter is $\Delta l > nD = n$. Since the wormhole traversals produce a backward time travel of $\Delta T = -nT_d = -n$, the demand that there be zero external time lapse between the first and second encounters, $\Delta l/v_1 + \Delta T = 0$, implies that the ball's initial speed is

$$v_1 > 1. \quad (4.1b)$$

Since each dangerous initial trajectory satisfies conditions (4.1a) and (4.1b), all dangerous initial trajectories are in the class for which we proved infinite multiplicity in Sec. III B; cf. Eq. (3.4).

B. $B < \frac{1}{2}$ and $R/B < \frac{1}{2}$

Turn next to a wormhole whose size is constrained only by $B < \frac{1}{2}$ (mouths do not overlap) and $R/B < \frac{1}{2}$ (tidal forces ignorable during traversal; cf. Sec. II A).

As in the extreme case of $R \ll B \ll 1$, so also here, all dangerous initial trajectories must extend directly from infinity to mouth 2, so as to initiate their backward time travel. This makes it advantageous to label the initial trajectories by a different triplet of parameters than those of Fig. 9(a) above. The previous parameters were the

initial speed v_1 of the ball's center, its impact parameter h , and its angle ψ_A relative to the wormhole mouths' line of centers. Our new parameters are v_1 and the two angles θ , ϕ shown in Fig. 11. The two sets of parameters are related by $h = -B \sin \theta$, $\psi_A = \theta + \phi$.

In order to make progress in the search for self-consistent solutions in this weakly constrained case of possibly large B and R/B , we have confined our search to self-consistent solutions (i) with just one collision, which (ii) is of the mirror-exchange type, and (iii) in which the ball first encounters the collision event before any wormhole traversal and then encounters it again after only one

traversal. We shall characterize such a self-consistent solution by (among others) the two angles α and β shown in Fig. 11; β is the ball's deflection angle when it first passes through the collision event, and α is the angle between the two incoming balls (old incarnation and new incarnation) at the collision event. In Appendix A we show that, corresponding to each nonspurious solution (α, β) of the following two equations, there exists a self-consistent solution of the full equations of motion for the billiard ball; and we give in Appendix A equations for computing all features of that solution. The two equations for α and β are

$$B \sin \alpha \sin \frac{\alpha - \beta}{2} \left[\sin \theta - \sin \left(\theta + \phi - \frac{\alpha - \beta}{2} \right) \right] + \sin \beta \sin \frac{\alpha - \beta}{2} \left\{ \sin(\theta + \phi) - B \left[\sin \theta + \sin \left(\theta + \phi + \frac{\alpha - \beta}{2} \right) \right] \right\} = (v_1 + d) \sin \frac{\alpha + \beta}{2} \sin \alpha \sin \beta, \quad (4.2)$$

$$B \sin \left(\frac{\alpha + \beta}{2} - \theta - \phi \right) (\sin \alpha + \sin \beta) + B \sin \theta \sin(\alpha - \beta) - \sin \beta \sin(\alpha - \theta - \phi) = -d \sin \alpha \sin \beta, \quad (4.3)$$

where

$$\rho = \frac{\sin[\frac{1}{2}(\alpha + \beta)]}{\sin[\frac{1}{2}(\alpha - \beta)]}, \quad (4.4a)$$

$$d = 2sR/(1 + \rho^2 + 2\rho \cos \alpha)^{1/2}, \quad s = \text{sign}(d); \quad (4.4b)$$

and if one is interested in the ball's speed between collisions, it is given by

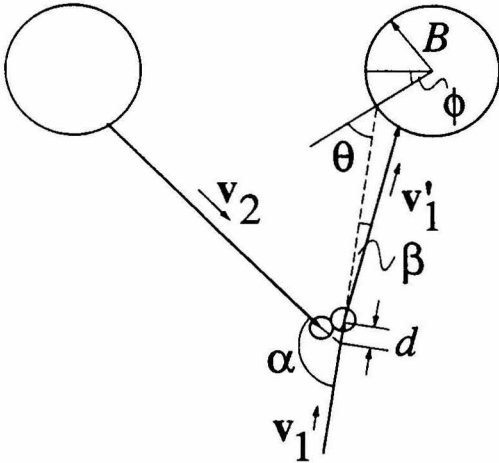


FIG. 11. Geometry of a self-consistent solution with one wormhole traversal and one billiard-ball collision. More details of this geometry are depicted in Figs. 17 and 18 of Appendix A. By convention all angles and distances (e.g., α , β , and d) are positive when their orientations are as shown here.

$$v_2 = v_1 \rho. \quad (4.5)$$

The parameter d is shown in Fig. 11; it is the distance that the ball's younger incarnation must travel *past* the point of intersection of the two incoming trajectories, to reach the collision event. One can choose its sign s arbitrarily in a search for solutions. If $s = +1$ (the case shown in Fig. 11), the ball's older incarnation passes behind the younger, the younger is deflected to the right ($\beta > 0$), and we call the collision "class I" [cf. Fig. 3(b)]. If $s = -1$, the older incarnation passes in front of the younger, the younger is deflected to the left ($\beta < 0$), and we call the collision "class II" [cf. Fig. 3(c)].

Equations (4.2) and (4.3) for α and β have the following set of *spurious solutions* that were introduced by manipulations carried out in Appendix A:

$$(\alpha, \beta) = (0, 0), (\pi, 0), (0, \pi), (\pi, \pi), (2\phi, 0), \quad (4.6a)$$

$$\text{any solution with } \rho < 0, \quad (4.6b)$$

$$\text{any solution with } \text{sign}(\beta) \neq \text{sign}(d) \equiv s. \quad (4.6c)$$

Equations (4.2) and (4.3) for α and β are so horribly nonlinear that we can say only one thing definitive and universal about their solutions: since there are two equations for two unknowns, the solutions must form a discrete set. It is far from obvious, just looking at the equations, whether there exist values of the wormhole and ball radii B , R and initial-trajectory parameters v_1 , θ , ϕ that produce zero solutions. Numerical exploration, and the analytic considerations of the next section, have not turned up any such zero-multiplicity trajectories.

$$C. B \ll 1 \text{ and } R/B < \frac{1}{2}$$

To make further progress in our search for dangerous initial trajectories with no self-consistent solutions, we shall retain $R/B < \frac{1}{2}$, but shall specialize to a wormhole with mouth radii small compared to their separation, $B \ll D = 1$. (Note that these relations imply $R \ll 1$.) We shall also limit ourselves to a large but not complete set of dangerous initial trajectories: those whose self-inconsistent solutions have the same form as the self-consistent solutions analyzed in the last section: the ball comes in from infinity, passes through (and ignores) its collision event, traverses the wormhole just once, and then hits its collision event a second (self-inconsistent) time. The parameters of such initial trajectories lie in the range

$$B/2 < \phi < \pi/2, \quad B - \phi < \theta < \phi, \quad v_{1\min} < v_1 < v_{1\max}, \quad (4.7)$$

where

$$\left. \begin{array}{l} v_{1\min} \\ v_{1\max} \end{array} \right\} = \frac{\cos \theta}{\cos \phi} (1 - 2B \cos \phi) \mp \frac{2R}{\cos \phi}. \quad (4.8)$$

The θ, ϕ part of this dangerous region is the interior of the thick-lined triangle of Fig. 12. We shall call this the "dangerous triangle." The constraint $\theta > B - \phi$ (lower left edge of dangerous triangle) is required so the ball will avoid entering mouth 1 before it reaches mouth 2; parameters (θ, ϕ) near this edge correspond to incoming trajectories that skim past mouth 1, go down mouth 2, emerge from mouth 1, and then collide self-inconsistently near mouth 1. The constraint $\phi < \pi/2$ (right edge of dangerous triangle) is required so the ball's path will intersect itself after passing through the wormhole; near this edge the outgoing path emerges from the wormhole nearly antiparallel to the ingoing path, thereby producing a self-inconsistent collision far from the wormhole. The constraint $\theta < \phi$ (upper left edge of dangerous triangle) is required to make the collision occur before the ball enters mouth 2 a second time; for (θ, ϕ) near this edge, the self-inconsistent collision occurs close to mouth 2. The constraint (4.8) on v_1 (not depicted in the figure) guarantees that the ball returns to the collision region at the right time to produce a self-inconsistent collision.

In Appendix B we carry out a search for self-consistent solutions throughout this range of dangerous initial trajectories. The strategy of the search is based on the physical idea that, because $R < B/2 \ll 1$, the ball travels a distance huge compared to its size R between its first and second encounters with the collision. This means that a very tiny deflection, $|\beta| \sim R \ll 1$, can significantly alter the geometry of the collision, and possibly change it from the self-inconsistent form of Fig. 3(a) to the class-I or class-II self-consistent form of Figs. 3(b) and 3(c). A tiny value of $|\beta|$ goes hand in hand with a tiny change of α from its self-inconsistent-solution value 2ϕ (which is dictated by the wormhole traversal rule shown in Fig. 4). This motivates us to search for solutions in the parameter range

$$|\beta| \ll 1, \quad |\epsilon| \ll 1, \quad \text{where } \epsilon \equiv \alpha - 2\phi. \quad (4.9)$$

In Appendix B we search in this range by expanding Eqs. (4.2) and (4.3) for α, β in powers of ϵ and β . In order to obtain real solutions, rather than just the spurious solutions of Eq. (4.6a), the equations are expanded to quadratic order, and they then are combined to yield one quadratic and one linear equation, Eqs. (B2) and (B12) [in which λ_1 is as defined in Eq. (4.10) below]. These equations have simple analytic solutions throughout the regime (4.7) of dangerous initial trajectories (throughout the interior of Fig. 12's dangerous triangle), except near the triangle's left corner and near its lower left edge.

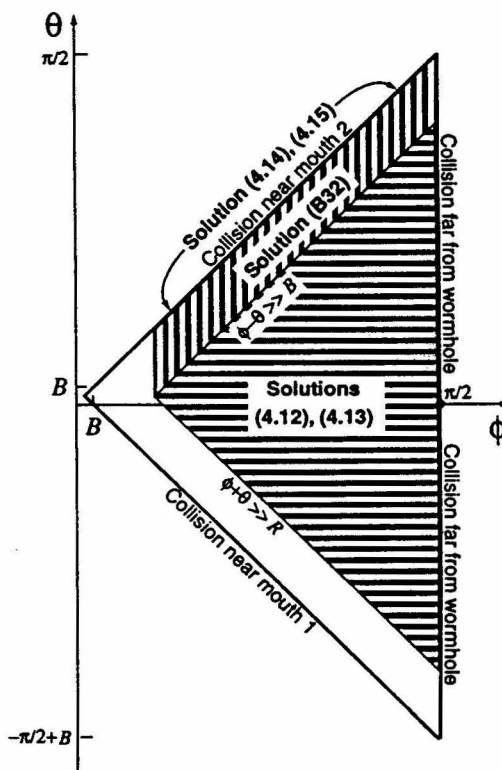


FIG. 12. Parameter space for the ball's initial trajectory when $B \ll 1$, $R/B < \frac{1}{2}$. The interior of the thick-lined triangle is the region of dangerous initial trajectories that produce a self-inconsistent collision after one wormhole traversal [Eq. (4.7)]. We call this the "dangerous triangle." Equations (4.2) and (4.3) govern solutions throughout this dangerous triangle. Simple analytic solutions of these equations are given, by the indicated shaded regions of the dangerous triangle, by the indicated equations. Analytic solutions cannot be derived by the techniques of Appendix B for the white regions of the triangle (left corner and lower left edge), but numerical solutions have been found in spot checks throughout that white region. Figure 14 below shows, as an example, a solution (part analytic, part numerical) all along the upper left edge of the dangerous triangle, including the left corner.

Near this corner and edge, tiny changes of the incoming trajectory produce huge changes in the location of the self-inconsistent solution; and correspondingly, it turns out that self-consistent solutions there typically have a large value of ϵ . This causes the power-series expansion of Appendix B to break down. However, near this corner and edge one can go back to the exact, nonlinear equations (4.2) and (4.3), and find solutions numerically. At all points near the left corner and lower left edge where we have tried, we found numerical solutions. Thus, it seems likely that solutions exist everywhere in the dangerous triangle.

The simple analytic solutions in the horizontally shaded central part of the triangle (i.e., for collisions not close to either mouth; cf. Fig. 12) are interesting and instructive. In describing these simple solutions we shall give formulas not only for β and ϵ (a surrogate for the angle α), but also for the ball's speed v_2 between collisions. Other parameters describing the solutions can be inferred from the equations in Appendix A. To simplify notation in the solutions, we shall characterize the initial speed v_1 and the speed between collisions v_2 by parameters λ_1 and λ_2 defined by

$$v_1 = v_{1\min} + \lambda_1(v_{1\max} - v_{1\min}), \quad (4.10)$$

$$v_2 = v_{1\min} + \lambda_2(v_{1\max} - v_{1\min}). \quad (4.11)$$

Note that the dangerous initial trajectories have $0 < \lambda_1 < 1$. In the central region of the triangle ($\phi - \theta \gg B$, $\phi + \theta - B \gg R$, and $\pi/2 - \phi \gg B$) there are two simple solutions to the quadratic and linear equations (B2) and (B12): one of class I, the other of class II. The class-I solution ($s = +1$) is

$$\beta = \frac{8 \sin \phi}{\cos \theta (\tan^2 \phi - \tan^2 \theta)} B R \lambda_1, \quad (4.12a)$$

$$\epsilon = \frac{8 \cos \phi}{\sin(\theta + \phi)} \lambda_1 R, \quad (4.12b)$$

$$\lambda_2 = \left(1 + \frac{2 \cos \phi}{\tan^2 \phi - \tan^2 \theta} B\right) \lambda_1. \quad (4.12c)$$

The class-II solution ($s = -1$) is

$$\beta = -\frac{8 \sin \phi}{\cos \theta (\tan^2 \phi - \tan^2 \theta)} B R (1 - \lambda_1), \quad (4.13a)$$

$$\epsilon = -\frac{8 \cos \phi}{\sin(\theta + \phi)} (1 - \lambda_1) R, \quad (4.13b)$$

$$1 - \lambda_2 = \left(1 + \frac{2 \cos \phi}{\tan^2 \phi - \tan^2 \theta} B\right) (1 - \lambda_1). \quad (4.13c)$$

These solutions, which when viewed as functions of λ_1 (i.e., of v_1) are linear, actually extend out of the region $0 < \lambda_1 < 1$ of dangerous initial trajectories: The class-I solution is valid for $R^{-1} \gg \lambda_1 > 1$, as well as for $0 < \lambda_1 < 1$, but it is spurious for $\lambda_1 < 0$ since there it predicts opposite signs for β and s ; cf. Eqs. (4.12a)

and (4.6c). Similarly, the class-II solution is valid for $-R^{-1} \ll \lambda_1 < 0$, as well as for $0 < \lambda_1 < 1$, but for $\lambda_1 > 1$ it predicts opposite signs for β and s and thus is spurious. At the point $\lambda_1 = 0$ or 1 where one of the solutions stops (becomes spurious), it actually joins onto (converts over into) a valid, collision-free solution in a manner depicted in Fig. 13.

These simple solutions for the interior region of the dangerous triangle (Fig. 12) break down near the triangle's upper left and lower left edges. There, in solving the coupled linear and quadratic equations (B2) and (B12), one must keep nonlinear terms. It is straightforward to do so, and thereby obtain solutions valid near the upper left edge, but not near the left corner or lower left edge. In Appendix B we analyze the region near the upper left edge (collisions that occur near mouth 2): $0 < \phi - \theta \lesssim B$, $\phi \gg B$. By combining Eqs. (B2) and (B12), we obtain a quadratic equation [Eq. (B29)], with rather simple coefficients, for the incoming ball's deflection angle β . Some of the solutions to this quadratic equation are spurious (wrong sign of β for a chosen sign of s). In Appendix B it is shown that, throughout our chosen region ($0 < \phi - \theta \lesssim B$, $\phi \gg B$), there is a nonspurious class-I ($s = +1$) solution, Eq. (B32), but in some parts of that region there is no nonspurious class-II solution. We suspect, but have not proved, that the missing class-II solution actually exists, but the ball first encounters its collision shortly after passing through the wormhole, rather than before, and therefore this solution is beyond the domain of validity of our analysis.

On the upper left edge of the dangerous triangle (at $\phi = \theta$), the class-I solution (B32) has the form depicted in Fig. 14. This figure is drawn for $\lambda_1 = \frac{1}{2}$, $B = 10^{-2}$

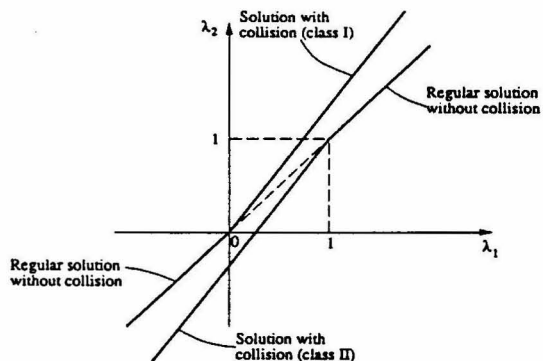


FIG. 13. Billiard-ball speeds for the two self-consistent solutions (4.12) and (4.13) in the central region of Fig. 12's dangerous triangle. (This central region represents collisions that occur neither very close to a wormhole mouth nor at huge distances from the wormhole.) The parameters plotted, λ_1 and λ_2 , are proportional to the speeds v_1 and v_2 [Eqs. (4.10) and (4.11)], and the dangerous range of incoming speeds is $0 < \lambda_1 < 1$. At each edge of the dangerous range, one of the solutions joins continuously onto a collision-free solution, and the other continues to exist as a solution with collision.

and $R = 10^{-5}$ (though the solution is valid also when R is close to B). Notice the sharp change in the deflection angle as one passes from $\phi > \pi/4$ to $\phi < \pi/4$, and from $\phi > \sqrt{B} = 0.1$ to $\phi < \sqrt{B} = 0.1$: At $\phi > \pi/4$, the deflection angle β is of order $R = 10^{-5}$ [This is rather larger than in the central region of the triangle, where it is of order BR ; cf. Eqs. (4.12a) and (4.13a)]. At $\sqrt{B} < \phi < \pi/4$, β is of order $B = 10^{-2}$. As ϕ decreases toward zero (as one moves toward the left corner of the dangerous triangle), ϵ grows large and the power series expansion of Appendix B begins to break down. We have solved numerically the full, nonlinear equations (4.2) and (4.3) for α and β in this corner region and have verified that a solution continues to exist right up to the corner.

The analytic solution (B32) takes on especially simple forms for a very small ball ($R \tan^2 \phi \ll B$), very near the upper left edge of the dangerous triangle ($|\phi - \theta| \tan^2 \phi \ll 1$), and away from the regions of rapidly changing β : At $\phi \gg \sqrt{B}$ and $\pi/4 - \phi \gg B$ the solution becomes

$$\beta = \sin \phi \cos 2\phi B, \quad \epsilon = \frac{\cos 2\phi \cos^2 \phi}{\sin \phi} B; \quad (4.14)$$

and at $\phi - \pi/4 \gg B$ (but $\pi/2 - \phi \gg \sqrt{R/B}$ and $\pi/2 - \phi \gg |\phi - \theta|^{1/2}$), it becomes

$$\beta = \epsilon = -\frac{4 \sin \phi}{\cos 2\phi} R \lambda_1. \quad (4.15)$$

These approximations to the solution are plotted as dashed lines in Fig. 14.

To recapitulate, self-consistent analytic solutions with $|\beta| \ll 1$ and $|\epsilon| \ll 1$ exist throughout the dangerous region of Fig. 12, except its left corner and lower left edge; and we have found numerical solutions in spot checks of

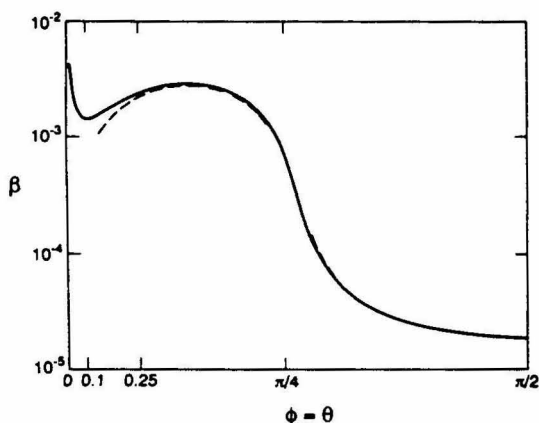


FIG. 14. A combination numerical and analytic solution for the ball's deflection angle β as a function of ϕ , along the upper edge $\theta = \phi$ of Fig. 12's dangerous triangle. This is the class-I solution ($\beta > 0$); the ball and wormhole radii are $R = 10^{-5}$ and $B = 10^{-2}$; and the incoming speed is at the center of the dangerous range, $v_1 = \frac{1}{2}(v_{1\max} + v_{1\min})$ [$\lambda_1 = \frac{1}{2}$; cf. Eq. (4.10)].

that corner and edge. We find no evidence, when $B \ll 1$ and $R/B < \frac{1}{2}$, for initial trajectories with zero multiplicity.

V. NONCOPLANAR TRAJECTORIES

In this section we shall extend most of the coplanar results of Secs. III and IV to initial trajectories that are slightly noncoplanar. Thereby we shall accumulate evidence which suggests, but does not really prove, that all noncoplanar initial trajectories have multiplicity larger than zero (i.e., have self-consistent solutions to the equations of motion). Throughout our discussion we shall confine attention to a wormhole with $B \ll 1$. [This same restriction was imposed throughout Sec. III and in all of Sec. IV except in the fully nonlinear equations of motion (4.2) and (4.3).]

As a first step, we shall ask ourselves how nearly coplanar a trajectory must be in order to be dangerous, i.e., in order to produce a self-inconsistent collision, if followed assuming no collision.

Consider an arbitrary initial trajectory. Define the wormhole's "equatorial plane" to be the unique plane that is parallel to this initial trajectory and contains the wormhole's line of centers. At any point along the ball's trajectory, denote by z the height of the ball's center above the equatorial plane, denote by l the distance the ball has traveled (from some arbitrary origin) parallel to the equatorial plane, and denote by $z' \equiv dz/dl$ the inclination of its trajectory to the equatorial plane. Our definition of equatorial plane guarantees that initially the trajectory has $z = \text{const} \equiv z_1$ and $z' = 0$. However, z' will be made nonzero by the first collision or wormhole traversal the ball encounters.

Now, follow the ball's initial trajectory assuming no collisions. In order for the trajectory to be dangerous, it must traverse the wormhole. The wormhole traversal will convert the trajectory's inclination from $z'_1 = 0$ to $z'_2 = \cos \theta \tan[2\arcsin(z_1/B)]$; cf. Fig. 15(a). Here θ is the angle at which the trajectory's equatorial projection intersects the equatorial normal to the wormhole mouth (as in Fig. 11 above). If it travels a subsequent distance $\Delta l = L_2$ parallel to the equatorial plane and then collides with itself (inconsistently), the height of its center at the collision will be $z_2 = z_1 + L_2 \cos \theta \tan[2\arcsin(z_1/B)]$. To guarantee a collision, we must have $|z_2 - z_1| < 2R$. Thus, the initial trajectory will be dangerous only if

$$z_1 < B \sin[\frac{1}{2} \arctan(2R/L_2 \cos \theta)]. \quad (5.1)$$

For typical dangerous initial trajectories, $L_2 \cos \theta$ will be of order unity, and thus much larger than B , which in turn is a little larger than R ; so the danger criterion (5.1) reduces to $z_1 \lesssim RB$. This means that the dangerous initial trajectories differ from coplanarity by no more than a fraction $B \ll 1$ of the ball's radius R .

We have not found a good way to analyze dangerous initial trajectories near the boundary of the region (5.1). However, for $z_1 \ll B \sin[\frac{1}{2} \arctan(2R/L_2 \cos \theta)]$, the ball's motions parallel to the equatorial plane (its "in-plane motions") decouple from its motions perpendicular to the equatorial plane (its "out-of-plane motions"), and this

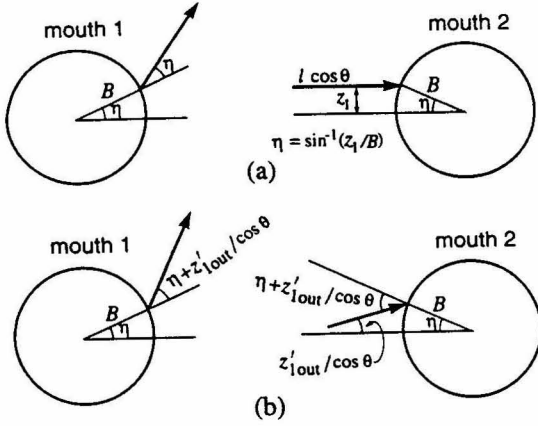


FIG. 15. Change in a noncoplanar trajectory's inclination z' when it traverses the wormhole from mouth 2 to mouth 1: (a) for a ball that does not collide before the traversal; (b) for a ball that collides and is vertically deflected before the traversal. (The change of inclination is a manifestation of the wormhole's "diverging-lens" effect.) The left and right halves of these two-dimensional diagrams are the projection of the ball's trajectory onto a plane that (i) is orthogonal to the equatorial plane (i.e., is vertical), and (ii) passes through the mouth's center and through the intersection of the trajectory with the mouth. The angle between the trajectory and this projection plane is θ , and correspondingly, horizontal distance along the projected trajectory is $l \cos \theta$.

permits us easily to extend to such trajectories most of the results of Secs. III and IV. We shall demonstrate this explicitly for self-consistent solutions that have just one wormhole traversal and one collision, and then shall argue that it is true also (though with a change in the allowed range of z_1) for all other self-consistent solutions.

Consider, then, a self-consistent solution in which the ball gets hit by itself, travels down mouth 2 and out of mouth 1, and then hits itself. We shall seek conditions on the degree of noncoplanarity that permit the in-plane motions to decouple from the out-of-plane motions.

Denote by z_1 and z_2 the out-of-plane displacements of the ball's younger and older incarnations at the moment of collision. Because the balls are round, the in-plane locations of the balls' centers are influenced by the out-of-plane displacements by amounts

$$\Delta l \sim R(1 - \cos \psi) \simeq R\psi^2/2 \simeq \frac{1}{2}R[(z_2 - z_1)/2R]^2, \quad (5.2)$$

where ψ is the angle shown in Fig. 16. Similarly, if the ball's center passes through the wormhole mouths at a height z_{mouth} , that height will influence the ball's in-plane motion in the same manner as would a decrease

$$\frac{\delta B}{B} \simeq -\frac{z_{\text{mouth}}^2}{2B^2} \quad (5.3)$$

in the wormhole's radius. The back action of the out-of-plane motion on the in-plane motion will be negligible

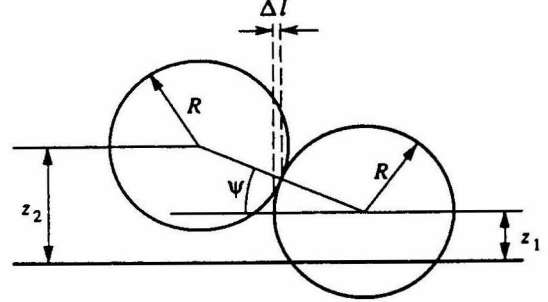


FIG. 16. Back action of a billiard ball's out-of plane motion on its in-plane motion.

in the collision and traversal if $\Delta l \ll R$ in (5.2) and $\delta B/B \ll 1$ in (5.3), i.e., if

$$|z_2 - z_1| \ll R \text{ and } z_{\text{mouth}} \ll B. \quad (5.4)$$

We now ask what values of z_1 lead to self-consistent solutions that satisfy this decoupling condition. [To keep formulas simple, we shall write them in approximate forms valid for the regime (5.4).]

In the collision, the z component of momentum transfer to ball 1 is

$$\Delta p_z = \frac{z_1 - z_2}{2R} \Delta p_l, \quad (5.5)$$

where $\Delta p_l = kmv_1\beta$ (with k typically of order unity) is the momentum transfer in the plane, m is the mass of the ball, v_1 is the ball's speed before the collision, and β is the deflection angle in the plane. This z -momentum transfer changes the inclination of the ball's trajectory from $z'_{\text{in}} = 0$ to

$$z'_{\text{out}} = \frac{z_1 - z_2}{2R} \frac{\Delta p_l}{p_l} = \frac{z_1 - z_2}{2R} k\beta \ll 1, \quad (5.6)$$

where $p_l = mv_1$ is the momentum in the plane. After traveling a distance L_1 from the collision point, the ball arrives at mouth 2 with height

$$z_{\text{mouth}} = z_1 + z'_{\text{out}}L_1 \ll B. \quad (5.7)$$

The wormhole's diverging-lens effect causes the ball to emerge from its traversal with inclination [Fig. 15(b)]

$$z'_2 = z'_{\text{out}} + \frac{2z_{\text{mouth}} \cos \theta}{B} \ll 1. \quad (5.8)$$

The height z_2 that the ball reaches after traveling through the wormhole and returning to the collision point is

$$z_2 = z_{\text{mouth}} + z'_2L_2. \quad (5.9)$$

Combining Eqs. (5.6), (5.7), (5.8), and (5.9), we obtain

$$z_2 - z_1 = \frac{(2L_2 \cos \theta/B)z_1}{1 + (k\beta/2R)(L_1 + L_2 + 2L_1L_2 \cos \theta/B)}, \quad (5.10a)$$

and correspondingly

$$z_{\text{mouth}} = \frac{[1 + (k\beta/2R)(L_1 + L_2)]z_1}{1 + (k\beta/2R)(L_1 + L_2 + 2L_1L_2 \cos \theta/B)} \quad (5.10b)$$

Note that, whatever may be the values of the parameters L_1 , L_2 , θ , and β , there always is a height z_1 that makes $z_2 - z_1$ and z_{mouth} small enough to satisfy the decoupling criteria (5.4). For the typical case of $\phi - \theta \gg B$, the distances of the collision from the mouths are $L_1 \sim L_2 \sim 1$ and the in-plane deflection angle in the collision is $\beta \sim BR$ [Eq. (4.12a)], so

$$z_2 - z_1 \sim z_1/B \quad \text{and} \quad z_{\text{mouth}} \sim z_1, \quad (5.11)$$

and both decoupling criteria (5.4) are satisfied if

$$z_1 \ll BR. \quad (5.12)$$

Unfortunately (and not surprisingly), this decoupled range is a small portion of the full range of dangerous initial trajectories $z_1 < B \sin[\frac{1}{2} \arctan(2R/L_2 \cos \theta)] \sim RB$. Thus, we can say nothing about the existence of solutions over the full range. However, in the decoupled range we can infer the following from the above analysis. (i) The in-plane motion is affected negligibly by the out-of-plane motion. (ii) If there exists a solution to the equations of motion for the in-plane motion, then there is also a solution for the out-of-plane motion, and it is described by the above equations. (iii) The in-plane motion is described by the same equations as for coplanar initial trajectories. (iv) Therefore, *to each solution for any slightly noncoplanar initial trajectory there corresponds a solution for the corresponding coplanar trajectory, and conversely*. We have derived this conclusion only for the case of solutions with a single collision and single wormhole traversal. However, it should be clear that the same method can be used to derive the same final conclusion for all self-consistent nearly coplanar solutions, regardless of the number of collisions and traversals. There will be a change in the precise criteria for decoupling of the in-plane motions from the out-of-plane motions, but there will always be some out-of-plane neighborhood of coplanar initial trajectories for which the conclusion holds true.

This implies that the results of Secs III and IV for coplanar trajectories are also valid for slightly noncoplanar trajectories. Specifically: (i) When $R \ll B \ll 1$ all initial trajectories have multiplicities greater than zero (i.e., have self-consistent solutions), and all dangerous initial trajectories have infinite multiplicity. (ii) When B is allowed to be of order unity (but no larger than $\frac{1}{2}$), and R/B is constrained only to be small enough to neglect tidal forces, the extensive set of dangerous initial trajectories investigated in Sec. IV and Appendix B all have self-consistent solutions even when they are perturbed slightly in a noncoplanar way.

To recapitulate, these conclusions hold only for a neighborhood of coplanarity (typically $z_1 \ll BR$) that is much smaller than the full range of dangerous initial trajectories (typically $z_1 \lesssim BR$). However, these conclusions make us suspect that even when $z_1 \sim BR$, all initial trajectories will have at least one self-consistent solution.

VI. CONCLUSIONS

We have found that the Cauchy problem for a billiard ball in a wormhole spacetime with closed timelike curves is ill posed in the sense that large, generic classes of initial trajectories have multiple, and even infinite numbers of self-consistent solutions to the equations of motion. On the other hand, we have seen no evidence for a stronger type of ill posedness: generic initial trajectories with no self-consistent solutions. In paper II [9] it will be shown that a sum-over-histories version of quantum mechanics restores well posedness to the Cauchy problem: Quantum mechanics predicts definite probabilities for a nearly classical billiard ball to follow this, that, or another of its classical solutions.

These results give a first glimpse of the behavior of interacting systems in wormhole spacetimes with closed timelike curves. It will be interesting to study more realistic, albeit more complex, classical and quantum systems, as some researchers are currently doing [10]. However, our results suggest that in general there might be no deep conflict between the existence of closed timelike curves and the standard laws of physics.

ACKNOWLEDGMENTS

We thank Joseph Polchinski for motivating this research by asking, in a letter to one of us, how the laws of physics could deal with paradoxical situations of the sort embodied in Fig. 3(a). For helpful discussions we thank John Friedman, Mike Morris, Nicolas Papastamatiou, Leonard Parker, and Ulvi Yurtsever. This paper was supported in part by National Science Foundation Grant No. AST-8817792.

APPENDIX A: DERIVATION OF EQUATIONS FOR COPLANAR SELF-CONSISTENT SOLUTIONS

In this appendix we derive a complete set of equations that govern self-consistent, coplanar solutions with $B < \frac{1}{2}$, R/B small enough to neglect tidal forces, and a single collision that the ball first encounters before any wormhole traversals and encounters the second time after just one traversal. The bottom line of our derivation will be a proof that, to each nonspurious solution of Eqs. (4.2) and (4.3) there corresponds a solution of the complete equations of motion.

Our derivation involves the geometric parameters depicted in Fig. 17, which is a more detailed version of Fig. 11. The first phase of our derivation is to construct a full set of equations of motion. The equations in our full set will be numbered; other equations along the way will be unnumbered. The full set consists of (i) three "main equations," which can be thought of as coupled equations for three unknowns, α , β , and v_2 , in terms of the wormhole and ball radii B , R and the parameters v_1 , θ , ϕ of the ball's initial trajectory, and (ii) a set of auxiliary equations, which express various geometric parameters appearing in the main equations in terms of the

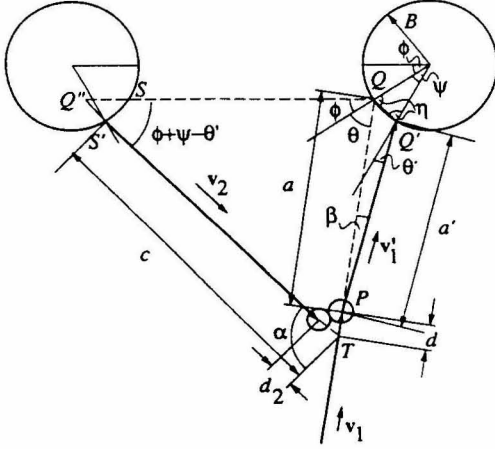


FIG. 17. Full geometry of a self-consistent solution with one wormhole traversal and one billiard-ball collision. This is the same as Fig. 11, but with many more details shown. By convention, all angles and distances (e.g., α , β , d , and d_2) are positive when their orientations are as shown here.

unknowns α , β , v_2 and the knowns B , R , v_1 , θ , ϕ .

We begin by constructing the three main equations. They are based on and embody the laws of mirror exchange (which guarantee conservation of momentum and energy), the geometry of the balls relative to each other and relative to their trajectories at the moment of collision, and the demand that the ball return to the event of collision at the same external time T as it left it. (These are all the laws of motion except for the wormhole traversal rules and the law of straight-line motion between collisions and traversal; those remaining laws are embodied in the auxiliary equations.)

The laws of mirror exchange (2.4a) can be rewritten as

$$v'_1 = v_2, \quad v'_1 \times (v_1 + v_2) = -v_2 \times (v_1 + v_2),$$

$$v'_2 = v_1, \quad v'_2 \times (v_1 + v_2) = -v_1 \times (v_1 + v_2)$$

(together with the requirement that we reject the spurious solutions $v'_1 = -v_2$, $v'_2 = -v_1$). The first pair of these determine v'_1 in terms of v_1 and v_2 , and will be crucial to our analysis. The second pair determine v'_2 , which is of no interest, and thus we can and shall ignore them. The first relation $v'_1 = v_2$ we shall automatically use throughout the analysis without even writing it down; i.e., nowhere will v'_1 appear; we shall always write v_2 in its place. The second relation $v'_1 \times (v_1 + v_2) = -v_2 \times (v_1 + v_2)$, which then becomes our sole embodiment of mirror exchange and hence of energy and momentum conservation, we rewrite in terms of the speeds and angles shown in Fig. 17:

$$v_2 \sin(\alpha - \beta) = v_1(\sin \alpha + \sin \beta).$$

In order to free this equation from its spurious solution $\alpha - \beta = \pi$ (i.e., $v'_1 = -v_2$), we divide both sides by

$2 \cos \frac{1}{2}(\alpha - \beta)$, thereby obtaining

$$v_2 \sin \frac{1}{2}(\alpha - \beta) = v_1 \sin \frac{1}{2}(\alpha + \beta). \quad (\text{A1})$$

This is our first main equation.

Turn, next, to the geometry of the collision. Letting the collision occur at time $T = 0$ and introducing a suitable origin of coordinates, we can write the incoming trajectories as

$$r_1(T) = v_1 T, \quad r_2(T) = v_2 T - 2sR \frac{v_1 + v_2}{|v_1 + v_2|};$$

cf. Eq. (2.4b). These two trajectories intersect spatially ($r_1 = r_2$) at times $T_1 = -d/v_1$ and $T_2 = d_2/v_2$, where d and d_2 are the distances shown in Fig. 17. By equating the above expressions for $r_1(T_1)$ and $r_2(T_2)$, we obtain

$$\frac{v_2}{v_2} d_2 + \frac{v_1}{v_1} d = 2sR \frac{v_1 + v_2}{|v_1 + v_2|}.$$

By forming the scalar products of this equation with $v_1 - v_2^{-2}(v_1 \cdot v_2)v_2$ (i.e., the component of v_1 orthogonal to v_2), and with $v_2 - v_1^{-2}(v_2 \cdot v_1)v_1$ (i.e., the component of v_2 orthogonal to v_1), we obtain several important relations: (i) our second main equation

$$\begin{aligned} |d|/v_1 &= 2R/|v_1 + v_2| \\ &= 2R/(v_1^2 + v_2^2 + 2v_1 v_2 \cos \alpha)^{1/2}; \end{aligned} \quad (\text{A2})$$

(ii) the relation

$$d_2/v_2 = d/v_1,$$

which we shall use below to eliminate d_2 from our third main equation; and (iii) the signs of d and d_2

$$\text{sign}(d_2) = \text{sign}(d) = s.$$

[Recall that s was originally defined as the sign of $v_2 - v_1$; cf. Eq. (2.4b).] These signs are also the same as that of β ,

$$\text{sign}(\beta) = \text{sign}(d) = s$$

[a relation embodied in the text's Eq. (4.6c)], as one can see from the following: The geometry of any collision dictates that the momentum transferred to ball 1 be along the line of centers from ball 2 to ball 1, i.e., $v'_1 - v_1 \uparrow \uparrow r_1 - r_2$ (where $\uparrow \uparrow$ means "points in the same direction as"). Combining this with Eq. (2.4b), we see that $v'_1 - v_1 \uparrow \uparrow s(v_2 + v_1)$. Taking the cross product with v_1 we see that $v'_1 \times v_1 \uparrow \uparrow s v_2 \times v_1$, which with the aid of Fig. 17 (and the fact that always $\sin \alpha > 0$) implies that $\sin \beta = s$.

Consider, next, the law that the total time lapse between the ball's first and second encounters with the collision must vanish. From Fig. 17, we see that the vanishing total time lapse is given by the time needed to travel the distances a' and $c - d_2$ both at speed v_2 , minus the time delay $\Delta T = 1$ introduced by the wormhole traversal:

$$\frac{a'}{v_2} + \frac{c - d_2}{v_2} - 1 = 0.$$

Using the preceding equation to eliminate d_2 , we obtain

our third main equation:

$$v_2 = \frac{a' + c}{1 + d/v_1} \quad (\text{A3})$$

The auxiliary equations, which embody the laws of straight-line motion between collisions and wormhole traversal, and also embody the wormhole traversal rules, are

$$c = \frac{\sin(\theta + \phi)}{\sin \alpha} \left(1 - 2B \cos \phi + 2B \frac{\sin(\psi/2) \cos \gamma_1}{\sin \gamma_2} \right) - 2B \frac{\sin(\psi/2) \cos \gamma_3}{\sin \gamma_2}, \quad (\text{A4})$$

$$d = -a + \frac{\sin \gamma_2}{\sin \alpha} \left(1 - 2B \cos \phi + 2B \frac{\sin(\psi/2) \cos \gamma_1}{\sin \gamma_2} \right), \quad (\text{A5})$$

$$a = \frac{B}{\sin \beta} [\sin(\theta - \beta) - \sin \theta'], \quad (\text{A6})$$

$$a' = a \frac{\cos[(\theta + \beta + \theta')/2]}{\cos[(\theta - \beta + \theta')/2]}, \quad (\text{A7})$$

$$\psi = \theta - \beta - \theta', \quad (\text{A8})$$

$$\gamma_1 = \frac{1}{2}(\theta - 3\theta' - \beta), \quad (\text{A9})$$

$$\gamma_2 = \theta + \phi - 2\theta' - \beta, \quad (\text{A10})$$

$$\gamma_3 = \frac{1}{2}(\theta - \theta' - \beta) + \phi, \quad (\text{A11})$$

$$\theta' = \phi + \theta - \frac{\alpha + \beta}{2}, \quad (\text{A12})$$

These auxiliary equations can be derived as follows:

It should be clear from Fig. 17 that $\overline{PQ} = a$ and $\overline{PQ'} = a'$, and that Q and Q' form an isosceles triangle with the center of the right-hand wormhole mouth. Hence, $\overline{QQ'} = 2B \sin(\psi/2)$ and $\eta = (\pi - \psi)/2$. The interior angles of the triangle PQQ' must add up to π :

$$\beta + (\pi - \eta - \theta) + (\pi - \eta + \theta') = \pi.$$

When η is reexpressed in terms of ψ , this immediately becomes Eq. (A8). Furthermore, applying the sine theorem to the triangle PQQ' yields (i) the relation

$$\frac{a}{\sin(\pi - \eta + \theta')} = \frac{a'}{\sin(\pi - \eta - \theta)},$$

which implies Eq. (A7); and (ii)

$$\frac{a}{\sin(\pi - \eta + \theta')} = \frac{2B \sin(\psi/2)}{\sin \beta},$$

which implies

$$2 \sin[(\theta - \beta - \theta')/2] \cos[(\theta - \beta + \theta')/2] = \frac{a}{B} \sin \beta,$$

which, by a well-known trigonometric formula, implies Eq. (A6).

Summing up the interior angles of the triangle TQQ'' , we find

$$(\phi + \psi - \theta') + (\phi + \theta) + (\pi - \alpha) = \pi,$$

which, when Eq. (A8) is used, yields Eq. (A12). Figure 18 expands on some details of Fig. 17. Applying the sine theorem to the triangle $Q''SS'$, we find

$$l_1 = 2B \sin(\psi/2) \frac{\sin(\eta + \theta')}{\sin(\phi + \psi - \theta')}$$

and

$$l_2 = 2B \sin(\psi/2) \frac{\sin(\eta - \phi)}{\sin(\phi + \psi - \theta')}.$$

For the triangle TQQ'' the sine theorem implies

$$c + l_2 = (1 - 2B \cos \phi + l_1) \frac{\sin(\phi + \theta)}{\sin(\pi - \alpha)}$$

and

$$a + d = (1 - 2B \cos \phi + l_1) \frac{\sin(\phi + \psi - \theta')}{\sin(\pi - \alpha)},$$

where we have used the relation $\overline{SQ} = 1 - 2B \cos \phi$. If, in the last two equations, we eliminate l_1 , l_2 , η , and ψ by using the relations found so far, we obtain Eqs. (A4) and (A5) with the auxiliary definitions (A6)–(A11). This completes our derivation of the auxiliary equations (A4)–(A12).

The next phase of our analysis is a derivation of the

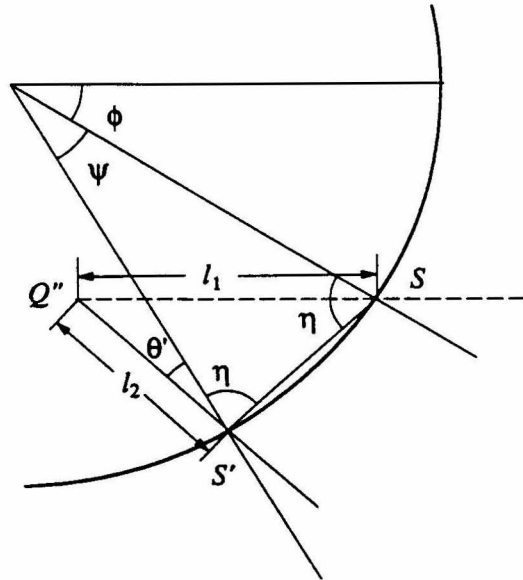


FIG. 18. Some details of Fig. 17 near the wormhole's left mouth (mouth 1).

text's equations (4.2) and (4.3) for the angles α and β . These coupled equations follow from our main and auxiliary equations in the following manner: First we define

$$\rho \equiv v_2/v_1, \quad (\text{A13})$$

and reexpress Eq. (A1) as

$$\rho = \frac{\sin[\frac{1}{2}(\alpha + \beta)]}{\sin[\frac{1}{2}(\alpha - \beta)]}. \quad (\text{A14})$$

Now, using Eq. (A2) d can be expressed in terms of ρ and α as

$$d = 2sR/(1 + \rho^2 + 2\rho \cos \alpha)^{1/2}, \quad (\text{A15})$$

where $s = \text{sign}(d)$. By combining Eqs. (A7), (A6), and (A12), it can be shown that

$$\begin{aligned} a' \sin \beta &= B[\sin \theta - \sin(\beta + \theta')] \\ &= B \left[\sin \theta - \sin \left(\theta + \phi - \frac{\alpha - \beta}{2} \right) \right]. \end{aligned} \quad (\text{A16})$$

From Eqs. (A9)—(A11) it can be seen that $\gamma_2 = \gamma_1 + \gamma_3$, and from (A10) and (A12) that $\alpha = \theta + \phi + \gamma_2$. Using these in Eq. (A4), one can show that

$$\begin{aligned} c \sin \alpha &= \sin(\theta + \phi)(1 - 2B \cos \phi) \\ &\quad - 2B \sin(\psi/2) \cos(\theta + \phi + \gamma_3). \end{aligned} \quad (\text{A17})$$

Next, using (A12) in (A8)—(A11), we obtain all the auxiliary angles in terms of α and β :

$$\psi = -\phi + \frac{1}{2}(\alpha - \beta), \quad \gamma_1 = -\theta - \frac{3}{2}\phi + \frac{3}{4}\alpha + \frac{1}{4}\beta, \quad (\text{A18})$$

$$\gamma_2 = \alpha - \theta - \phi, \quad \gamma_3 = \frac{1}{2}\phi + \frac{1}{4}(\alpha - \beta).$$

Using these expressions and some trigonometric manipulations, Eq. (A17) can be simplified further, giving

$$\begin{aligned} c \sin \alpha &= \sin(\theta + \phi) \\ &\quad - B \left[\sin \left(\theta + \phi + \frac{\alpha - \beta}{2} \right) + \sin \theta \right]. \end{aligned} \quad (\text{A19})$$

Finally, eliminating v_2 between (A13) and (A3), and replacing ρ , a' , and c from (A14), (A16), and (A19), we obtain the first of our equations for α and β : Eq. (4.2); and we obtain the second, Eq. (4.3) by eliminating a between (A5) and (A6), using the values (A18) and (A12) of the auxiliary angles, and performing some algebraic manipulations.

Notice that, in the process of deriving our two equations (4.2) and (4.3), we multiplied them by $\sin \alpha \sin \beta \sin[(\alpha - \beta)/2]$ [Eq. (4.2)], and by $\sin \alpha \sin \beta$ [Eq. (4.3)]. This introduced the first four spurious solutions of Eq. (4.6a). The fifth spurious solution in (4.6a) is the self-inconsistent solution. Since v_2 and v_1 are both positive by definition, $\rho \equiv v_2/v_1$ must also be positive, so any solution for α and β which produces a negative ρ via Eq. (A14), or equivalently via (4.4a), must be spurious. This accounts for Eq. (4.6b). Finally, as was discussed following Eq. (A2), the collision geometry rules out as spurious any solutions with $\text{sign}(\beta) \neq \text{sign}(d)$, which accounts for Eq. (4.6c).

The last phase of our analysis is to explain why, to every nonspurious solution of Eqs. (4.2) and (4.3) for α and β , there exists a full solution of the billiard ball's equations of motion. The reason is that (i) the main and auxiliary equations (A1)—(A12) embody all the equations of motion (as well as a lot of geometrical constructions); and (ii) by regarding the auxiliary equations (A4)—(A12) and the third main equation (A3) as definitions of other variables in terms of α , β , B , R , v_1 , θ , ϕ , and by inserting a nonspurious solution of (4.2) and (4.3) into these equations, we automatically produce a solution of the remaining two main equations (A2) and (A1).

APPENDIX B: SELF-CONSISTENT SOLUTIONS FOR $B \ll 1$

In this appendix we derive the properties of self-consistent solutions quoted in Sec. IV C, for a wormhole and ball with $B \ll 1$ and $R/B < \frac{1}{2}$. We restrict attention to dangerous initial trajectories in the range (4.7) [interior of the dangerous triangle depicted in Fig. 12], and restrict our search to self-consistent solutions with a single collision of the type shown in Fig. 17 and with $|\beta| \ll 1$ and $|\epsilon| \ll 1$, where $\epsilon \equiv \alpha - 2\phi$; cf. Eqs. (4.9).

We begin our derivation in Appendix B 1 by expanding the highly nonlinear, coupled equations (4.2), (4.3) in powers of β and ϵ to the leading orders that produce nonspurious solutions. Then in Appendix B 2 we derive explicit solutions to those approximate equations for the central region of the dangerous triangle, and in Appendix B 3 for the upper-edge region of the triangle.

1. Approximate equations

In this section we derive the approximate equations for β and ϵ by power-series expansions of Eqs. (4.2) and (4.3). To facilitate the expansion of Eq. (4.2), we first divide it by $\sin(\alpha/2)$ (a factor that appears in each term in the limit of vanishing β). When we then expand, the resulting equations are homogeneous in β and ϵ and at linear order admit only spurious solutions, so we move on to quadratic order. Up through quadratic order the expanded equations take the forms

$$M\epsilon + N\epsilon^2 + P_1\beta + Q_1\beta^2 + S_1\beta\epsilon = 0, \quad (\text{B1})$$

$$M\epsilon + N\epsilon^2 + P_2\beta + Q_2\beta^2 + S_2\beta\epsilon = 0, \quad (\text{B2})$$

for which the coefficients M and N of ϵ and ϵ^2 are identically the same in the two equations. The expressions for all the expansion coefficients are

$$M = \frac{1}{2}B \sin 2\phi \cos \theta, \quad (\text{B3})$$

$$N = \frac{1}{2}B(\cos 2\phi \cos \theta + \frac{1}{4} \sin 2\phi \sin \theta), \quad (\text{B4})$$

$$\begin{aligned} P_1 &= -\sin(\phi - \theta) - 2(4\lambda_1 + s - 2)R \sin \phi \\ &\quad + B \left[\frac{3}{4} \sin(2\phi - \theta) - \frac{1}{4} \sin(2\phi + \theta) - \sin \theta \right], \end{aligned} \quad (\text{B5})$$

$$Q_1 = -\cos \phi \cos \theta - \frac{1}{2} \cot \phi \sin(\phi + \theta) - 2(2\lambda_1 - 1)R \cos \phi + B\left[\frac{1}{2}(9 \cos^2 \phi - 1) \cos \theta + \frac{1}{4} \sin \theta \cot \phi (7 \cos^2 \phi - 3)\right], \quad (\text{B6})$$

$$S_1 = -\cos 2\phi \cos \theta / \cos \phi + R[2(2\lambda_1 - 1) / \cos \phi + (4 - 8\lambda_1 - s) \cos \phi] + B[\cos \theta (\frac{3}{2} \cos^2 \phi - 1) + \frac{1}{4} \sin 2\phi \sin \theta], \quad (\text{B7})$$

$$P_2 = -\sin(\phi - \theta) + 2sR \sin \phi + B(-2 \sin \theta \cos^2 \phi + \frac{1}{2} \sin 2\phi \cos \theta), \quad (\text{B8})$$

$$Q_2 = -sR \cos \phi + B(\frac{1}{2} \cos \theta - \frac{3}{8} \sin 2\phi \sin \theta), \quad (\text{B9})$$

$$S_2 = -\cos(\phi - \theta) + sR \cos \phi + B(\cos \theta \cos^2 \phi + \frac{5}{4} \sin \theta \sin 2\phi). \quad (\text{B10})$$

Here the notation is that of Sec. IV and Appendix A, including the use of λ_1 as a surrogate for the ball's initial speed v_1 ; cf. Eqs. (4.10) and (4.8) which imply

$$v_1 = \frac{1}{\cos \phi} [(1 - 2B \cos \phi) \cos \theta + 2R(2\lambda_1 - 1)]. \quad (\text{B11})$$

By subtracting Eq. (B2) from Eq. (B1) and dividing by β , we obtain the linear equation

$$Q\beta + S\epsilon + P = 0, \quad (\text{B12})$$

where

$$Q = -\cos \phi \cos \theta - \frac{1}{2} \cot \phi \sin(\phi + \theta) - (4\lambda_1 - s - 2)R \cos \phi + B(-\cos \theta + \frac{3}{2} \cos^2 \phi \cos \theta + \cos^2 \phi \cot \phi \sin \theta), \quad (\text{B13})$$

$$S = \cos \theta / \cos \phi - \cos(\phi + \theta) + R[2(1 - 2\lambda_1) \cos 2\phi / \cos \phi - 2s \cos \phi] + B(-\cos \theta + \frac{1}{2} \cos \theta \cos^2 \phi - \sin 2\phi \sin \theta), \quad (\text{B14})$$

$$P = -4R \sin \phi (2\lambda_1 + s - 1). \quad (\text{B15})$$

We shall use Eqs. (B2) and (B12) as our approximate, coupled equations for β and ϵ . Since one is quadratic and the other is linear, they can be combined to form a single quadratic equation for β or for ϵ , but the coefficients in that quadratic equation are so complicated that we shall not write it down explicitly except in special regimes where the coefficients simplify.

The coefficients in our quadratic and linear equations (B2) and (B12) change drastically (because $R \ll 1$ and $B \ll 1$) as one approaches the edges of the dangerous triangle (Fig. 12), $\phi - \theta \rightarrow 0$, $\phi + \theta \rightarrow B$, $\phi \rightarrow \pi/2$. Correspondingly, the structures of the solutions change drastically as one approaches the edges. In Appendix B 2 we shall consider the central region (extending out to the right edge), and in Appendix B 3, the upper-left-edge region. Near the lower left edge and the left corner, ϵ

grows large, invalidating the power-series expansion that underlies our quadratic and linear equations (B2) and (B12), and thus the methods of this appendix are not usable there.

2. Solutions in the central region

We specialize, now, to the central region of the dangerous triangle, $\phi - \theta \gg B$, $\phi + \theta - B \gg R$; and we retain our previous assumptions, $B \ll 1$, $R/B < \frac{1}{2}$. In one of our manipulations we shall require an additional constraint: $\epsilon \ll \phi - \theta$. Since $\phi - \theta \gg B$ and ϵ has already been assumed small, this additional constraint is not severe.

These constraints on the parameters imply that in (B2) the terms in ϵ^2 , β^2 , and $\beta\epsilon$ can be neglected compared to the first-order terms. The result is the linear relation

$$\beta = \frac{\sin 2\phi \cos \theta}{2 \sin(\phi - \theta)} B \epsilon \ll \epsilon. \quad (\text{B16})$$

Inserting this relation into our linear equation (B12), we find that ϵ is (very nearly) independent of B :

$$\epsilon = \frac{8 \cos \phi}{\sin(\theta + \phi)} (\lambda_1 - \sigma) R, \quad (\text{B17})$$

with

$$\sigma \equiv \frac{1}{2}(1 - s) = \begin{cases} 0 & \text{if } s = +1, \\ 1 & \text{if } s = -1. \end{cases} \quad (\text{B18})$$

Inserting this back into Eq. (B16), we obtain

$$\beta = \frac{4 \sin 2\phi \cos \phi \cos \theta}{\sin(\phi - \theta) \sin(\phi + \theta)} (\lambda_1 - \sigma) B R = \frac{8 \sin \phi}{\cos \theta (\tan^2 \phi - \tan^2 \theta)} (\lambda_1 - \sigma) B R, \quad (\text{B19})$$

and by inserting these relations into Eqs. (A13), (A14), and (4.11), we obtain the dimensionless parameter λ_2 that describes the speed v_2 of the ball between its encounters with the collision

$$\lambda_2 - \sigma = \left[1 + \frac{\cos^3 \phi \cos^2 \theta}{2 \sin(\phi - \theta) \sin(\phi + \theta)} B \right] (\lambda_1 - \sigma) = \left(1 + \frac{2 \cos \phi}{\tan^2 \phi - \tan^2 \theta} B \right) (\lambda_1 - \sigma). \quad (\text{B20})$$

Equations (B17)–(B20) are the simple form of the solutions for self-consistent collisions of class I ($s = +1$, $\sigma = 0$) and class II ($s = -1$, $\sigma = 1$), which we quoted and discussed in Sec. IV B [Eqs. (4.14) and (4.15)].

3. Solutions in the upper-edge region

We turn, finally, to the upper-left-edge region of the dangerous triangle, $0 \leq \phi - \theta \lesssim B$; and in order to obtain valid solutions with $|\beta| \ll 1$ and $|\epsilon| \ll 1$, we bound ourselves away from the triangle's left corner—i.e., we assume that $\phi \gg B$. In our formulas we shall characterize the difference $\phi - \theta$ by a dimensionless parameter

$$\mu \equiv (\phi - \theta) / B. \quad (\text{B21})$$

As in the preceding subsection, our constraints on ϕ and θ make the ϵ^2 and β^2 terms in Eq. (B2) negligible compared to the first-order terms; but now the $\beta\epsilon$ term is not *a priori* negligible. As a result, Eq. (B2) takes the form

$$k_1\beta + k_2\epsilon + k_3\beta\epsilon = 0, \quad (\text{B22})$$

where

$$k_1 = -\mu B + 2sR\sin\phi - B\sin\phi\cos^2\phi, \quad (\text{B23})$$

$$k_2 = B\sin\phi\cos^2\phi, \quad (\text{B24})$$

$$k_3 = -1. \quad (\text{B25})$$

Our other, linear, equation for ϵ and β [Eq. (B12)] also simplifies; its coefficients become

$$Q = -2\cos^2\phi, \quad (\text{B26})$$

$$S = 2\sin^2\phi, \quad (\text{B27})$$

$$P = -8R\sin\phi(\lambda_1 - \sigma). \quad (\text{B28})$$

By combining our two equations and eliminating ϵ , we obtain the following quadratic equation for β :

$$\beta^2 + p\beta + q = 0, \quad (\text{B29})$$

with

$$\beta = \sin\phi\cos 2\phi B, \quad \epsilon = \frac{\cos 2\phi\cos^2\phi}{\sin\phi} B \quad \text{if } \phi - \pi/4 \ll -R\lambda_1, \quad (\text{B34})$$

and

$$\beta = \epsilon = -\frac{4\sin\phi}{\cos 2\phi} R\lambda_1 \quad \text{if } \phi - \pi/4 \gg +R\lambda_1. \quad (\text{B35})$$

Notice that in (B34) β and ϕ are independent of λ_1 , while in (B35) they are proportional to it. These are the solutions quoted in Eqs. (4.14) and (4.15).

$$p = 2\tan^2\phi[2(\lambda_1 - \sigma) - s\sin\phi]R - (\sin\phi\cos 2\phi - \mu\tan^2\phi)B, \quad (\text{B30})$$

$$q = -4BR\sin^2\phi(\lambda_1 - \sigma). \quad (\text{B31})$$

In discussing the solutions of this quadratic equation we shall restrict attention to the region $0 < \lambda_1 < 1$ of dangerous initial trajectories.

By examining the signs of the coefficients in Eq. (B29), it is easy to see that when $s = +1$ (class-I collision) there always exist two real solutions for β , one positive and thus acceptable; the other negative and thus spurious (recall that $\beta > 0$ for class I and $\beta < 0$ for class II; cf. Fig. 3). On the other hand, when $s = -1$ there is always a range of ϕ where $p^2/4 - q < 0$ and there is no solution. For $R \ll 1$ and $\mu \ll 1$, this no-solution region is $\phi \sim \pi/4$.

Focus attention on the always existent class-I solution, $s = +1$ (and $\sigma = 0$). Since $q < 0$ in this case, the solution is

$$\beta = -p/2 + \sqrt{p^2/4 - q}. \quad (\text{B32})$$

When one continuously varies ϕ in the range of our analysis, $\phi \gg B$, p passes through 0 at some point and changes sign. Since q is second order in the small radii B and R , while p is first order, there is a sharp change in the form of the solution (B32) at that point:

$$\beta = \begin{cases} -q/p & \text{if } p \gg |q|, \\ -p & \text{if } p \ll -|q|. \end{cases} \quad (\text{B33})$$

When $R\tan^2\phi \ll B$ and $\mu\tan^2\phi \ll 1$, the change of sign for p occurs very close to $\pi/4$, and the solution (B33) on the two sides of $\pi/4$ is

- [1] M.S. Morris, K.S. Thorne, and U. Yurtsever, *Phys. Rev. Lett.* **61**, 1446 (1988).
- [2] V.P. Frolov and I.D. Novikov, *Phys. Rev. D* **42**, 1057 (1990); see also I.D. Novikov, *Zh. Eksp. Teor. Fiz.* **95**, 769 (1989) [*Sov. Phys. JETP* **68**, 439 (1989)].
- [3] S.-W. Kim and K.S. Thorne, *Phys. Rev. D* **43**, 3929 (1991).
- [4] V.P. Frolov, *Phys. Rev. D* **43**, 3878 (1991); U. Yurtsever, *Class. Quantum Grav.* **8**, 1127 (1991).
- [5] G. Klinkhammer, *Phys. Rev. D* **43**, 2542 (1991); U. Yurtsever, *Class. Quantum Grav. Lett.* **7**, L251 (1990); R.M. Wald and U. Yurtsever, *Phys. Rev. D* **44**, 403 (1991).
- [6] J. Friedman, M.S. Morris, I.D. Novikov, F. Echeverria, G. Klinkhammer, K.S. Thorne, and U. Yurtsever, *Phys.*

- Rev. D* **42**, 1915 (1990); cited in text as "the consortium."
- [7] J. Friedman and M.S. Morris, *Phys. Rev. Lett.* **66**, 401 (1991); and (in preparation).
- [8] U. Yurtsever, *J. Math. Phys.* **31**, 3064 (1990).
- [9] G. Klinkhammer and K.S. Thorne (in preparation); cited in text as paper II.
- [10] I.D. Novikov and V. Petrova (research in progress).
- [11] I.D. Novikov (unpublished).
- [12] R.L. Forward conceived this example for use in his forthcoming science fiction novel, *Timemaster*.
- [13] M. Morris and K.S. Thorne, *Am. J. Phys.*, **56**, 395 (1988).

Epilogue

...and having, ..., by my own merits and energy, raised myself to one of the highest social positions that any man in England could occupy, I determined to enjoy myself as became a man of quality for the remainder of my life.

William Makepeace Thackeray,

The Memoirs of Barry Lyndon, Esq.